

UNIVERSITÀ DEGLI STUDI DI MILANO

Graduate School in Experimental and Clinical Pharmacological Sciences

Department of Pharmacological and Biomolecular Sciences

XXX course



**PCSK9 (proprotein convertase subtilisin/kexin type 9)
and glucose metabolism: which connection?**

Bio/14

Balzarotti Gloria

Matr. N. R11002

Supervisor: **Chiarissimo Prof. Alberico Luigi Catapano**

Coordinator: **Chiarissimo Prof. Alberico Luigi Catapano**

A.A. 2016-2017

PCSK9 (proprotein convertase subtilisin/kexin type 9) and glucose metabolism: which connection?

Background: PCSK9 (proprotein convertase subtilisin/kexin type 9), is a protein, mainly synthesized and secreted by the liver, which binds to specific target proteins and escorts them towards lysosomes for degradation. The best defined activity of PCSK9 is its ability to modulate the hepatic uptake of LDL cholesterol (LDL-C), by enhancing the intracellular degradation of the LDL receptor (LDLR). In humans, several mutations in PCSK9 gene were described, both “gain-of-function” mutations associated to hypercholesterolemia and “loss of function” mutations linked to low LDL-C levels [1]. These findings suggest PCSK9 inhibitors as a promising class of drugs for the treatment of patients with severe hypercholesterolemia or at very high cardiovascular risk. However, some gaps regarding the potential role of PCSK9 in targeting the LDLR in organs other than the liver are still open. Indeed, the LDLR is abundantly expressed in pancreatic β -cells, where it plays a key role in the uptake of plasma LDL particles [2]. Therefore, further investigations are needed to better clarify the physiological role of PCSK9, also in light of its pharmacological targeting.

Methods: WT, PCSK9 KO, LDLR KO, PCSK9/LDLR DKO, albumin (Alb)Cre⁺/PCSK9^{LoxP/LoxP} (liver selective PCSK9 KO mice) and AlbCre⁻/PCSK9^{LoxP/LoxP} mice were fed a HFD (High Fat Diet – 45% Kcal fat) or SFD (Standard Fat Diet – 10% Kcal fat) for 12 or 20 weeks. GTT, ITT, insulin and C-peptide plasma levels, pancreas morphology and cholesterol accumulation in pancreatic islets were studied in the different animal models.

Results: Glucose clearance was significantly impaired in PCSK9 KO mice fed a SFD or a HFD for 20 weeks compared to WT animals, with both diet. On the contrary, insulin sensitivity was not affected as both animals showed a similar decrease in plasma glucose levels following insulin injection (ITT). Plasma insulin and C-peptide levels were reduced in PCSK9 KO mice compared to WT and accordingly fasting and refeeding experiments showed increased plasma glucose but reduced insulin levels in PCSK9 KO compared to controls. A detailed analysis of pancreas morphology of PCSK9 KO mice vs WT littermates revealed larger islets with increased accumulation of cholesteryl esters, paralleled by increased insulin intracellular levels. This phenotype was completely reverted in PCSK9/LDLR DKO mice implying the LDLR as the PCSK9 target responsible for the phenotype observed. Further studies in AlbCre⁺/PCSK9^{LoxP/LoxP}, which lack detectable circulating PCSK9, also showed a complete recovery of the phenotype, thus indicating that circulating, liver-derived PCSK9 does not impact β -cells function and insulin secretion.

Conclusion: The PCSK9/LDLR axis affects β -cells function and control insulin secretion. Our data indicate that this effect is independent of circulating PCSK9, and is probably related to local effects of PCSK9 suggesting the possibility that anti-PCSK9 antibodies or liver specific therapies, such as siRNAs, might have a limited impact on LDLR expression in pancreas and β -cells dysfunction.

Ruolo di PCSK9 (proteina convertasi subtilisina/kexina di tipo 9) nel metabolismo glucidico

Obiettivo: PCSK9, enzima della classe delle proteasi, viene secreto nel circolo sanguigno dove regola i livelli plasmatici di lipoproteine a bassa densità (LDL), favorendo la degradazione dei recettori per le LDL (LDLR) principalmente a livello epatico. Numerose mutazioni nel gene codificante per PCSK9 sono state descritte, associate sia ad ipercolesterolemia che a bassi livelli di LDL colesterolo (LDL-C) e ridotto rischio cardiovascolare [3]. Queste osservazioni hanno favorito il rapido sviluppo di diverse strategie volte all'inibizione farmacologica di PCSK9, soprattutto nel trattamento di soggetti con ipercolesterolemia familiare (FH). Tuttavia, la presenza del LDLR e di altri recettori target di PCSK9 in numerosi tessuti extra-epatici [4], potrebbe significare un ruolo critico della proteina in diverse patologie metaboliche. In particolare, lo scopo del seguente progetto è stato quello di valutare l'impatto di PCSK9 nel pancreas e nel metabolismo glucidico, avvalendosi di differenti modelli animali.

Materiali e metodi: Topi maschi WT, PCSK9 KO, LDLR KO, PCSK9/LDLR DKO, albumin(Alb)Cre+/PCSK9^{LoxP/LoxP} (topi PCSK9 KO condizionali) e AlbCre-/PCSK9^{LoxP/LoxP}, sono stati alimentati per 12 o 20 settimane con una dieta standard (SFD) o con una dieta ricca in lipidi (HFD), in grado di indurre obesità e disfunzione metabolica. GTT, ITT, livelli plasmatici di insulina e C-peptide, espressione del LDLR, morfologia e contenuto lipidico delle isole pancreatiche sono stati valutati nei differenti gruppi sperimentali.

Risultati: Test di tolleranza al glucosio (GTT) e test di tolleranza all'insulina (ITT) hanno evidenziato una marcata intolleranza al glucosio nei topi PCSK9 KO rispetto ai topi WT, con entrambe le diete, non associata allo sviluppo di insulino-resistenza. I livelli plasmatici di insulina e C-peptide sono risultati significativamente ridotti nei topi PCSK9 KO, in associazione ad un accumulo di insulina nel pancreas, suggerendo un'alterazione nel processo di secrezione dell'ormone a livello delle cellule β pancreatiche. Queste osservazioni sono state confermate dall'analisi morfologica di isole di topi PCSK9 KO e WT. L'assenza di PCSK9 si associa inoltre ad una maggiore espressione del LDLR a livello pancreatico, con conseguente accumulo di lipidi. Al contrario, topi PCSK9/LDLR DKO non presentano alterazioni metaboliche rispetto ai controlli LDLR KO, suggerendo il ruolo chiave del LDLR alla base del fenotipo osservato nei topi PCSK9 KO. Anche studi in topi AlbCre+/PCSK9^{LoxP/LoxP}, che mancano di PCSK9 solo a livello epatico, non mostrano differenze rispetto ai controlli.

Conclusioni: PCSK9 modula l'espressione del LDLR a livello pancreatico, svolgendo un ruolo cruciale nella funzionalità delle cellule β e nel processo di secrezione di insulina dalle stesse. I dati riportati indicano inoltre che l'effetto osservato a livello del pancreas è indipendente da PCSK9 circolante, principalmente prodotto a livello epatico, ma probabilmente associato alla proteina prodotta localmente. Queste osservazioni forniscono informazioni chiave riguardo il ruolo di PCSK9 nel metabolismo glucidico, utili soprattutto in ottica della sicurezza degli inibitori farmacologici di PCSK9.

Index

Index	4
Abbreviations.....	7
Introduction	10
1. Diabetes Mellitus	11
1.1 Physiology of glucose homeostasis	12
1.2 Type 1 Diabetes Mellitus	16
1.3 Type 2 Diabetes Mellitus	18
2. Glucose metabolism: focus on insulin	22
2.1 Insulin structure and biosynthesis	22
2.2 Regulation of insulin transcription	24
2.3 Regulation of insulin translation	25
2.4 Regulation of insulin secretion	26
2.5 Insulin receptor and its signal transduction network	29
3. Factors influencing beta cell function	30
3.1 Beta cell physiology	30
3.2 Dysfunctional beta cells	31
3.2.1 Hyperglycemia and glucotoxicity	32
3.2.2 Lipotoxicity	33
3.2.3 Inflammation and autoimmunity	35
4. PCSK9	36
4.1 Structure, cellular biology and targets: focus on LDLR	36
4.2 Regulation of PCSK9 expression and plasma levels	39
4.3 PCSK9 targets beyond LDLR	41
4.4 Role of PCSK9 in extrahepatic tissue	42

4.4.1 Brain	43
4.4.2 Pancreas	44
4.4.3 Vascular tissue	46
4.4.4 Small intestine	47
4.4.5 Adipose tissue	48
4.4.6 Kidney and adrenals.....	49
4.5 PCSK9-based therapy	50
4.5.1 CRISPR/Cas9 platform	51
4.5.2 Antisense oligonucleotides (ASOs)	52
4.5.3 Small interference RNA (siRNA)	53
4.5.4 Berberine and oleanolic acid	54
4.5.5 Anti-PCSK9 monoclonal antibodies (mAbs)	55
4.5.6 Vaccines	61
4.5.7 Mimetic peptides	62
4.5.8 Adnectins	63
Aim of the project	64
Materials and methods	66
1. Mice	67
2. DNA isolation and genotyping	67
3. Dietary regimen	68
4. Glucose Tolerance Test (GTT) and Insulin Tolerance Test (ITT)	71
5. Fasting and refeeding test	71
6. Magnetic resonance for imaging (MRI)	71
7. Plasma cholesterol and triglycerides measurement	72
8. Insulin, C-Peptide and PCSK9 measurement	72
9. Western Blot Analysis	73
10. Immunofluorescence staining and analysis	73
11. Image acquisition and analysis	74
12. Pancreatic islets isolation and FACS analysis	74

13. Cholesterol and fatty acid content in pancreatic islets	75
14. RNA isolation and real time quantitative PCR (RT-PCR)	75
15. Statistical analysis	76
Results	77
1. Setting of a mouse model of obesity and metabolic dysfunction ...	78
2. Impact of PCSK9 deficiency on lipid metabolism and ectopic fat accumulation	82
3. PCSK9 deficiency results in impaired glucose tolerance but not in insulin resistance	85
4. PCSK9 deficiency results in the impairment of insulin secretion and histological abnormalities in pancreatic islets	90
5. PCSK9 effect on glucose metabolism is dependent on the presence of the LDLR	94
6. Circulating PCSK9 does not impact glucose metabolism and beta cells function	101
Discussion	107
References	114

Abbreviations

2h PG	2h Plasma Glucose
ABCA1	ATP-Binding Cassette Transporter A1
ABCG1	ATP-Binding Cassette Transporter G1
ACAT1	Acetyl-CoA Acetyltransferase
AD	Alzheimer's Disease
ADH	Autosomal Dominant Hypercholesterolemia
ApoB	Apolipoprotein B
ApoER2	Apolipoprotein E Receptor 2
ASOs	Antisense Oligonucleotides
AUC	Area Under the Curve
A β	Amyloid B-Peptide
BACE1	B-site Amyloid Precursor Protein (APP)- Cleaving Enzyme 1
CD36	Cluster Of Differentiation 36
CGN	Cerebellar Granule Neurons
CRE	Cyclic AMP Response Element
DM	Diabetes Mellitus
DPP-4	Dipeptidyl Peptidase 4
DRP1	Dynamin-Related Protein 1
ECs	Endothelium Cells
EGF-A	Epidermal Growth Factor-A
eIF2a	Eukaryotic Initiation Factor 2a
ENaC	Epithelial Na ⁺ Channel
ER	Endoplasmic Reticulum
FFA	Free Fatty Acid
FH	Familial Hypercholesterolemia
FPG	Fasting Plasma Glucose
G6P	Glucose 6-Phosphate
GDM	Gestational Diabetes
GIP	Glucose-Dependent Insulinotropic Peptide
GK	Glucokinase
GLP-1	Glucagon-Like Peptide 1
GLP-1R	GLP-1 Receptor
GLUT2	Glucose Transporter 2
GLUT4	Glucose Transporter 4
GOF	Gain-Of-Function
GSIS	Glucose Stimulated Insulin Secretion
GTT	Glucose Tolerance Test

GWAS	Genome-Wide Association Studies
HbA1c	Hemoglobin A1c
HFD	High Fat Diet
HLA	Human Leukocyte Antigen
HMGCoA-R	3-Hydroxy-3-Methylglutaryl-Coenzyme A Reductase
HNF1 α	Hepatocyte Nuclear Factor 1 α
ICA512	Islet Cell Autoantigen 512
IL-6	Interlukin-6
IMT	Intima Media Thickness
IPGTT	Intraperitoneal Glucose Tolerance Test
IR	Insulin Receptor
IRS	Insulin Receptor Substrate
ITT	Insulin Tolerance Test
KATP channel	ATP-Sensitive Potassium channel
LDL	Low Density Lipoprotein
LDL-C	LDL Cholesterol
LDLR	LDL Receptor
LOF	Loss-Of-Function
LXR	Liver X Receptor
mAbs	Monoclonal Antibodies
MRI	Magnetic Resonance for Imaging
MTNR	Melatonin Receptor
NAFPD	Nonalcoholic Fatty Pancreas Disease
NARC-1	Neural Apoptosis-Regulated Convertase 1
nNOS	Neuronal NO Synthase
OA	Oleanolic Acid
OGTT	Oral Glucose Tolerance Test
oxLDL	Oxidized LDL
PC	Proprotein Convertase
PCR	Polimerase Chain Reaction
PCSK9	Proprotein convertase subtilisin/kexin type 9
PDX-1	Duodenal Homeobox-1
PERK	Pancreatic ER Kinase
PP1	Protein Phosphatase 1
PPAR	Peroxisome Proliferator-Activated Receptor
RIPE3b	Rat Insulin Promoter Element 3b
ROS	Reactive Oxygen Species
RTK	Receptor Tyrosine Kinase
RT-PCR	Real Time Quantitative Polymerase Chain Reaction

SCAT	Subcutaneous Adipose Tissue
SFD	Standard Fat Diet
SH2	Src-Homology 2
siRNA	Small Interfering Rna
SMCs	Smooth Muscle Cells
SNPs	Single Nucleotide Polymorphisms
SRE	Sterol-Responsive Elements
SREBP1c	Sterol Regulatory Element-Binding Protein 1c
T1DM	Type 1 Diabetes Mellitus
T1R2	Taste Receptor Type 1
T2DM	Type 2 Diabetes Mellitus
TCA Cycle	Tricarboxylic Acid Cycle
TG	Triglycerides
TNF- α	Tumor Necrosis Factor-A
UCP-2	Uncoupling Protein-2
UPR	Unfolded Protein Response
VAT	Visceral Adipose Tissue
VLDLR	Very Low Density Lipoprotein Receptor

Introduction

1. Diabetes Mellitus

Diabetes mellitus (DM) is a group of metabolic disorders characterized by a chronic hyperglycemic condition due to dysfunction in insulin secretion, insulin action or both. The chronic hyperglycemia causes long-term damage, dysfunction and failure of different tissues and organs, such as the eyes, heart, kidneys, nerves and blood vessels. The pathogenic processes involved in the onset and development of diabetes include both autoimmune disorders, associated with the destruction of the pancreatic β -cells, and deficient action of insulin on target tissues, resulting in abnormalities in carbohydrate, fat and protein metabolism [5].

Particularly, there are three main types of diabetes mellitus:

- Type 1 DM: is a consequence of the pancreatic failure in producing enough insulin, due to autoimmune β -cell destruction. This form was previously known as "insulin-dependent diabetes mellitus" (IDDM) or "juvenile diabetes".
- Type 2 DM: begins with insulin resistance, a condition in which cells respond to insulin less than expected, leading to a progressive loss of β -cell insulin secretion. This form was referred to as "non insulin-dependent diabetes mellitus" (NIDDM) or "adult-onset diabetes".
- Gestational diabetes (GDM): occurs when pregnant women, without a previous history of diabetes, develop hyperglycemia. It is usually diagnosed in the second or third trimester of pregnancy.

The prevalence of diabetes is increasing rapidly worldwide and it is estimated that currently 415 million adults (8.4%) have diabetes. In 2015 the International Diabetes Federation predicted that one-third of adults are expected to have diabetes in 2050 in the USA and that there will be 71.1 million adults living with diabetes in Europe [6].

1.1 Physiology of glucose homeostasis

Glucose, a fundamental source of cellular energy, represents an important precursor for the synthesis of several biomolecules and plays an important role in cell signalling. Plasma glucose concentration depends on the rate of glucose entering the circulation balanced by the rate of glucose removed from the circulation. A considerable fraction of plasma glucose derives from the intestinal absorption during the fed state, while other sources of circulating glucose derive from hepatic processes (glycogenolysis and gluconeogenesis) during the fasting state [7]. The maintenance of circulating glucose levels in a relatively narrow range is strictly dependent on glucoregulatory hormones release and activity. They include insulin, amylin and glucagon, produced in the pancreatic islets of Langerhans, and glucagon-like peptide 1 (GLP-1) and glucose-dependent insulinotropic peptide (GIP), known as incretins and derived from the intestine [8].

Among the various hormones involved in glucose modulation, insulin and glucagon are the most relevant. Insulin is secreted by pancreatic β -cells in response to increased blood glucose and amino acids in the postprandial state. Insulin is able to reduce circulating glucose levels by enhancing the uptake of glucose into insulin-sensitive cells and promoting its storage in liver via glycogenesis (conversion of glucose to glycogen) and lipogenesis (fat formation). In addition, insulin inhibits glucagon secretion, thus stopping the hepatic production of glucose via glycogenolysis and gluconeogenesis [9]. Glucagon is secreted from pancreatic α -cells. It is produced in response to fasting hypoglycemia and acts increasing glucose levels by enhancing hepatic glycogenolysis and gluconeogenesis [10]. The hormone amylin, released from pancreatic β -cells, contributes to reduce glucagon in postprandial state, as well as slowing of gastric emptying. GIP and GLP-1, glucose-dependent hormones, are secreted only when glucose levels rise above normal fasting glycemia and are involved in the regulation of blood glucose, acting on insulin and glucagon release [11].

The absorptive state or fed state, which occurs when we consume and digest a meal absorbing the nutrients (fats, proteins and carbohydrates), is characterized by increased glucose concentrations in the bloodstream, that in turn stimulates pancreatic β -cells to release insulin. Postprandially, the secretion of insulin occurs in an initial phase of rapid

release of preformed insulin, followed by increased insulin synthesis and release in response to blood glucose [7]. Basically, the major factors that influence postprandial glucose homeostasis are those affecting the suppression of endogenous glucose release and those that concern the hepatic and extrahepatic glucose uptake. Insulin primarily stimulates the uptake of glucose mainly by hepatocytes, adipocytes and muscle cells, taking advantage of glucose transporters (GLUTs). GLUT2, a high-capacity and low-affinity glucose transporter, is highly expressed in the liver, while GLUT4 is detected in insulin sensitive tissues such as skeletal and cardiac muscle, brown and white adipose tissue [12]. Once inside, glucose is immediately converted into glucose 6-phosphate (G6P), leading to a reduction in intracellular glucose levels which further increases glucose uptake. At the same time, insulin suppresses both hepatic gluconeogenesis and glycogenolysis, responsible for the endogenous glucose production [13] (Fig. 1).

The postabsorptive state or fasting state, occurs when food has been digested, absorbed and stored. The drop in blood glucose levels several hours after a meal leads to a decrease in insulin release, paralleled with a rise in glucagon secretion from pancreatic α cells. Glucagon acts mainly in the liver, where it inhibits the synthesis of glycogen and stimulates the glycogenolysis, the breakdown of stored glycogen back into glucose [14]. The large amount of glucose derived from glycogen is then released in the circulation to be used by the peripheral tissues and the brain. Anyway, muscle and liver start to use fatty acids as fuel when the blood glucose levels drop, while the entry of glucose into muscle and adipose tissue decreases in response to a low insulin level, contributing to the maintenance of the blood glucose homeostasis. Finally, to replace the glycogen stores that have been depleted in the liver, the gluconeogenesis allows the generation of glucose from non-carbohydrate carbon substrates such as lactate, citric acid cycle intermediates, amino acids and glycerol [15]. When fasting is prolonged to the point of starvation, glycolysis is shut off in cells that can use alternative fuels, such as skeletal muscle cells that switch from using glucose to fatty acids, converting them into acetyl CoA, used in the tricarboxylic acid cycle (TCA) cycle to produce ATP. As starvation continues, fatty acids and triglycerides stores are used to create ketone bodies, which become the major source of fuel for the heart and other organs [16] (Fig. 2).

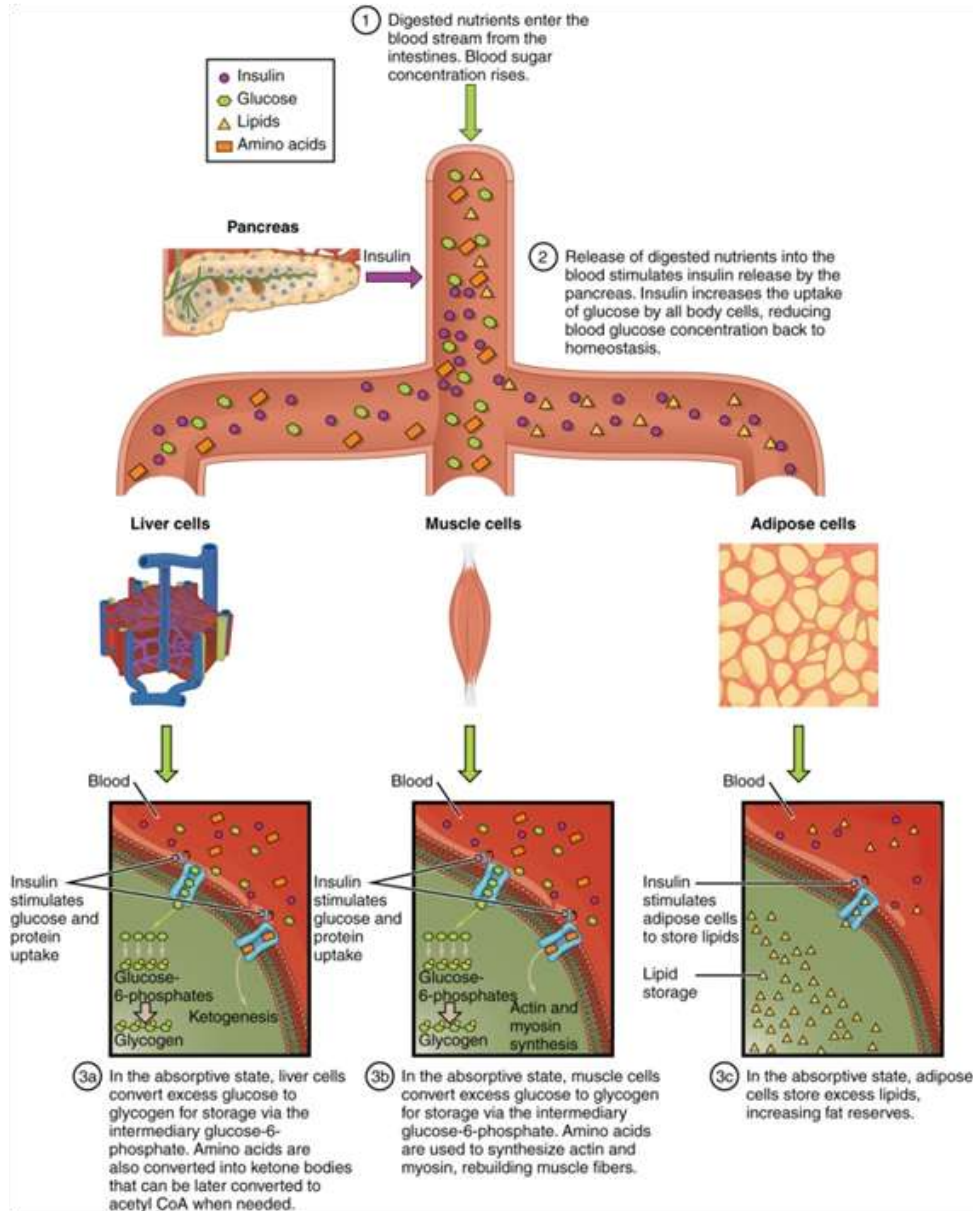


Figure 1. Absorptive State. During the absorptive state, the body digests food and absorbs the nutrients. (Anatomy and Physiology - BC Open Textbook project)

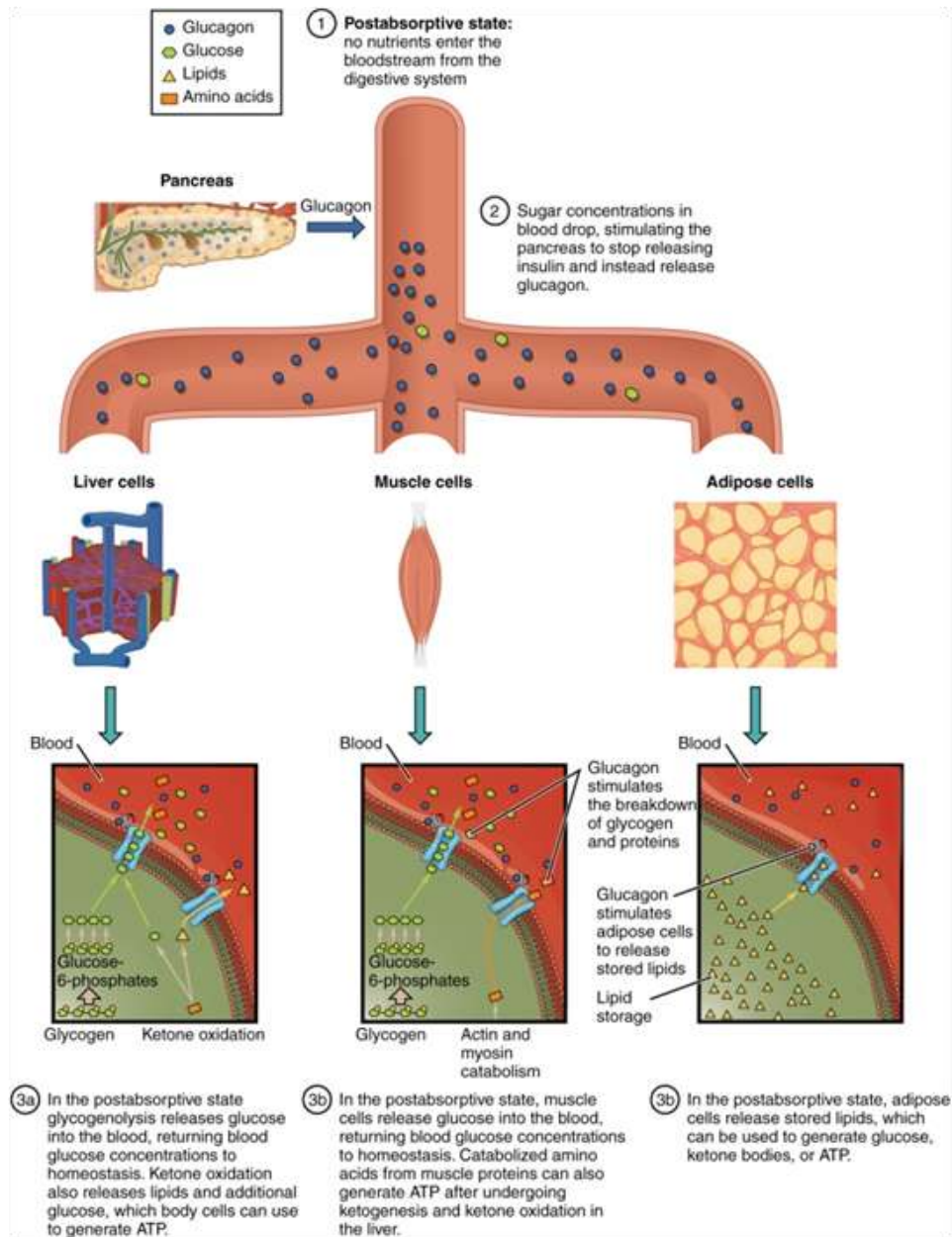


Figure 2. Postabsorptive State. During the postabsorptive state, the body must rely on stored glycogen for energy (Anatomy and Physiology - BC Open Textbook project)

1.2 Type 1 Diabetes Mellitus

Type 1 diabetes mellitus (T1DM) is an autoimmune disease resulting in the destruction of pancreatic β -cells and in the consequent development of hyperglycemia, after a prolonged and variable latent period. Although T1DM can be diagnosed at any age, it is one of the most common chronic diseases of childhood [17]. T1DM is a multifactorial disease resulting from a complex interplay between host genetics, immune system and environment. Although genetic predisposition are clearly important, the increased incidence can only be explained by changes in environment or lifestyle [18]. The presence of auto-antibodies against the pancreatic islet cells is the hallmark of T1DM, even if their role in the pathogenesis of the disease is still unclear. Beyond islet cells auto-antibodies, there are auto-antibodies against insulin (IAA), glutamic acid decarboxylase (GAD, GAD65), protein tyrosine phosphatase (IA2 and IA2 β) and zinc transporter protein (ZnT8A) [19].

T1DM is clearly a polygenic disorder, with approximately 50 loci known to affect disease susceptibility. The human leukocyte antigen (HLA) class II genes show the strongest association with T1DM (especially the HLA-DRB1, HLA-DQA1 and HLA-DQB1 loci), as well as HLA class I genes, which are responsible for 40–50% of the genetic risk [20]. Moreover, multiple non-HLA loci have been reported to contribute to disease risk, including INS, CTLA4, PTPN22, IL2RA, IFIH1, CAPSLIL7R, CLEC16A, and PTPN2 [21]. However, also the environment factors play a key role in the pathogenesis of the disease. The main environmental factors associated with T1DM are drugs, pollutants, dietary factors, stress, infections and gut microbiota [22]. Pentamidine, alloxan and streptozotocin can be toxic to β -cells, while among persistent organochlorine pollutants (POPs), dioxins inhibits glucose uptake and lowers insulin production [23]. Several studies showed that dietary factors are involved in T1DM pathogenesis, including cow's milk and wheat gluten as risk factors, while breastfeeding and Vitamin D seems to have protective effects. The role of the psychological stress is still debate but it may induce T1DM associated autoimmunity and β -cell stress, thereby accelerating its development [24]. Finally, a number of viral infections associate with T1DM onset in humans, including enterovirus, rotavirus and cytomegalovirus (CMV) [25]. The mechanisms by which these factors affect T1DM are still

unclear. So far, it has been proposed that these environmental factors may induce immune responses by generating novel antigens, as well as directly or indirectly inducing epigenetic alterations, which regulate gene expression in immune cells [22].

T1DM is a chronic autoimmune disorder associated with selective destruction of insulin-producing pancreatic β -cells, histologically characterized by cells inflammation (insulinitis) and damage. The pathogenesis of β -cells destruction within the islet in T1DM is difficult to follow due to the marked heterogeneity of the pancreatic lesions. Although symptoms usually occur when 90–95% of β -cells are lost, recent studies suggest that 40%–50% β -cells viability may be present at the onset of hyperglycemia. The rate of β -cells destruction is quite variable, being rapid in some individuals, mainly infants and children, and slow in others, such as in adults [26]. The immunological events occurring in T1DM involve macrophages, dendritic cells (DCs) and T lymphocytes, both CD4+ and CD8+ T cells. Among CD4+ T cells, Th1 and Th17 cells produce proinflammatory cytokines, while CD4+ Th2 cells have been recognized to have protective effects against autoimmunity [27]. CD4+ T regulatory (Treg) cells exhibit potent regulatory functions and are necessary to maintain immune tolerance. In addition to CD4+ T cells, also CD8+ T cells are involved in the pathogenesis of T1DM. Studies in NOD mice demonstrated that the activation of CD8+ T cells can cause damage to pancreatic islets, contributing to the onset and development of the disease [28].

The classical symptoms of T1DM, which typically develop over a short period of time, are polydipsia, polyuria, enuresis, lack of energy, extreme tiredness, polyphagia, weight loss, poor healing, chronic infections and blurred vision, with severe dehydration and diabetic ketoacidosis in children and adolescents. In patients with classic symptoms, T1DM is diagnosed based on plasma glucose criteria, either the fasting plasma glucose (FPG) or the 2h plasma glucose (2h PG) value after a 75g oral glucose tolerance test (OGTT) or Hemoglobin A1c (HbA1c). FPG \geq 126 mg/dL (7.0 mmol/L), 2h PG after OGTT \geq 200 mg/dL (11.1 mmol/L), HbA1c \geq 6.5% (48 mmol/mol) or a random plasma glucose \geq 200 mg/dL (11.1 mmol/L) along with symptoms of hyperglycemia, are diagnostic of the disease [29]. A key distinguishing feature between type 1 and type 2 disorders is the presence of auto-antibodies against β -cells antigens, observed in more than 90% of subjects with newly

diagnosed T1DM. An accurate diagnosis of the disease in childhood and adolescence is crucial for optimum care and avoiding complications [30].

Regarding the management of T1DM, the discovery of insulin in 1921 was clearly the most significant therapeutic event in the history of the disease. Currently, the administration of exogenous insulin through daily injections or computerized pumps remain the most noticeable treatment for T1DM patients [31]. Exogenous insulin administration significantly increases life expectancy and helps normalize blood glucose, but can expose patients to episodes of hypoglycemia, one of the worst side effects of this treatment [31]. Recently, notable progresses have been made in the development of immunotherapy approaches using pharmaceutical compounds, such as cyclosporine. These compounds are designed to manipulate the immune system in order to avoid β -cell destruction, successfully blocking the progression of the disease [32]. Alternative immunotherapy methods, including autoantigen-specific immune therapy, immunoregulatory-based approach and activation of Treg cells, have been proposed and are currently in preclinical and clinical studies [33]. In some cases, whole pancreas or islet transplantations can be effective for T1DM treatment, even though they are limited by donor scarcity and life-long immunosuppression. Therefore, development of novel therapies that can tackle these issues is highly desirable [34].

Type 2 Diabetes Mellitus

Type 2 diabetes mellitus (T2DM) is a long-term metabolic disorder characterized by relative (rather than absolute) insulin deficiency, peripheral insulin resistance and consequent hyperglycemia. In 2013, the global prevalence of T2DM in adults (20-79 years old) was 8.3% (382 million people) and this number is expected to rise beyond 592 million by 2035 [35]. More than 90-95% of diabetes patients belong to T2MD and most of these patients are adults. However, the number of young people (< 20 years) with the disease is rapidly increasing, mainly due to changes in the lifestyle of children in terms of more sedentary life and less healthy food [36]. T2DM is indeed characterized by a strong genetic predisposition, even though the environmental factors also play a key role in this types of disorder [37].

Despite several genome-wide association studies (GWAS) have identified a large array of gene mutations and single nucleotide polymorphisms (SNPs) associated with T2DM, these variants explain less than 15% of disease heritability [38]. A study conducted in different countries on T2DM patients identified various diabetes putative loci positioned in and around the CDKAL1, CDKN2A/B, HHEX/IDE and SLC30A8 genes, providing strong evidences that common genetic determinants, including common specific genes, are linked to diabetes [39, 40]. Genetic variants and polymorphisms in the interleukin and related genes, including interleukin-6 (IL-6) and tumor necrosis factor- α (TNF- α) genes, were found to be associated with increased risk of developing T2DM [41]. Interestingly, also variants and SNPs in the antioxidant genes, such as superoxide dismutase and glutathione peroxidase, are implicated in the risk and pathogenesis of T2DM [35]. However, beyond the genetic causes, environmental and lifestyle changes significantly contribute to the rapid global increase in T2DM prevalence and incidence in recent decades. It has been demonstrated that an unhealthy energy-dense diet in association with a sedentary lifestyle are the primary cause of obesity and T2DM [42]. Despite the wide range of diet types consumed worldwide, generally plant food is associated with reduced T2DM risk than meat, while refined grains or sugar-sweetened beverages appear to promote obesity and diabetes risk [43]. Unfortunately, epidemiological studies cannot exclude the impact of confounding factors such as those of physical activity, which is difficult to assess in queries or interviews. Indeed, high total physical activity is associated with a reduction in relative diabetes risk by approximately 30%, compared to low one [44]. Other contributing factors for T2DM are the duration and quality of sleep, paralleled with housing environment such as the exposure to residential traffic, noise, fine airborne particulate, UV or ionising radiation, toxins or allergens [43]. The relationship between depressive mood, stress or infections and diabetes is still debated. Of note, except high levels of nutrients and their metabolites in blood, only few environmental or lifestyle factors directly affect β -cell function. They usually have different sites of action, such as the immune system, vascular tissue, adipose tissue, liver, muscle, brain or intestine [43].

Regarding the pathophysiology, T2DM is characterised by hyperglycemia, insulin resistance and relative pancreatic β -cell failure, with up to 50% cell loss at diagnosis. More than 90-95% of T2DM patients are adults, even though recently the incidence of

this disease in young people is significantly increased, where the β -cell loss occurs more rapidly compared to adults [45]. Insulin resistance is a pathological condition in which cells fail to respond normally to insulin and occurs primarily within hepatocytes, adipocytes and myocytes. As a consequence, insulin resistance increases the demand for insulin in these tissues, leading to an initial period of euglycaemic hyperinsulinaemia [46]. Subsequently, insulin secretion decreases with the increased demand for insulin by time due to the gradual destruction of β -cells, causing some T2DM patients to be dependent on insulin [47]. Increasing evidences support that T2DM is strongly modulated by β -cell dysfunction and apoptosis, mainly due to a glucose toxicity effect. Particularly, hyperglycemia-induced β -cell apoptosis has been extensively studied regarding the balance between pro-apoptotic Bcl-2 proteins (Bad, Bid, Bik, and Bax) and anti-apoptotic Bcl family (Bcl-2 and Bcl-xL). Apoptosis occurs when the concentration of pro-apoptotic proteins exceeds that of anti-apoptotic ones [48].

The classical symptoms associated with T2DM, which usually come on slowly, include increased thirst, frequent urination, unexplained weight loss, increased hunger and tiredness. The long-term complications caused by high blood glucose levels are heart disease, strokes, diabetic retinopathy, kidney failure and reduced blood flow in the limbs, which may lead to amputations. As described for T1DM, T2DM is diagnosed using either the estimation of plasma glucose (FPG or OGTT) or HbA1c. FPG \geq 126 mg/dL (7.0 mmol/L), 2h PG after OGTT \geq 200 mg/dL (11.1 mmol/L), HbA1c \geq 6.5% (48 mmol/mol) or a random plasma glucose \geq 200 mg/dL (11.1 mmol/L) along with symptoms of hyperglycemia are diagnostic of the disease [35]. Of note, HbA1c has the advantage to be a stable diagnostic measure that does not require fasting and is equivalent to FPG regarding the prediction of the development of retinopathy [49]. T2DM can be distinguished from T1DM considering that it is characterized by hyperglycemia in the context of insulin resistance and relative insulin deficiency, while in T1DM there is an absolute insulin deficiency due to destruction of pancreatic islet cells. However, if the diagnosis is in doubt, antibody testing may be useful to confirm T1DM [50].

Management of T2DM mainly focuses on lifestyle interventions and pharmacological treatments, in order to reach the goal of HbA1c around 7% or fasting glucose $<$ 130 mg/dL.

Considering that around 60% of patients with T2DM are obese (BMI ≥ 30 kg/m²) and show insulin resistance, diet and lifestyle are effective tools for T2DM prevention and management [51]. Regarding the pharmacological management, the initial T2DM management approach recommend monotherapy, usually with metformin, but if the HbA1c goal has not been met within approximately 3 months of starting initial therapy, treatment should be intensified by adding a second or third agent [52]. Metformin reduces hepatic glucose production, enhances peripheral insulin sensitivity and stimulates GLP-1 secretion. Moreover, it effectively decreases HbA1c levels, is weight neutral, does not cause hypoglycemia and can have modest beneficial effects on blood pressure and lipid profile [42]. Sulfonylureas, which act on β -cells promoting insulin secretion [53], and thiazolidinediones, that stimulate peroxisome proliferator-activated receptors (PPARs), are usually chosen for dual therapy [54]. Glucagon-like peptide-1 receptor agonists (GLP-1 RAs) are synthetic analogues of the native human GLP-1 with improved pharmacokinetic properties. They trigger GLP-1-like effects, including increased insulin secretion, reduced glucagon released, reduced hepatic glucose output, delayed gastric emptying and increased satiety [55]. Dipeptidyl peptidase 4 (DPP-4) inhibitors, such as sitagliptin, saxagliptin and alogliptin, act reducing the enzymatic degradation of the incretin hormones GLP-1 and GIP. This leads to an increased availability of endogenous incretins, stimulating insulin secretion from pancreatic β -cells and inhibiting glucagon release from pancreatic α -cells in a glucose-dependent manner [56]. Finally, insulin remains the most potent glucose-lowering agent, particularly for patients with high HbA1c levels. However, there are multiple barriers to initiating insulin therapy and the decision to add insulin will require discussion between the prescribing physician and the patient, taking into consideration the patient's motivation, general health, age, risk of hypoglycemia and cardiorenal complications [57].

2. Glucose metabolism: focus on insulin

The pancreas is a centralized organ vital for whole body metabolic homeostasis and the nutrient metabolism in pancreatic cells is not only essential for providing them energy, but also acts as a mechanism to sense and react to circulating levels of macronutrients. The pancreas, located behind the stomach and connected to liver, spleen and small intestine, produces exocrine enzymes to aid digestion and endocrine hormones to regulate blood glucose. The exocrine pancreas represents around 98% of the pancreatic mass and is responsible for synthesis, storage and secretion of digestive enzymes into the duodenum. The endocrine pancreas, representing about 2% of the total mass, is made up of the islets of Langerhans, containing different cell types: α - β - δ - ϵ - and γ (PP) cells [58]. Adult pancreatic β -cells express and secrete insulin in response to relevant stimuli. Despite the primary regulatory factor for insulin synthesis and secretion is glucose, other stimuli, such as amino acids, fatty acids, hormones and neuronal signals, also play important roles in these processes. Once released in blood stream, insulin binds to its receptor found in several tissues, especially in liver, muscle and adipose tissue, to facilitate glucose uptake and storage. An efficient energy metabolism in pancreatic β -cells is necessary to prevent dysfunction of this metabolic framework, such as T2DM, whose prevalence has been dangerously increasing over the past few decades [59].

2.1 Insulin structure and biosynthesis

Insulin was the first peptide hormone to be discovered. In the mid 1950's Sanger showed that insulin is a two-chain heterodimer, consisting of a 21 amino acid residue "A" chain and a 30 amino acid residue "B" chain, bound by two disulfide linkages (A7-B7 and A20-B19) [60]. Although this primary structure provided important information concerning the amino acid composition and size of the molecule (5,8 kDa), questions regarding the processes of insulin biosynthesis and secretion remained unclear until the late 1960's, when proinsulin was discovered [61]. This precursor protein (~9 kDa) consists of both the A and B chain, joined through an intervening fragment, known as C-peptide. Finally, only in 1976 Chan et al. demonstrated that there was an additional and larger precursor of

insulin, preproinsulin. This single-chain polypeptide (~12 kDa) consists of proinsulin extended at the amino-terminus by a 24-residue signal peptide [62].

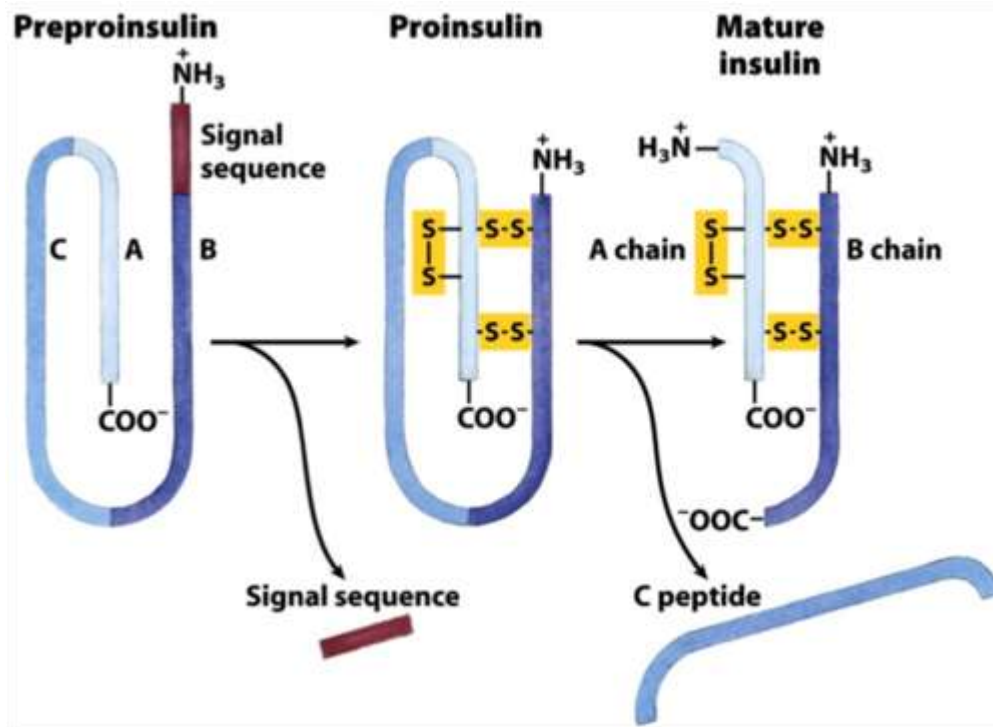


Figure 3. Insulin synthesis and maturation. (2004 Beta Cell Biology Consortium)

Preproinsulin, once encoded, is translocated across the rough endoplasmic reticulum (rER) membrane into the lumen, via interactions of its signal peptide with the signal recognition particle (SRP) and SRP-receptor in the rER membrane [63]. On the luminal side of the rER membrane, the preproinsulin signal peptide is cleaved to yield proinsulin, which undergoes folding and formation of three disulfide bonds to generate the native tertiary structure, the direct precursor of insulin. Finally, the folded proinsulin is transported from the ER to the Golgi apparatus where it enters immature secretory vesicles and is cleaved to yield insulin and C-peptide. Insulin and C-peptide are then stored in these secretory granules together with islet amyloid polypeptide (IAPP or amylin) and other less abundant β -cell secretory products [64]. Both proinsulin and insulin monomers tend to form dimers when their concentration rises, while in the presence of zinc (Zn) and favorable pH the monomers assemble into hexamers [65]. The hexamer,

despite it is inactive, presents long-term stability, which protects the highly reactive insulin, yet readily available. Once the hexamers are secreted from the β -cell and diffuse into circulation, a combination of electrostatic repulsion and decreased concentration of insulin favors the dissociation of insulin into its active monomeric form [66].

2.2 Regulation of insulin transcription

Insulin content in β -cells is highly dynamic, enhancing in the presence of nutrients and decreasing in response to fasting. This ability of β -cells to rapidly respond to cellular signals is mainly due to transcriptional regulation. Several elements within the promoter region of insulin gene (A, C, E, Z, and CRE elements) provide binding sites for different β -cell transcription factors that regulate insulin gene expression [67]. The A elements contain a TAAT motif in the core region, that represents the central DNA binding recognition site for several proteins, including duodenal homeobox-1 (PDX-1), Cdx2/3 and Isl-1 [68]. The expression of PDX-1, which was initially characterized as an insulin and somatostatin transcriptional factor, is generally restricted to islet β -cells (~91%) in adult pancreas. Cdx2/3, despite it is expressed both in β -cells and α -cells, appears to play a less important role in islet function, because Cdx2/3 KO mice presents defects only in intestinal function. Isl-1, which is expressed by all types of islet cells and plays an essential role in islet formation during embryo development, is able to activate somatostatin, glucagon and IAPP gene expression [59]. There are two C elements in the insulin gene promoter, C1 and C2 element. Rat insulin promoter element 3b (RIPE3b)¹ is the major factor binding the C1 element, which has been demonstrated to play a key role in regulating insulin transcription [69]. The C2 element contributes to insulin, glucagon and somatostatin transcription in α -, β -, and δ -cells, respectively. In particular, the activator of insulin C2 element PAX6, a member of the Pax transcription factor family, which is required for normal transcription of these genes and islet development [70]. Regarding the E elements, rodents have two separated mini-enhancer units within the insulin gene, while other mammals have only one. The most important E element activators are BETA2/NeuroD1, E2/5, E12 and E47 [71]. Pancreatic islets are especially enriched in BETA2/NeuroD1, which is fundamental in regulating insulin gene expression and β -cell survival [72]. The Z element is located upstream of the A element and is present only in

the human insulin gene promoter. Of note, recent studies demonstrated that A element activation depends on the presence of the Z element. The Z element functions as both a potent glucose-responsive transcriptional enhancer in primary cultured islet cells and as a transcriptional repressor in transformed β -cell lines and primary fibroblast cells [73]. Finally, the human insulin gene promoter contains 4 Cyclic AMP response element (CRE) sites: CRE1, CRE2, CRE3 and CRE4, which contain within the core a sequence similar to the CRE consensus sequence. Several transcription factors, that are members of the CRE binding protein (CREB)/ATF family, regulate insulin gene transcription by binding to the consensus CRE [74].

2.3 Regulation of insulin translation

Glucose metabolism is no doubt the most influential physiological event that stimulates insulin gene transcription and mRNA translation, despite insulin biosynthesis depends on multiple factors. In response to nutrients, β -cells are able to enhance their overall protein translation, which is mostly controlled by the phosphorylation/dephosphorylation of eukaryotic initiation factor 2a (eIF2a). Protein phosphatase 1 (PP1) is responsible for the eIF2a dephosphorylation, while the pancreatic ER kinase (PERK) phosphorylates eIF2a, thereby regulating insulin translation [75]. Interestingly, PERK seems to be required during the fetal and neonatal phases for proper development of β -cell mass, while not necessary in adults for maintaining β -cell mass [76]. Moreover, β -cells have developed a mechanism for detecting the amount of insulin stored in granules and secreted, in order to adjust insulin synthesis accordingly. For example, the islet cell autoantigen 512 (ICA512), a granule transmembrane protein, plays a crucial part in this feedback control. When the granule membrane fuses to the cell membrane to release insulin, the cytosolic fragment of ICA512 is released from granules and targets the transcriptional factor STAT5 in the nucleus, which in turn upregulates insulin transcription [77]. Therefore, the release of insulin from secretory granules is rapidly communicated to the nucleus, which serves as a positive feedback mechanism to start insulin translation, in order to maintain a sufficient amount of stored insulin [59].

In addition, β -cells also adjust insulin production in response to immediate environmental triggers by modulating the speed of insulin translation. The acute glucose-stimulated

insulin production is independent of mRNA synthesis within the first 45min, considering that blockage of transcription occurs only after that time frame. For example, when rat islets are exposed to 25 mM glucose for 1h, occurs a significant induction in intracellular proinsulin levels, while proinsulin mRNA content remains almost the same [78]. Moreover, insulin mRNA stability, which depends on nutrient status, is a crucial factor that influences insulin biosynthesis. In particular, both in vitro and in vivo studies demonstrated that insulin mRNA stability decreases under lower glucose levels and increases under high glucose conditions. Rats fasted for 3 days present only 15–20% of the pancreatic insulin mRNA measured in the control animals. Thus, translation regulation controls the immediate insulin synthesis, while regulation at the transcriptional level contributes to the modulation of delayed insulin synthesis [59].

2.4 Regulation of insulin secretion

Secretion of insulin from β -cells represents a crucial step in the regulation of glucose homeostasis and in healthy subjects it precisely meet the metabolic demand. However, abnormalities in insulin secretion have been demonstrated to be an integral component of both T1DM and various forms of T2DM. Insulin is stored in large dense granules and released by exocytosis, through a multistep process that involves the transport of the secretory vesicles to the plasma membrane, then docking, priming and finally their fusion with the plasma membrane. Only a small part of the insulin stored in granules is released, even under maximum stimulation, suggesting that systemic insulin levels are regulated by secretion rather than by biosynthesis [66]. To sense the nutritional state, β -cells are clustered in islets strategically connected to the circulation, which allows them to receive a greater amount of blood than cells in the surrounding exocrine regions. In addition to glucose, some amino acids and fatty acids impact on insulin secretion, a process that is modulated cooperatively by nutrients, hormones and neurotransmitters in association with electrical depolarization of the β -cells [59] (Fig. 4).

exocytosis of insulin-containing granules. Interestingly, also some products derived from the anaplerosis/cataplerosis can act as insulin secretion signals, including NADPH, malonyl-CoA, and glutamate [81].

Single amino acids, at physiological concentrations, are usually poor insulin secretagogues, but certain combinations of amino acids or higher levels can enhance glucose stimulated insulin secretion (GSIS). For example, during fasting proteins in skeletal muscle are catabolized and amino acids, such as alanine and glutamine, are released into circulation. These free amino acids acts as potent glucagon secretagogues, leading to an elevation in blood glucose levels, which then triggers insulin secretion [82]. Dietary amino acids can also induce insulin secretion via incretin-dependent mechanisms. GIP and GLP-1, the two major incretin hormones secreted from the gastrointestinal tract, directly act on β -cells by binding to their specific cell-surface receptors, augmenting GSIS [83]. Beyond glucose and amino acids, also free fatty acids (FFAs) can influence β -cell secretion of insulin. In T2DM, FFAs potentiate insulin secretion to compensate the increased insulin need consequently of insulin resistance [84].

Finally, several hormones are able to modulate insulin secretion. Despite β -cells are not considered classic estrogen targets, their receptors are present in islets and the effects of 17β -estradiol on β -cells are well described. At physiological concentrations, 17β -estradiol significantly decreases KATP channel activity, which causes membrane depolarization and subsequent opening of voltage-gated Ca^{2+} channels, influencing insulin secretion [85]. The effect of melatonin, a hormone secreted by the pineal gland, on insulin secretion is controversial, despite melatonin receptors (MTNRs) has been discovered on both clonal β -cells and human islets [86]. GLP-1, secreted from small intestinal L-cells in response to nutrient load, is involved in insulin secretion in order to meet the increased demand for insulin after a meal. Analogs of GLP-1 have been studied as a potential therapy for T2DM for many years, with the long-lasting GLP-1 analog exenatide introduced to clinics in 2005. Upon activation of the GLP-1 receptor (GLP-1R), adenylyl cyclase is activated, leading to the generation of cAMP, which significantly potentiates GSIS [87]. Leptin, secreted by adipocytes, exerts an inhibitory effect on insulin secretion. Indeed, has been demonstrated that leptin deficiency is associated with hyperinsulinemia in both mice and humans [88].

2.5 Insulin receptor and its signal transduction network

Although insulin is generally viewed as a glucose homeostasis regulating hormone, actually it is known to have a much extended pleiotropic role. Insulin acts through a receptor located in the membrane of several target organs and tissues, including β -cells. The insulin receptor (IR) belongs to the receptor tyrosine kinase (RTK) superfamily, whose members generally regulate several cellular functions, including cell proliferation, survival, differentiation, migration and metabolism [89]. The receptor, synthesized as single chain preproreceptors, is processed into α and β chains by a furin-like proteolytic enzyme and subsequently glycosylated, folded and dimerized to yield the mature form. Each monomer is structurally organized into 8 distinct domains: a leucine-rich repeat domain (L1), a cysteine-rich region (CR), an additional leucine rich repeat domain (L2), three fibronectin type III domains (FnIII-1, FnIII-2 and FnIII-3), an insert domain inside FnIII-2 (ID, containing the α/β furin cleavage site), a transmembrane helix (TH) and intracellular juxtamembrane (JM) region, just upstream of the intracellular tyrosine kinase (TK) catalytic domain, responsible for subsequent intracellular signaling pathways [66].

Insulin, IGF-I and IGF-II bind to the α -chain of the IR inducing structural changes within the receptor, which leads to the autophosphorylation of the tyrosine residues within the intracellular TK domain of the β -chain. These changes create binding sites for signaling protein partners containing src-homology 2 (SH2) domains or phosphotyrosine-binding (PTB) domains. Unlike other RTKs, IR do not bind signaling proteins directly, but works through key signaling intermediates, the insulin receptor substrate (IRS) proteins as well as the adapter Shc (SH2 domain containing). The IRS proteins are a family of cytoplasmic adaptor molecules that transfer signals from the IR to evoke a cellular response [90]. The central portion and the C-terminal domain of the IRS proteins contain up to 20 potential phosphorylation sites that bind to signaling proteins containing SH2 domains, when phosphorylated by the IR. The two major IR signaling cascades are the PI3K/AKT pathway and the Grb2-SOS-Ras-MAPK (also known as ERK) pathway. The PI3K pathway is responsible for most metabolic effects of insulin and is connected exclusively through IRS. On the contrary, the ERK pathway, linked both with IRS and Shc, is involved in the regulation of gene expression and, together with the PI3K pathway, in the control of cell growth (mitogenesis) and differentiation [91].

3. Factors influencing beta cell function

The pancreas and especially β -cells play crucial roles in maintaining whole body energy balance. Nutrient metabolism in β -cells is not only essential for providing them energy, but also allow them to sense and respond to circulating levels of macronutrients, putting pancreatic metabolism central in the regulation of whole body energy homeostasis. Many factors could affect pancreatic β -cells function, such as hyperglycemia/glucotoxicity, lipotoxicity, autoimmunity, inflammation, adipokines, incretins and insulin resistance [92]. In particular, chronic hyperglycemia may result in deleterious effects on insulin synthesis and secretion, cell survival and insulin sensitivity. Moreover, in the presence of hyperglycemia, extended exposure to increased free fatty acids (FFAs) leads to the accumulation of toxic metabolites into the cells (lipotoxicity), causing decreased insulin gene expression and impaired insulin secretion. In addition recent studies, focusing on nonalcoholic fatty pancreas disease (NAFPD), demonstrated that the accumulation of FFAs within the pancreas, possibly due to inefficient lipid metabolism, disrupts insulin secretion and may contribute to the development of the disease [58].

3.1 Beta cell physiology

β -cells represent the most important glucose sensors among pancreatic cell types and their function is absolutely necessary for proper glucose balance within the whole body. In healthy subjects, glucose enters β -cells through facilitated diffusion via GLUT2. Once inside, glucose is metabolized to generate pyruvate and NADH via glycolysis, which in turn are used to produce ATP through the TCA cycle and the oxidative phosphorylation. The resulting increased ATP/ADP ratio causes the fusion of insulin granules with the plasma membrane, promoting the hormone release into the circulation [93]. Several studies, both in vitro and in vivo, convincingly demonstrated the importance of nutrient metabolism for β -cell function and the key role of mitochondria for an efficient GSIS. For example, the deficiency of dynamin-related protein 1 (DRP1) in β -cells, that prevents mitochondrial fission, reduces GSIS limiting substrate availability to mitochondria. Of note, GSIS is rescued in these cells by the simple addition of pyruvate, suggesting that

mitochondrial dynamics is able to impact metabolic pathways outside of the mitochondria, including glycolysis [94].

Besides glucose, β -cells respond to several macronutrients such as other monosaccharides, amino acids and FFAs, as well as to hormones and neurotransmitters. For example, although fructose is largely metabolized in liver, mouse and human β -cells secrete insulin in response to fructose, when it interacts with the sweet taste receptor type 1 (T1R2) on the β -cell membrane [95]. Amino acids are essential nutrients for β -cells, with both positive and negative effects on insulin release, depending on time, concentration and type [58]. FFAs modulate insulin secretion via different metabolic signalling mechanisms. Once inside β -cells, FFAs are converted into FA-CoA and can enter the glycerolipid/FFA cycling (lipogenesis and lipolysis) or can be oxidized to acetyl-CoA to enter TCA cycle. In order to improve ATP production, metabolites produced in these pathways can independently modulate insulin release through other parallel mechanisms [96].

In addition to nutrients, also circulating hormones interfere with the modulation of β -cells metabolism. Non-pancreatic hormones, such as the incretins GLP-1 and GIP, are important for glucose homeostasis. They are both released from the intestine in response to food intake and activate their corresponding G-protein-coupled receptors (GLP-1R or GIPR) on the surface of β -cells [97]. GLP-1 and GIP are able to stimulate insulin secretion when glucose is high, but it is still debated if this directly depends on their effects on nutrient metabolism in β -cells. Recent evidences suggest that GLP-1 and related peptides have beneficial effects on mitochondrial metabolism, biogenesis and reactive oxygen species (ROS) production in different cell types [58].

3.2 Dysfunctional beta cells

Nowadays, western diets and sedentary lifestyle represent the major contributors to obesity and insulin resistance, which are strictly associated with metabolic syndrome. Pancreatic β -cells, which are the primary nutrient-sensors in our bodies, respond to chronically higher-than-normal levels of circulating nutrients increasing in mass, in order to compensate for higher insulin requirements. However, the slow rate of proliferation

and regeneration of this highly differentiated cells is not enough to completely maintain glucose homeostasis [58]. High levels of circulating glucose and lipids have also their own detrimental effects on β -cells (gluco/lipotoxicity), while inflammation associated with obesity, both in peripheral tissues and in pancreas, negatively impacts on β -cell function. In addition, stress caused by increased mitochondrial metabolism leads to over-production of ROS, thus damaging DNA and proteins. Taken together, these insults ultimately lead to β -cell failure and death, triggering dependence on exogenous insulin for maintenance of glucose balance [98].

3.2.1 Hyperglycemia and glucotoxicity

Pancreatic β -cells are very sensitive to blood glucose levels and changes in its homeostasis strongly influence their function and dynamics. Several studies have demonstrated that the chronic exposure to abnormally high blood glucose has deleterious effects on insulin synthesis and secretion, cell survival and insulin sensitivity through different mechanisms. In turn, this glucotoxicity leads to hyperglycemia and finally to the vicious circle of endless deterioration of β -cells function. Glucotoxicity impacts irreversibly the cellular pathways of insulin production and secretion, as opposed to beta cell desensitization and beta cell exhaustion, which are reversible. Chronic hyperglycemia is able to impair β -cells function and cause β -cells apoptosis through multiple pathways and mechanisms [99].

Firstly, prolonged exposure to increased glucose levels leads to a reduced activity of key regulators of insulin promoter activity and other β -cells specific genes, causing a gradual loss of insulin gene expression. These processes are, at least in part, mediated by oxidative stress. Indeed, long-term sustained hyperglycemia, that increases the metabolic flux into the mitochondria, induces a massive production of reactive oxygen species (ROS) [100]. In hyperglycaemic conditions, ROS are excessively produced by mitochondrial oxidative phosphorylation during anaerobic glycolysis and through alternative pathways, which occur when the glycolytic capacity is exceeded. The oxidative stress subsequently activates different stress-induced pathways in β -cells, inducing dysfunctional insulin biosynthesis and secretion, and ultimately apoptosis [101]. Recent data show a closely correlation between the oxidative stress and ER stress. Cellular ROS can increase the

accumulation of misfolded proteins in the ER, which amplifies ROS production that in turn further enhances the ER stress, impairing insulin production and favoring cell death. The ER stress is also induced by β -cells exposure to an increased insulin secretory request during hyperglycaemic condition, which increases the demand on ER for the synthesis of proinsulin. Despite ER stress triggers the unfolded protein response (UPR) in order to restore the ER homeostasis, in case of severe ER stress and strong UPR, apoptosis occurs β -cells [92]. Besides ER stress, several studies indicate that chronic hyperglycemia is associated with decreased number of mitochondria and changes in their morphology, such as increased volume, reduction of the proteins in the inner membrane and increased variability in mitochondrial size [102]. Finally, evidence exists that chronic hyperglycemia induces non-immune mediated inflammatory pathways, enhancing the production of interleukin (IL)-1 β , nuclear factor-kB (NF-kB) and Fas receptor in β -cells, even though this requires to be confirmed [92].

3.2.2 Lipotoxicity

Lipids, which represent no doubt a vital energy source for β -cells, can exert both positive and negative effects on their survival and insulin secretory function, depending on concentration, duration and glucose abundance. Indeed, prolonged lipid exposure has been recently shown to activate cell stress responses including oxidative stress, ER stress and autophagy. For example, diabetes is often associated with changes in lipoprotein profiles and increased FFA concentrations. Chronic exposure to FFAs determine many of the key features of β -cells failure, including apoptosis, defective pro-insulin processing, diminished insulin content and gene expression and subsequent reduced GSIS [103]. For example, evidence suggests that the uncoupling protein-2 (UCP-2), a ubiquitously expressed mitochondrial carrier that uncouple the respiratory chain from ATP synthesis, plays a role in lipotoxicity. UCP-2 KO mice are characterized by increased circulating insulin levels and are protected from genetic and nutritional diabetes, while UCP-2 expression is increased in β -cells derived from high-fat feeding rodents [104]. Prolonged exposure to FFAs is also able to impair insulin gene expression in the presence of high glucose. In particular, palmitate inhibits insulin gene transcription modulating the activity of pancreatic duodenal homeobox 1 (PDX-1), a transcriptional factor that plays a central role in β -cells function and survival. In vitro, saturated FFAs induce β -cell apoptosis, while

unsaturated ones are usually protective, probably due to their greater ability to form intracellular triglycerides. Several mechanisms have been proposed to mediate FFAs induced apoptosis in β -cells, including ceramide formation, generation of oxidative stress and inflammation. In insulin secreting cells, palmitate, but not oleate, induces markers of ER stress, causing alterations in its morphology [104] (Fig. 5).

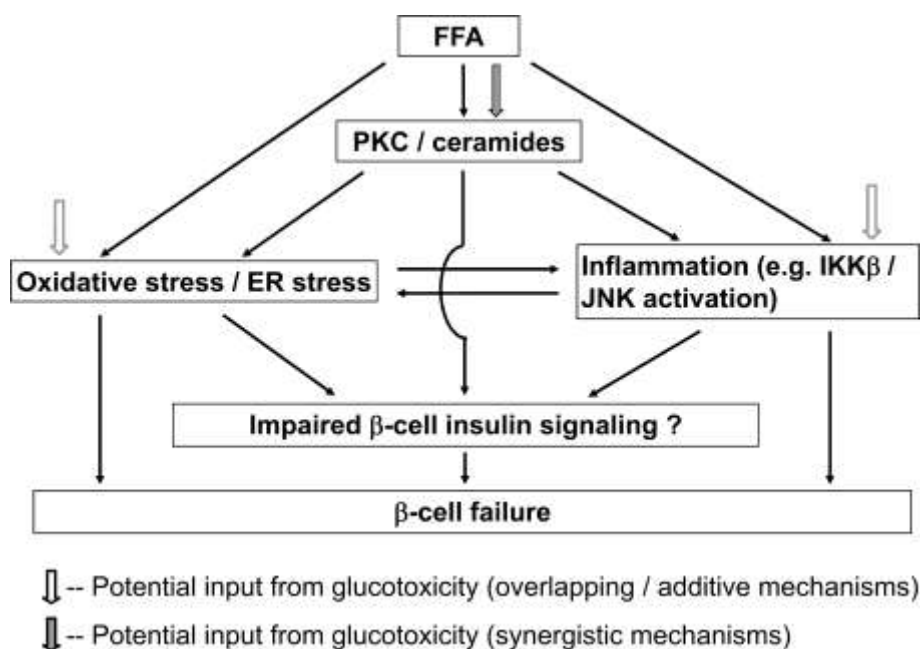


Figure 5. Mechanisms of β -cell lipotoxicity: FFA leading to oxidative stress/ER stress/inflammation, resulting in β -cell failure. [105]

Although most of the studies have been focused on the effects of FFAs on β -cells function, emerging data suggest that cholesterol and lipoprotein fractions may also play a role in the progression of β -cells failure. LDL, oxidized LDL and VLDL reduce preproinsulin expression levels in isolated β -cells, while HDL particles seems to be protective [106]. Interestingly, despite the role of cholesterol in β -cells is still debate, recent findings indicate it as an important modulator of β -cells function and survival. The disruption of cholesterol transport by reduced function of the ATP-binding cassette (ABC) transporters ABCA1 and ABCG1 results in increased fasting glucose levels and impaired glucose tolerance. The combined deficiency of ABCA1 and ABCG1 also leads to a significant islet inflammation, underlined by enhanced expression of IL-1 β and macrophage infiltration

[107]. More recently, also the liver X receptor (LXR) alpha, a receptor for cholesterol-related compounds, is demonstrated to be crucial for insulin secretion. LXR α , upregulating the sterol regulatory element-binding protein 1c (SREBP1c), has been demonstrated to interfere with glucose metabolism, ATP production and calcium channel flux in β -cells [103]. Hao et al. showed a new possible potential mechanism linking cholesterol with glucose homeostasis. They demonstrated that excess cellular cholesterol is directly linked to reduced GSIS and that normal secretion could be restored by cholesterol depletion. The cholesterol regulation of GSIS may involve modification of neuronal NO synthase (nNOS) and glucokinase (GK) activity through cholesterol-rich membrane microdomains on the insulin granules [108]. Moreover, considering that in β -cells insulin granules are the major sites of intracellular cholesterol accumulation, excess cholesterol is specifically delivered to granules, where it causes their enlargement and retention [109].

3.3.3 Inflammation and autoimmunity

The role of autoimmunity in T1DM has been long recognized, however reports have shown that about 10% of subjects with T2DM present diabetes-specific autoantibodies, with a higher percentage in young people. These evidences suggest a possible role of immune system also in the pathogenesis of T2DM. Although the mechanisms and the factors behind autoimmunity might be different, the immune-cell infiltration in pancreatic islets and the increased production of local cytokines are common of both types of DM [110]. β -cells are metabolically and immunologically up-regulated when functionally stressed by hyperglycemia. Indeed, in T2DM, chronic metabolic stress such as high levels of blood glucose and FFAs, induces an inflammatory response in β -cells, increasing the production of cytokines and chemokines. Among them, IL-1 β plays a crucial role, regulating in turn many other pro-inflammatory cytokines, cytotoxic factors and chemokines. IL-1 β also contributes to apoptosis and β -cells function impairment [111]. Additionally, adipose tissue-derived factors, such as pro-inflammatory adipokines, present local and systemic effects on metabolism and contribute to the chronic inflammatory process, which triggers β -cells death and is a risk factor for autoimmunity. Indeed, apoptotic β -cells may themselves present antigens and stimulate the development of an autoimmune response [92].

4. PCSK9

Proprotein convertase subtilisin kexin type 9 (PCSK9) is the ninth and last member belonging to a particular family of proteases known as the proprotein convertases (PCs), which includes 8 other members sharing identities to bacterial subtilisin and yeast kexin (PC1/3, PC2, Furin, PC4, PC5/6, Pace4, PC7 and SKI-1/S1P) [112]. PCSK9, originally called neural apoptosis-regulated convertase 1 (NARC-1), was discovered in primary cerebellar neurons, where it plays an important role in brain development as well as in cortical neuron differentiation. At the same time, Abifadel et al. identified two mutations in the PCSK9 gene associated with autosomal dominant hypercholesterolemia (ADH), in two French families without mutations in the candidate genes encoding LDL receptor (LDLR) and apolipoprotein B (apoB) [113]. Structural and functional studies revealed that the clinical output of these functional variations in PCSK9 gene were linked to an enhanced degradation of LDLR. These observations highlighted a strong association between PCSK9 and circulating levels of LDL-C and quickly other PCSK9 mutations were described around the world. The identification of both loss-of-function (LOF) mutations linked to low LDL-C levels and gain-of-function (GOF) mutations causing hypercholesterolemia, revealed that PCSK9 consistently contribute to the regulation of cholesterol homeostasis. Even if the frequency of PCSK9 mutations in patients affected by familial hypercholesterolemia (FH) is low (1–2%), these findings established PCSK9 as one of the most promising target for the development of new therapies in the treatment of hypercholesterolemia [3]. Nevertheless, further analysis on the global physiological function of PCSK9 still have to be evaluated, since this protein may have unknown roles beyond LDL-C lowering.

4.1 Structure, cellular biology and targets: focus on LDLR

Human PCSK9 gene is located on the small arm of chromosome 1p32 and contains 12 exons and 11 introns [114]. PCSK9 is initially synthesized as a 692-amino acid precursor (~75 kDa) which is composed of a signal peptide (aa 1–30), a prodomain (aa 31–152), a catalytic serine protease domain (aa 153–451) and a Cys- and His-rich C-terminal domain (CHRD; aa 452–692) [115]. PCSK9 zymogen shows an atypical activation pathway when compared with the 8 other members of PC family. After the cleavage of its signal peptide

in the ER, the zymogen proPCSK9 (aa 31–692) undergoes an autocatalytic intramolecular processing between Gln152 and Ser153, which is required for the release of the mature and active PCSK9 (~62 kDa) [3]. Indeed, has been recently described a mutation which prevents autocatalytic processing and PCSK9 secretion, associated with a 48% reduction in plasma LDL-C levels [116]. After cleavage, the prodomain remains tightly associated via hydrogen bonds to the catalytic site of the protein, preventing the access of other potential substrates to the catalytic pocket of PCSK9. Therefore the only known substrate of PCSK9 for proteolytic cleavage is itself and its activity is related to its binding to specific target proteins and to escort them toward intracellular degradation compartments [117] (Fig.6).

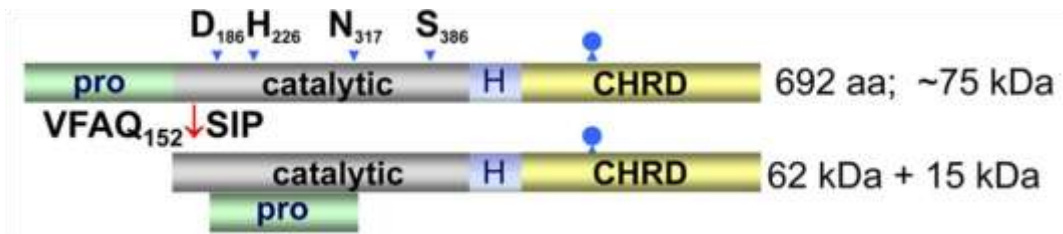


Figure 6. Schematic representation of proprotein convertase subtilisin kexin 9 (PCSK9) zymogen processing [3].

The first PCSK9 target to be identified is the LDLR at the surface of hepatocytes. Secreted PCSK9 binds the epidermal growth factor-A (EGF-A) domain of the LDLR *via* its catalytic domain, as well as the analogous domain discovered in other LDLR superfamily members (very low density lipoprotein receptor [VLDLR], apolipoprotein E receptor 2 [ApoER2] [118], cluster of differentiation 36 [CD36] [119] and lipoprotein receptor-related protein 1 [LRP1] [120]). Normally, the LDLR/LDL-C complex is internalized through clathrin heavy chain-coated vesicles and then proceeds to the endosomes, where the acidic pH causes the dissociation of the LDLR and its recycling to the cell surface, whereas the LDL-C is directed to lysosomes for degradation [121]. Conversely, when secreted PCSK9 binds the LDLR, the complex does not dissociate at acidic pH, but is rather more tightly associated and it is escorted to lysosomes for degradation [122]. The majority of attention has been

focused on the interaction between secreted PCSK9 and the cell-surface LDLR. However, it is probable that beyond the extracellular pathway, PCSK9 can induce the degradation of the LDLR via an intracellular pathway. Indeed, some degradation of the LDLR precursor was observed following PCSK9 overexpression, showing that the LDLR might interact with PCSK9 before its O-linked glycosylation in the Golgi apparatus [123, 124]. The presence of two different pathways is supported by a recent observation which reveals that PCSK9 lacking the M2 domain of the CHR1 domain can still degrade the LDLR intracellularly but not when added outside cells. However, both the intracellular and the extracellular LDLR degradation activities of PCSK9 require the presence of the CHR1 domain, necessary for the delivery of the PCSK9/LDLR complex to lysosomes. Whether these two pathways are functional in all tissues is still unknown [125] (Fig. 7).

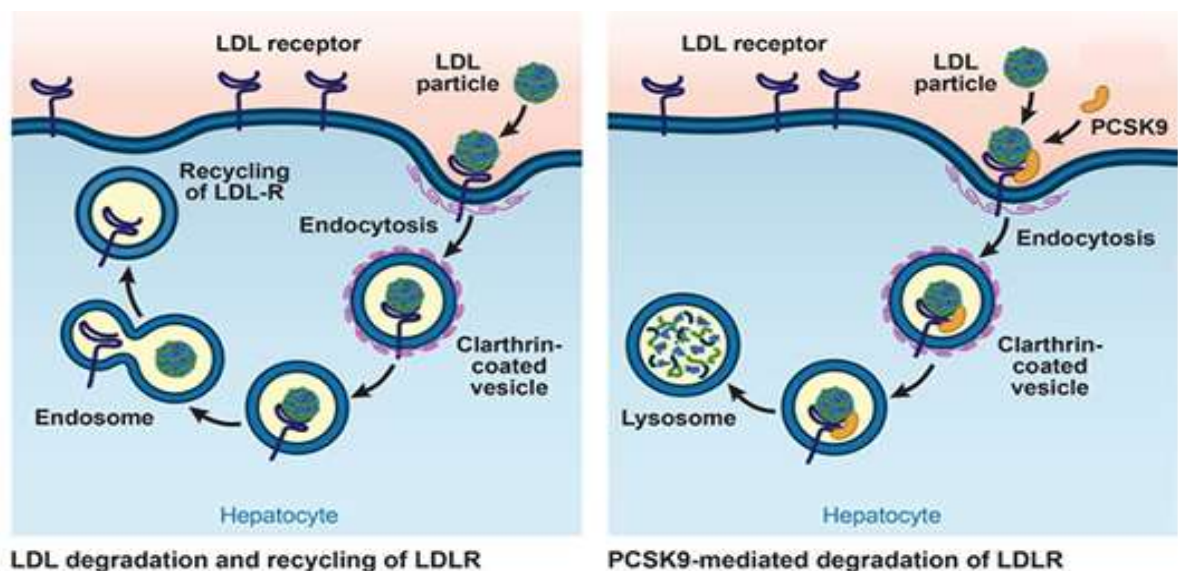


Figure 7. PCSK9-mediated degradation of LDLR. A complex of LDL-C, LDLR, and PCSK9 is internalized into hepatocytes into clathrin-coated pits and subsequently undergoes lysosomal degradation [126].

4.2 Regulation of PCSK9 expression and plasma levels

The regulation of PCSK9 expression is a quite complex process which, as it occurs with any other gene, begins at transcription. A tight scanning of the proximal promoter of the PCSK9 gene revealed that the promoter region carries a specificity protein 1 (Sp1) site, a hepatocyte nuclear factor 1 α (HNF1 α) site and two sterol-responsive elements (SREs) [127, 128]. Intracellular cholesterol content is the main factor that controls PCSK9 gene expression. SRE, the most conserved among the transcriptional motifs and the binding site for SRE-binding proteins (SREBPs), mediates the response of PCSK9 to cholesterol depletion, statins and SREBPs. PCSK9 expression is strongly downregulated by a high-cholesterol diet in mice and upregulated in transgenic mice overexpressing nuclear SREBP-1a or SREBP-2 [127, 129]. Accordingly, Dubuc et al. demonstrated *in vitro* that statins, which inhibit HMGCoA reductase, the rate-limiting enzyme in cholesterol biosynthesis, resulting in a feedback activation of nuclear SREBP-2, increased the level of PCSK9 mRNA in HepG2 [128]. Moreover, SREBP-1c is involved in postprandial insulin upregulation of PCSK9 gene expression in primary mouse and rat hepatocytes, as well as *in vivo*, during hyperinsulinemic-euglycemic clamp procedures performed on mice [130]. SREBPs activation of the PCSK9 gene promoter is enhanced by HNF1 α , which binds to an element residing 28 bp upstream from SRE. Recently, Li et al. provided evidence suggesting that HNF1 α site works cooperatively with SRE and that HNF1 α mutation reduced PCSK9 promoter activity >90% in transfected HepG2 cells [131]. Upregulation of HNF1 α expression by statins contributes to sustained PCSK9 production/secretion, which reduces the LDLR-mediated clearance of plasma LDL-C induced by these drugs, while its expression is downregulated by the natural hypocholesterolemic compound berberine [131, 132]. The PCSK9 promoter is also regulated by ligand-activated nuclear receptors, such as peroxisome proliferator-activated receptors (PPARs). Mice treated with the PPAR α agonist fenofibrate show a 50% decrease expression of hepatic PCSK9, in a PPAR α -dependent manner [133], while in humans PCSK9 plasma levels are slightly (8.5%), but significantly, reduced in diabetic patients upon fenofibrate treatment, paralleling a 13% reduction in LDLC levels [134].

PCSK9 mature protein also undergoes post-transcriptional modifications. PCSK9 is susceptible to the proteolytic cleavage by other members of the PCs family, such as furin

and PC5/6A, which cleave the mature PCSK9 at Arg218, generating a truncated protein (~55 kDa). The activity of this truncated protein is discussed, but studies in cultured hepatocytes and in furin hepatic conditional KO mice suggest that furin-cleaved PCSK9 is inactive. The natural gain-of-function mutations R218S, F216L and D374Y, associated with hypercholesterolemia, result in total or partial loss of furin/PC5/6A processing [135]. However, Lipari et al. recently demonstrated that circulating furin-cleaved PCSK9 is able to regulate LDLR and serum cholesterol levels, although somewhat less efficiently than intact PCSK9 [136].

Overall, beyond transcriptional and post-transcriptional regulation, the key concept is that PCSK9 expression is mainly regulated by variation of cholesterol levels. Throughout the day and in response to fasting and cholesterol depletion, circulating PCSK9 displays significant variation, probably related to oscillations in hepatic cholesterol content and consequent modification in cholesterol biosynthesis [137]. As a consequence, PCSK9 expression is consistently increased following cholesterol-lowering pharmacological treatments with agents such as statins [138], ezetimibe [139], or bile acid-binding resins [140]. In particular, statins induce SREBP-2 activity by inhibiting HMG-CoA reductase, which in turn increases hepatic LDLR expression and plasma LDL-C clearance. However, increased PCSK9 expression under these same conditions could attenuate statin efficacy by promoting LDLR degradation [141]. The effect of fibrates on circulating PCSK9 is still unclear, both reduced and increased PCSK9 levels were reported. Lambert and coworkers showed that plasma PCSK9 concentrations correlate with LDL-C and total cholesterol in diabetic patients and are decreased by fenofibrate treatment, while Costet et al. demonstrated that fenofibrate and atorvastatin increase circulating PCSK9 in diabetic patients, with no additive effect after 6 weeks of combined therapy [134, 142]. Finally, also the nutritional status and hormones such as glucagon, growth factor and sex hormones are surely involved in the regulation of PCSK9 plasma levels. Premenopausal women have higher PCSK9 levels when compared with men while in boys PCSK9 decreases during puberty, although the mechanisms are still unclear [143, 144].

4.3 PCSK9 targets beyond LDLR

PCSK9 binds the extracellular domains of a highly selective subset of transmembrane receptors and escorts them to lysosomes for degradation, through a mechanism that is independent of its proteolytic activity. Although the LDLR is no doubt the main studied target of PCSK9, probably due to its physiological relevance in modulating the levels of circulating LDL-C, PCSK9 targets other receptor members of the LDLR superfamily [3]. This family consists of structurally closely related transmembrane proteins, among which VLDLR and ApoER2 are the closest to LDLR (59% and 46% identity, respectively). Poirier et al. demonstrated that PCSK9 *in vitro* affects, in an LDLR-independent manner, the levels of both VLDLR and ApoER2 and that the gain-of-function D374Y mutant is more active in enhancing the degradation of these receptors [118]. *In vivo*, endogenous PCSK9 negatively regulates the levels of VLDLR in adipose tissue. The analysis of different mouse models reveals that this regulation is achieved by circulating, and not local, PCSK9. Indeed, liver-specific PCSK9 KO mice show a dramatic increase in adipose VLDLR protein, while the expression of PCSK9 in the liver of PCSK9 KO mice reverts this phenotype [145]. More recently, it has been discovered that PCSK9 enhances the degradation of LRP1 in mouse B16F1 melanoma cells and in Chinese hamster ovary (CHO) cells, although proof of this activity *in vivo* is still lacking. However, the observation that the LDLR is not sensitive to PCSK9 in B16F1 cells suggests a distinct targeting mechanism for these receptors [120]. CD36, a major receptor involved in transport of long-chain fatty acids and triglyceride storage, is also suspected to be a PCSK9 target in intestinal epithelial cells and adipose tissue. The overexpression of PCSK9 induces CD36 degradation and reduces the uptake of the palmitate analog Bodipy FL C16 and oxidized LDL in 3T3-L1 adipocytes and hepatic HepG2 cells, respectively [119].

Beyond transmembrane receptors, PCSK9 could improve the degradation of certain targets within the ER/ER-Golgi intermediate compartment, such as BACE1 (β -site amyloid precursor protein (APP)-cleaving enzyme 1) and ENaC (epithelial Na⁺ channel). BACE1 is transiently acetylated in the lumen of the ER/ER-Golgi intermediate compartment. The acetylated protein is able to reach the Golgi apparatus, while the nonacetylated one is retained and degraded in a post-ER compartment. PCSK9 contributes to the disposal of nonacetylated BACE1, enhancing the generation of amyloid β -peptide (A β) [146].

Moreover, within the ER/ER-Golgi intermediate compartment of epithelial cells of the renal collecting duct, PCSK9 induces the degradation of the ENaC, that is critical for Na⁺ homeostasis and blood pressure control [147].

4.4 Role of PCSK9 in extrahepatic tissues

Several experimental studies clearly show that the liver is simultaneously the key organ modulating PCSK9 plasma levels and the main target of PCSK9 activity, where it is involved in the binding and degradation of LDLR. However, PCSK9 is expressed in many extrahepatic tissues and organs, where it plays additional functions [1] (Fig. 8).

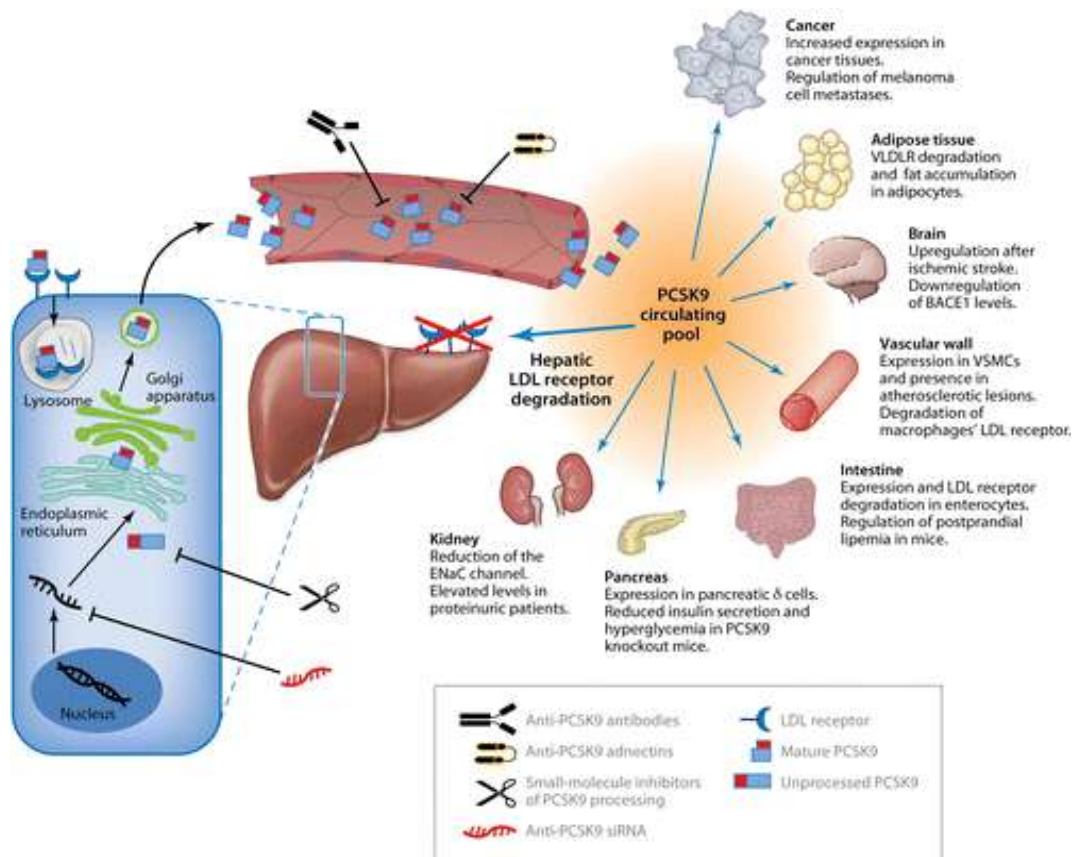


Figure 8. Extrahepatic targets of PCSK9 besides liver [1].

4.4.1 Brain

Despite PCSK9 was originally discovered in brain (NARC-1), its role in this tissue is still debate, with evidence of both pro-apoptotic effects and protective activities in the development of the nervous system. PCSK9 is highly expressed in cells with a significant proliferative index, including the embryonic brain telencephalon and cerebellum neurons, which present a higher recruitment rate of undifferentiated neural progenitor cells, when transfected to overexpress PCSK9 [148]. PCSK9 and LDLR are co-expressed in the telencephalon and cerebellum during active neurogenesis and in the rostral extension of the olfactory peduncle (RE-OP) of adult animals. Although the levels of LDLR are similar in the adult brain of PCSK9 KO and WT mice, PCSK9 is able to downregulate LDLR expression during brain development and following transient ischemic stroke. Of note, following experimental transient ischemic stroke in mice, PCSK9 is not expressed in the infarct and penumbra areas (suggesting that it may not play a role in cell death) but rather in the area where neurogenesis takes place [149]. Anyway, PCSK9 KO mice are viable, without any relevant alterations in the cerebellum, hippocampus or cortex, according to the observation that humans carrying complete LOF mutations of PCSK9 show no major neurological defects [150].

Cholesterol plays a key role in neuronal development as well as in brain function, and the reduction of plasma cholesterol levels to a large extent might negatively impact brain function. On the contrary, hypercholesterolaemia is considered an important risk factor for neurodegenerative diseases such as Alzheimer's disease (AD), and lipid-lowering therapies can reduce the risk to develop these pathological conditions. BACE1 (β -site amyloid precursor protein (APP)-cleaving enzyme 1) is the β -secretase enzyme required for the production of the neurotoxic β -amyloid (A β) peptide, which have a crucial early role in the etiology of AD. In vitro, PCSK9 overexpression leads to a reduction in endogenous BACE1 levels, whereas the down-regulation of PCSK9 by siRNA completely normalized the levels of BACE1. In vivo, PCSK9 KO mice showed higher levels of BACE1 and A β in the neocortex, suggesting that in the brain PCSK9 is able to regulate the metabolism of BACE1 and the rate of A β production [146]. However, in randomized clinical trials the treatment with PCSK9 mAbs is not associated with increased incidence of neurocognitive adverse events, as well as in PCSK9 LOF carriers [151-153].

Finally, PCSK9 has been identified to be up-regulated during apoptosis induced by withdrawal of potassium and serum in cultured cerebellar granule neurons (CGN). The transient overexpression of recombinant PCSK9 in CGNs is pro-apoptotic and only partially sensitive to caspase inhibitors, thus defining both a caspase-dependent and a caspase-independent component of PCSK9 pro-apoptotic effect [154]. On the contrary, PCSK9 overexpression promoted cell proliferation in a model of human neuroglioma, suggesting an anti-apoptotic effects in these cells [155]. Therefore, even if PCSK9 inhibitors are already used in the clinic for controlling plasma lipids, we are far from fully understanding the physiological role of this protein.

4.4.2 Pancreas

The link between PCSK9 and metabolic dysfunction goes beyond the modulation of the VLDLR in adipocytes, since PCSK9 is detectable also in mouse and human isolated pancreatic islets. Immunohistochemistry analysis showed that PCSK9 co-localizes specifically with somatostatin in human pancreatic δ -cells, while α - and β -cells apparently do not secrete detectable levels of PCSK9, although they respond to exogenously added PCSK9 [156]. Moreover, the LDLR is abundantly expressed in pancreatic β -cells in humans, mice and rats, where it plays a pivotal role in the uptake of plasma LDL [2, 157]. Cholesterol homeostasis is crucial for β -cells function and survival and excessive cholesterol accumulation causes a significant reduction in islets' ability to secrete insulin in response to glucose [108]. All these findings support the investigation of a possible involvement of PCSK9 in glucose homeostasis.

Mbikay and co-workers proved that old male PCSK9 KO mice express more LDLR in pancreatic islet cells, when compared with controls. The increased LDLR expression is paralleled with morphological abnormalities of pancreatic islets, although it is not clear whether this phenotype is correlated with impaired insulin secretion [158]. Indeed, contradictory results have been obtained in two different studies: one shows no effect of PCSK9 on insulin secretion and glucose tolerance [156], while the other reveals that PCSK9 KO mice are hypoinsulinaemic, hyperglycaemic and intolerant to glucose. In the latter study, PCSK9 KO islets present signs of malformation, apoptosis and inflammation [158]. These discrepancies are probably age dependent (8–10 weeks vs 4–5 months) and strain dependent (mice with different genetic background). However, as the

LDLR-cholesterol axis has been suggested to play a crucial role in modulating β -cell function and insulin secretion, a potential physiological role of PCSK9 in the pancreas cannot be excluded.

Also in humans data from carriers of PCSK9 LOF mutations, which present undetectable or very low levels of the circulating protein, are discordant. Some studies report no pancreatic dysfunction or increased incidence of diabetes in carriers compared to controls [153, 159], while others link PCSK9 LOF to an increased incidence of diabetes. The FH individuals carrying the PCSK9 InsLEU genetic variant (LOF) seem to be protected from major cardiovascular events but show increased occurrence of prediabetes and diabetes status [160]. In the cohort of the Dallas Heart Study, it has been shown a significant correlation among PCSK9 levels and fasting serum glucose, insulin and HOMA-IR [143], confirming the data obtained both in healthy volunteers and in a cohort of children [161, 162]. Moreover, Yang et al. established a positive correlation between PCSK9 levels and hemoglobin (Hb)A1c in T2DM patients, while not in patients without [163]. Interestingly, a genetic score consisting of independently inherited polymorphisms in the PCSK9 gene in more than 110.000 subjects, although resulting into reduced LDL-C levels and cardiovascular events, associates to increased risk of diabetes [164, 165]. Conversely, patients with familial hypercholesterolemia (decreased LDLR function) appear to have a lower risk of diabetes [166] (Fig. 9).

Regarding the clinical evidences, the effect of Alirocumab on the onset of new cases of diabetes has been evaluated in the ODYSSEY LONG TERM trial. No significant difference has been reported between the Alirocumab and placebo arms after a follow-up of 78 weeks [112]. In the OSLER-1 and OSLER-2 studies, conducted with Evolocumab, no measurable effects on glycemic parameters, including fasting plasma glucose, HbA1c and new-onset diabetes, have been showed after one year of treatment [167]. However, despite no evidence of PCSK9 inhibition effect on glucose metabolism, longer period and larger population could be necessary in order to reveal possible side effects. Indeed, the increased of T2DM observed with the use of statins was appreciated only after the analysis of several prospective and retrospective clinical trials.

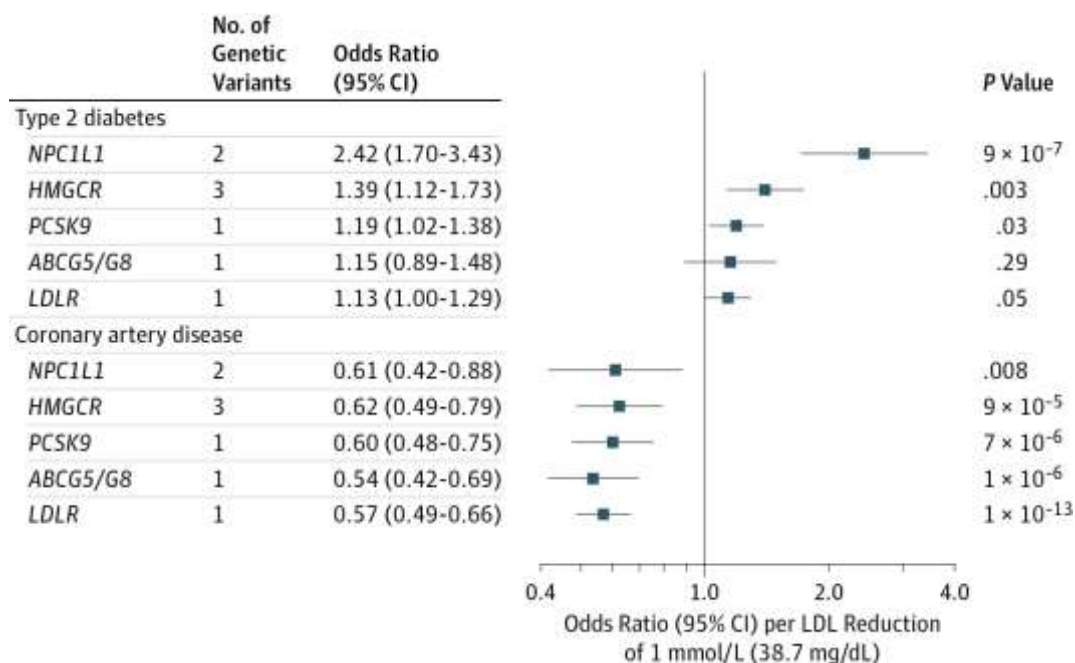


Figure 9. Association of Low-Density Lipoprotein Cholesterol (LDL-C)-Lowering Genetic Variants With Coronary Artery Disease and Type 2 Diabetes [165]

4.4.3 Vascular tissue

Beyond the extensively studied role of PCSK9 in liver, recent evidences report that PCSK9 is also present in human carotid atherosclerotic lesions. Among the cells of the artery wall, smooth muscle cells (SMCs) express significant levels of PCSK9, while its expression in endothelium cells (ECs) and macrophages is still debated [4]. The vascular expression of PCSK9 is notable higher in regions with low shear stress and is coupled with reactive oxygen species (ROS) production and inflammation [168].

In vascular SMCs PCSK9 is processed and released through a mechanism similar to the one described in hepatocytes. PCSK9 derived from SMCs is functionally active and capable of reducing LDLR expression at the surface of arterial macrophages, modulating the LDL accumulation in the artery wall. This finding suggests a possible role for PCSK9 in oxidized LDL (oxLDL) and foam cell formation and in atherogenesis, directly affecting the function of vascular cells [169]. Notably, siRNA directed against PCSK9 attenuates OxLDL-dependent apoptosis in endothelial cells, while OxLDL are able to induce the expression

of PCSK9 in these cells [170]. Denis et al. investigated the role of PCSK9 and LDLR on the atherosclerotic process in vivo, using WT, apoE KO and LDLR KO mouse models. They showed that PCSK9 deficiency ameliorates atherosclerosis in apoE KO mice by improving their lipid profile, but not in LDLR KO mice, proposing that the observed effect is dependent on the increased levels of LDLR in PCSK9 KO/apoE KO mice [171]. Moreover, two recent studies reported an association between serum PCSK9 levels and carotid intima media thickness (IMT), a surrogate marker of preclinical atherosclerosis, both in hypertensive and in FH patients. This correlation occurs independently of the plasma lipid profile and suggests that circulating PCSK9 may have an important role in early pathogenesis of the disease [172, 173]. Whether PCSK9 is expressed by macrophages is currently a subject of discussion. Murine J774A macrophages do not express PCSK9 [169], whereas Giunzioni and colleagues demonstrated that murine peritoneal macrophages secrete functional PCSK9 [174].

Anyway, systemic and local PCSK9 (by SMCs or macrophages) affects macrophages LDLR expression, while the absence of the LDLR mitigates the negative effect of PCSK9 on atherosclerosis and inflammation. Currently there are no studies that elucidate the potential role of PCSK9 in heart function. PCSK9 could indirectly affect cardiomyocytes by modulating the plasma concentrations of LDL-C and oxLDL, which effects on cardiomyocytes are less well reviewed as those to vascular cells [175].

4.4.4 Small intestine

Despite notable levels of PCSK9 mRNA are detectable in the small intestine and the intestine is a key player in maintaining cholesterol balance, the knowledge of the role of PCSK9 in this tissue is still partial. PCSK9 is highly expressed both in rat and mouse embryos and adult ileum and jejunum [148, 176], while in humans immunohistochemical analysis reveal that PCSK9 is present almost exclusively in the epithelial barrier of the duodenum and ileum, both in enterocytes and goblet cells [177]. Interestingly, Levy and coworkers have recently shown that in Caco-2/15 cells PCSK9 is secreted from basolateral site to the culture medium, suggesting that PCSK9 synthesized by the enterocytes may be released in the circulation [178].

As it occurs in liver, PCSK9 is able to trigger the degradation of the LDLR expressed at the basolateral surface of the enterocytes, modulating cholesterol homeostasis and chylomicron metabolism. Indeed, Caco-2/15 cells treated with exogenous PCSK9 show reduced levels of the LDLR on the basolateral membrane paralleled with increased cholesterol uptake and apoB48 synthesis and output [178]. The positive correlation between PCSK9 levels and apoB48 secretion observed in Caco-2/15 cells has been confirmed in *in vivo* studies. PCSK9 KO mice exhibit a significantly decreased postprandial triglyceridemia after olive oil gavage, caused by reduced lymphatic apoB48 and TG-rich lipoproteins output and by increased capacity to clear chylomicrons from the blood [177]. Although the LDLR is involved in this process, the chylomicrons clearance rate probably requires the ability of PCSK9 to target other receptors, such as the VLDLR and apoER2 [118].

The involvement of PCSK9 in the postprandial response was also investigated in humans, where Cariou et al. pointed out that heterozygous PCSK9 missense mutations may associate with profound hypobetalipoproteinemia. [179]. In addition, PCSK9 seems to affect intestinal cholesterol absorption. The addition of exogenous PCSK9 to cultured enterocytes reduce LDLR expression and cholesterol uptake from the basolateral media. Under these conditions, cholesterol uptake through the apical membrane is increased via the upregulation of cholesterol transporters (NPC1L1, CD36) [178].

4.4.5 Adipose tissue

Although PCSK9 is a key modulator of hepatic LDLR and circulating LDL-C levels, its involvement in the regulation of adipogenesis requires further investigation. In addition to the LDLR, PCSK9 is able to target other receptors of the LDLR superfamily, such as the VLDLR and ApoER2 [118]. The VLDLR, highly expressed on the adipocytes surface, plays a key role in the hydrolysis of triglyceride-rich lipoproteins, a critical step for fat storage in this tissue.

Interestingly, despite adipocytes do not express PCSK9, circulating PCSK9 negatively regulates the levels of VLDLR in adipose tissue. Indeed, together with a lower postprandial triglyceride levels, PCSK9 KO mice present adipocyte hypertrophy and a significant increased visceral adiposity. In particular, a detailed analysis demonstrated

that PCSK9 KO mice are characterized by a larger perigonadal (+70%) and perirenal (+90%) depots compared to WT littermates. Of note, this phenotype was demonstrated to be independent by the LDLR expression but rather to be mediated by the VLDLR and CD36 modulation [119, 145]. In humans, although a modest positive correlation between circulating PCSK9 levels and the BMI has been reported [143], specific studies aimed at analyzing the association between plasma PCSK9 and obesity are necessary to clarify the role of PCSK9 in adipogenesis. Interestingly, the levels of resistin, an adipose tissue derived adipokine, is inversely correlated with circulating PCSK9 in lean, but not obese, subjects, thus raising questions about the physiological relevance of resistin in the control of PCSK9 in vivo [180].

4.4.6 Kidney and adrenals

PCSK9 is abundantly expressed in renal tissues, but surprisingly it only marginally interferes with kidney and adrenals LDLR expression. This might be due to a lower local concentration of PCSK9 or to a different expression of cofactors necessary for PCSK9-dependent LDLR degradation. Adrenals are enriched in annexin A2, a natural endogenous inhibitor of PCSK9, which could prevent its function on the LDLR. Indeed, Anxa2-KO mice present double PCSK9 plasma levels and LDLR reduction by \approx 50% in some extrahepatic tissues, such as adrenals and small intestine but not in liver [181]. Another possibility is that the extrahepatic tissues, which do not respond to PCSK9, are unable to sort efficiently the PCSK9/LDLR complex to lysosomes, as recently shown in fibroblasts [182].

Nevertheless these tissues express reasonable amount of PCSK9, recommending a possible additional functions of PCSK9 beyond the regulation of LDLR expression and cholesterol homeostasis. The epithelial Na⁺ channel (ENaC) was lately identified as a PCSK9 target in the collecting duct of the kidney. PCSK9 regulates ENaC trafficking and cell surface expression through its ER degradation, suggesting that reductions in PCSK9 might result in increased Na⁺ renal absorption and increased risk of hypertension [147]. However, subjects carrying LOF mutations of PCSK9 do not exhibit increased prevalence of hypertension compared with non-carriers [183] and in studies with anti-PCSK9 mAbs no effect on blood pressure has been reported to date [152, 184]. Many studies have recently proposed a role for PCSK9 in the development of dyslipidaemia in renal pathologies. Subjects with renal failure and proteinuria present significant increased

PCSK9 plasma levels compared with matched healthy individuals [185], as well as patients with nephrotic syndrome. These subjects show elevated LDL-C levels, with a significant direct correlation with plasma PCSK9 concentrations, suggesting that increased PCSK9 can cause LDLR deficiency, which in turn contributes to the onset of hypercholesterolaemia [186]. Despite the physiological role of PCSK9 in kidney and adrenals is still not clear and it requires further investigation, these findings indicate that PCSK9 inhibition could be a therapeutic strategy for improving dyslipidemia associated with chronic kidney disease.

4.5 PCSK9-based therapy

After its discovery in 2003, PCSK9 was rapidly recognized as a key player in LDL metabolism, because of its ability to prevent the recycling of the LDLR to the hepatocytes surface. The crucial role of PCSK9 in lipid metabolism was disclosed performing genetic studies, which revealed a strong association between PCSK9 variants and alterations in cholesterol levels. GOF mutations in PCSK9 were identified to be involved in FH [187], while a range of LOF mutations resulted in reduced LDL-C levels and concomitant decreased risk of cardiovascular events [188]. Moreover, preclinical studies showed that statin-mediated LDL-C reduction, which occurs through increased LDLR expression on hepatocytes along with increased LDL turnover, is associated with induced PCSK9 expression. This increased expression and secretion of PCSK9 with statin therapy attenuates, at least in part, the LDL-lowering efficacy of statins and also of ezetimibe [128]. These observations suggest that PCSK9 inhibition may represent a promising therapeutic target for LDL-C lowering, also in statin-treated patients.

Since PCSK9 acts both intracellularly as a chaperone targeting the LDLR to the lysosomes and extracellularly by promoting LDLR internalization [189], the inhibition of both its synthesis and its interaction with the LDLR represents an attractive approach to obtain a lipid-lowering effect. The interaction between PCSK9 and the LDLR can be diminished by removing PCSK9 from the circulation (monoclonal antibodies and vaccines) or proposing alternative binding partners rather than LDLR (mimetic peptides or adnectins). Alternatively, the inhibition of PCSK9 can be performed at the expression level (CRISPR/Cas9 system, berberine, silencing RNA and oligonucleotides) [175]. To date the

best approach is related to the use of a monoclonal antibodies (mAb) against PCSK9, that block its binding to the LDLR via an allosteric mechanism. Thanks to the advance production technologies, it is now possible to generate humanized (bococizumab, LY3015014) or fully human (Evolocumab, Alirocumab) antibodies with a significant reduced immunogenicity compared with the antibodies of the early-generation [190] (Fig. 10).

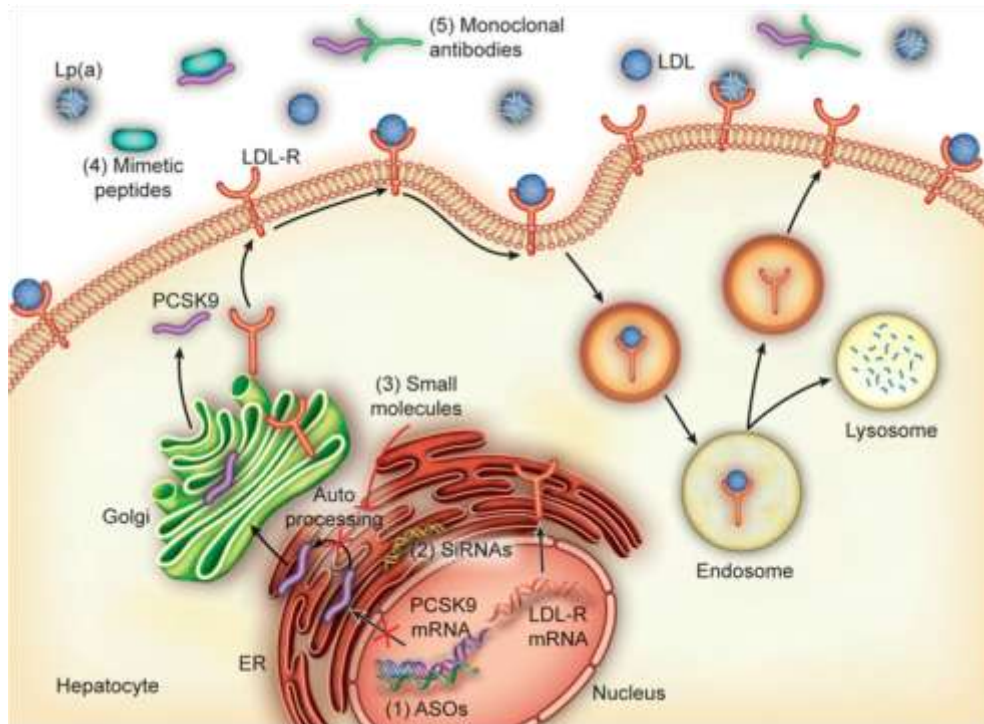


Figure 10. Metabolism of lipoproteins when therapies that target proprotein convertase subtilisin/kexin type 9 (PCSK9) are used [191].

4.5.1 CRISPR/Cas9 platform

The CRISPR/Cas system, found in approximately 40% of sequenced bacterial genomes, is an adaptive immune system that awards resistance against the invasion of foreign nucleic acids, including viruses and plasmids. Recently, a simple version of the CRISPR/Cas system, CRISPR/Cas9, has been modified to edit genomes. It includes a synthetic guide RNA (gRNA) linked to the Cas9, which delivers the complex to the cellular genome that can be cut at a desired location, removing the existing genes and/or adding new ones

[192]. Ding et al., using the CRISPR/Cas9 system to target PCSK9 in mouse liver, demonstrated that after the administration of the virus, the mutagenesis rate of PCSK9 in the liver is higher than 50%. This results in increased hepatic LDLR expression, decreased plasma PCSK9 levels and decreased plasma cholesterol levels (by 35-40%) [193]. In a study using FRG KO mice, which have chimeric-humanized liver, the treatment with CRISPR/Cas9 system to target the human PCSK9 gene induces a significant down-regulation of PCSK9 both in liver and in the circulation. This technique reveals an high on-target mutagenesis (around 50%) with a minimal off-target mutagenesis, yields important information on the efficacy and safety of CRISPR-Cas9 therapy [194]. Although the CRISPR/Cas9 platform targeting PCSK9, causing a permanent PCSK9 alteration, is a promising genome editing technology, many questions remain unresolved.

4.5.2 Antisense oligonucleotides (ASOs)

Antisense oligonucleotides (ASOs) are short, single-stranded, synthetic nucleotide sequences designed to specifically bind to a target messenger RNA (mRNA). This binding induces a selective degradation of the mRNA or prevents the translation of the selected mRNA into protein. ASOs are successfully deliver to the hepatic nucleus and have the ability to inhibit unique targets with high specificity [195]. Preclinical trials revealed that the administration of a second generation PCSK9 ASO (ISIS 394814) to high fat-fed mice for 6 weeks reduces total cholesterol and LDL-C by 53% and 38%, respectively, and the levels of PCSK9 mRNA by 92%. The inhibition of PCSK9 expression is associated with a 2-fold increase in hepatic LDLR protein levels [196]. Antisense oligonucleotides that contain at least one locked nucleic acid (LNA) present a higher binding affinity and specificity to mRNA. LNA ASOs reduce the mRNA and protein levels of PCSK9, with a concomitant increase in LDLR protein levels, both in cell lines (HepG2 and HuH7 cells) and mouse liver. In particular, the intravenous administration of LNA ASOs in mice leads to a significant reduction in PCSK9 mRNA levels (-60%). This effect lasts more than 16 days, as well as the twofold up-regulation of the hepatic LDLR protein levels [197]. Also when translated in non-human primates, this technology (LNA SPC5001 and LNA SPC4061) produces a very long lasting reduction of LDL-C, paralleled with an important decrease of both PCSK9 mRNA and protein levels [198]. Although the promising preclinical data, the first phase I clinical trials in healthy human subjects and individuals with FH were terminated early

(NCT01350960). SPC5001 was seen to cause mild to moderate injection site reactions and renal tubular toxicity. Kidney biopsy revealed multifocal tubular necrosis and signs of LAN accumulation, a damage reversible upon termination of SPC5001 treatment [199, 200]. Further development of SPC4061 was discontinued for undisclosed reasons. Therefore, even if ASOs present high affinity and specificity, the high production cost, the undesired side effects and the required routes for intravenous or subcutaneous administration limit its use in individuals with hyperlipidemia.

4.5.3 Small interfering RNA (siRNA)

Small interfering RNA (siRNA) is a class of double-stranded RNA molecules, 20-25 base pairs long, that interfere with the expression of specific genes with complementary nucleotide sequences, leading to the degradation of the mRNA after transcription, resulting in no translation. Delivery systems based on liposomes and lipid nanoparticles (LNPs) are the most commonly used nonviral vectors for siRNA delivery, both in academic studies and clinical trials [201]. Studies in mice and rats have reported that liver-specific siRNA silencing of PCSK9 is able to decrease the PCSK9 mRNA levels by 50–70% and the plasma LDL-C concentrations by 60%. Also in transgenic mice expressing human PCSK9, siRNAs silence the human PCSK9 transcript by >70%, with a significant reduction of the plasma protein levels. In nonhuman primates, siRNA mediated knockdown of PCSK9 is rapid, sustained and reversible and lasts for 3 weeks after a single intravenous administration. The reduced levels of circulating PCSK9 is paralleled with a decrease in apoB and LDL-C, without measurable effects on either HDL-C or TGs [202]. In humans, Fitzgerald and coworkers investigated the safety and efficacy of siRNA ALN-PCS, administered intravenously in healthy subjects with raised cholesterol who were not on lipid-lowering treatment. They showed a dose-dependent reduction in plasma PCSK9 and LDL-C levels, with the highest dose (0.4 mg/kg) conferring 70% and 40% reductions in PCSK9 and LDL-C levels respectively. ALN-PCS has a long lasting effect, sustained for 2–3 weeks after a single administration, and overall is well tolerated with side effects being similar to placebo [203]. More recently, has been tested the subcutaneous administered of ALN-PCS, both in single and multiple doses, in healthy volunteers with an LDL-C level of at least 100 mg/dl. In this phase I trial, no severe side

effects were observed and the doses of 300 mg or more (in single or multiple doses) is enough to reduce the levels of PCSK9 and LDL-C for at least 6 months [204].

4.5.4 Berberine and oleanolic acid

Despite small molecules have received considerable attention because of their low cost, the efforts to develop small-molecule inhibitors of PCSK9 have often been unsuccessful. However, other small molecules which directly inhibit PCSK9 expression, such as berberine and oleanolic acid, seem to be promising [205]. Berberine (BBR), usually found in the roots, rhizomes, stems and bark of several plants, is a quaternary ammonium salt from the protoberberine group of isoquinoline alkaloids. BBR is endowed with several pharmacological activities, including anti-microbial, glucose and cholesterol-lowering, anti-tumoral and immunomodulatory properties. BBR exerts its protective role in atherosclerosis increasing hepatic LDLR expression, due to increased LDLR mRNA stability, with a higher LDL uptake in BBR-treated cells [206]. While statins increase the expression of hepatic PCSK9, BBR has been shown to reduce PCSK9 mRNA and protein levels in HepG2 cells, in a time and dose dependent manner. This effect is not due to changes in the PCSK9 mRNA stability but most likely to an impaired transcription of the PCSK9 gene [207]. Indeed, BBR reduces the cellular levels of both hepatocytes nuclear factor 1 α (HNF1 α) and sterol regulatory element-binding protein 2 (SREBP2), which co-regulate the transcription of PCSK9. Although SREBP2 plays a key role also in LDLR transcription, it is not altered by the treatment with BBR, suggesting that the overall effect of BBR is in favor of the LDLR expression [131]. Recently, studies in mice and hamsters revealed that the administration of BBR to hyperlipidemic animals decreases both hepatic PCSK9 mRNA levels (-46%) and circulating PCSK9 concentrations (-50%), while significantly increases the LDLR protein in liver (+67%). Interestingly, hepatic HNF1 α protein levels result markedly reduced after the BBR treatment, while no difference in HNF1 α gene expression, suggesting a mechanism linked with an accelerated degradation of the protein [208].

Oleanolic acid (OA), widely distributed in food and plants, is a naturally occurring pentacyclic triterpenoid related to betulonic acid. OA presents several beneficial properties, such as antioxidative, anti-cancer, hepatoprotective, anti-inflammatory, hypolipidemic and anti-atherosclerotic effects [209, 210]. In db/db mice, the treatment

with OA improves lipid and lipoprotein metabolism, reducing serum TG, LDL-C, free fatty acids and hepatic lipid accumulation, while increasing circulating HDL-C. In vitro, OA decreases the levels of PCSK9 protein and mRNA in HepG2 cells, in a time and dose dependent manner. However, the underlying mechanism is still unknown and the OA efficiency is limited because of its low bioavailability and insolubility in water [205].

4.5.5 Anti-PCSK9 monoclonal antibodies (mAbs)

Monoclonal antibody therapy is a form of immunotherapy that uses monoclonal antibodies (mAbs) to specifically target certain cells or proteins. Therapeutic mAbs act through several mechanisms, such as blocking the activity of targeted molecules, inducing apoptosis in cells which express the target or modulating signalling pathways. Currently, PCSK9 mAbs, that bind to PCSK9 and allow the LDLR to recycle to its higher potential, represent the most advanced and promising class of PCSK9 inhibitors. Two fully-human PCSK9 mAbs, Alirocumab and Evolocumab, were approved by the FDA (US Food and Drug Administration) and the EMA (European Medicines Agency) in 2015. The humanized PCSK9 mAb Bococizumab was discontinued from further clinical development due to increased immunogenicity and limited LDL-C lowering in 2016. Actually, a third humanized PCSK9 mAb, LY3015014, is under development [211].

Alirocumab

Alirocumab (REGN727/SAR236553), which is marketed by Sanofi/Regeneron under the brand name Praluent, was studied both in phase I and phase II trials. The phase I trials revealed that Alirocumab is able to reduce, in healthy volunteers, LDL-C in a dose-dependent way (-65% at maximal doses), both after an intravenous and subcutaneous administration. In non-FH patients on atorvastatin and LDL > 100 mg/dL or with LDL > 130 mg/dL being managed by diet alone, Alirocumab reduces LDL-C up to 65% and up to 60% respectively [212]. The phase II trials, which studied the efficacy of Alirocumab in patients with FH, showed that the most efficacious regimen of 150 mg every 2 weeks (Q2W) reduces LDL-C up to 70%, paralleled with a significant reduction in apoB levels and increased HDL-C. Interestingly, in patients on statin therapy, the Alirocumab mediated LDL-C reduction is independent from different doses of atorvastatin (10 mg vs 80 mg) [213, 214].

The phase III randomized, double-blinded ODYSSEY trials were designed to evaluate Alirocumab for long-term safety, efficacy and adverse events and include data from different open label studies. CHOICE I trial was designed to evaluate Alirocumab in patients with poorly controlled hypercholesterolemia and showed that Alirocumab (300 mg every 4 weeks; Q4W) significantly reduces LDL-C both in statin-naive patients (-52%) and in patients on maximally tolerated statins (-59%), when compared to placebo. Similarly, COMBO I and II trials studied the effect of Alirocumab treatment in patients with LDL-C > 70 mg/dL and high cardiovascular risk on maximally tolerated statin therapy. COMBO I (316 patients) demonstrated that Alirocumab (75 mg Q2W, increased to 150 mg Q2W at week 12 if at week 8 LDL-C was ≥ 70 mg/dL) reduces LDL-C up to 50% after 24 weeks of treatment, compared to placebo. COMBO II (720 patients), comparing Ezetimibe (10 mg/die) to Alirocumab (75 mg Q2W) in patients on background statin therapy, showed that Alirocumab induces a 50% LDL-C reduction vs 20% reduction with ezetimibe at 24 weeks [215]. OPTIONS I trial randomized 355 patients with hypercholesterolemia and LDL > 70 mg/dL and found that the addition of Alirocumab (75 mg Q2W increased to 150 mg Q2W) to atorvastatin (20 mg/die or 40 mg/die) produced the greatest reduction in LDL-C as compared to addition of ezetimibe, doubling atorvastatin dose or switching to rosuvastatin [216]. OPTIONS II trial studied the association between Alirocumab and rosuvastatin using a similar protocol and obtaining results comparable with those obtained in OPTIONS I [184]. CHOICE II and ODYSSEY ALTERNATIVE evaluated Alirocumab in patients intolerant to statin therapy. In CHOICE II trial 241 patients with a history of statin intolerance demonstrated a 56% reduction in LDL-C when treated with Alirocumab (150 mg Q4W), while the ODYSSEY ALTERNATIVE trial (314 patients) showed a 45% reduction in LDL-C with Alirocumab (75 mg Q2W) as opposed to 15% reduction in LDL-C with ezetimibe (10 mg/die), at 24 weeks [217]. FH I and FH II trials were designed to evaluate a total of 735 patients (486 and 249, respectively) with heterozygous FH, insufficiently controlled on lipid lowering therapy. These trials showed that Alirocumab (75 mg Q2W, increased to 150 mg Q2W at 12 week if at week 8 LDL-C was ≥ 70 mg/dL) is able to reduce LDL-C levels by 48.8% (FH I study) and by 48.7% (FH II study), compared to placebo [218]. Finally, ODYSSEY LONG TERM trial, which was recently published, evaluated 2341 patients with hyperlipidemia on maximally tolerated statins and high risk for coronary heart disease (CHD). The patients treated with 150 mg

Alirocumab Q2W showed lower LDL-C by 62% at 24 weeks, compared to placebo. These results persisted at 78 weeks and the reduction in LDL-C appeared to be associated with reduction in the combined end-point of death from CHD, nonfatal MI, fatal or nonfatal ischemic stroke or unstable angina [112]. The ODYSSEY Outcomes trial (NCT01663402) is still ongoing and will assess the effects of Alirocumab on cardiovascular events in 18000 patients on maximally tolerated statin therapy, with results expected in February 2018 [219].

The side effects of Alirocumab have been evaluated on 2476 patients, that participate to the clinical trials mentioned above. The most common adverse effects observed with Alirocumab include nasopharyngitis, injection site reactions (erythema, itchiness, swelling, pain or tenderness), influenza, sinusitis, bronchitis, urinary tract infection, myalgia and muscle spasms. Alirocumab is contraindicated in patients who develop serious hypersensitivity reactions such as hypersensitivity vasculitis or allergic reactions, which require hospitalization. Among these adverse effects, the most common causes that lead to drug discontinuation are allergic reactions and elevated liver enzymes [219].

Evolocumab

Evolocumab (AMG 145), marketed by Amgen under the brand name Repatha, is a fully human monoclonal antibody inhibiting PCSK9. It has a molecular weight of 144 kDa and is usually administered by subcutaneous injection at a dose of 140 mg Q2W or 420 mg Q4W [205]. The phase I trials demonstrated that in healthy volunteers Evolocumab, administered both subcutaneously and intravenously, leads to a short-term dose-dependent reduction in LDL-C by up to 75% with a maximally dose of 420 mg, compared to placebo. Similar results were obtained in hypercholesterolemic statin-treated subjects, including those with heterozygous FH or taking the highest doses of atorvastatin or rosuvastatin. No serious adverse events occurred [220]. The phase II trials were subsequently performed to show the benefits of Evolocumab in LDL-C lowering when added to maximally tolerated statin therapy in patients with hypercholesterolemia (including FH). In LAPLACE-TIMI57 trial, 631 patients on stable statin therapy and LDL-C > 85 mg/dL were treated with Evolocumab 70 to 140 mg Q2W or 280 to 420 mg Q4W, obtaining an LDL-C reduction up to 65% and up to 50%, respectively [221]. The MENDEL trial studied Evolocumab, used as monotherapy, in 406 patients with

hypercholesterolemia. The optimal frequency of Evolocumab therapy was shown to be twice monthly to determine a 50% to 60% reduction in LDL-C, when combined with statins. However, when used as a monotherapy, also a frequency of one administration Q4W would be acceptable [222].

Evolocumab was subsequently evaluated in PROFICIO phase III program, which includes 14 trials performed in different populations. In LAPLACE-2 study, 1899 patients with fasting hyperlipidemia were randomized to a daily moderate or high intensity statin regimen and after 4 weeks further randomized to receive Evolocumab (140 mg Q2W or 420 mg Q4W) or placebo. After 12 weeks of treatment, Evolocumab reduces LDL-C levels by 75% (both on Q2W and Q4W regimen), when compared to placebo, both in moderate and high intensity statin groups [223]. MENDEL-2 trial compared the efficacy of biweekly (140mg) and monthly (420mg) Evolocumab with placebo and oral ezetimibe in 614 patients with fasting LDL-C ≥ 100 mg/dL and < 190 mg/dL and low risk on Framingham scale ($\leq 10\%$). Evolocumab treatment is able to reduce LDL-C by up to 57% more than placebo and 40% more than ezetimibe [151]. GAUSS-2 trial was designed to evaluate the efficacy and safety of subcutaneous Evolocumab compared to oral ezetimibe in hypercholesterolemic patients who are statin intolerant, predominantly due to muscle-related side effects. In this 12-week double-blind study, 307 patients were treated with Evolocumab (140 mg Q2W or 420 mg Q4W) and compared to daily oral or subcutaneous placebo (both placebo groups on 10mg ezetimibe). At 12 week, Evolocumab group showed a reduction in LDL-C by 56% vs 39% in the other groups (placebo + ezetimibe arm) [224]. Similarly, GAUSS-3 trial assessed the efficacy of Evolocumab in 218 statin intolerant patients, enrolled after an initial phase of the study which included administration of atorvastatin (20 mg) for 10 weeks vs placebo. The patients who experienced muscle related adverse effects received Evolocumab (420 mg Q4W, divided in 3 doses) vs ezetimibe (10 mg/die). After 24 weeks, LDL-C was reduced by 53% with Evolocumab compared to 17% with ezetimibe, with no difference in muscle related side effects [225]. DESCARTES trial evaluated 901 patients with hyperlipidemia, comparing subcutaneous administration of Evolocumab (420 mg Q4W) vs placebo, for a period of 52 weeks. The patients were under lipid lowering therapy, including diet alone, low intensity atorvastatin (10 mg), high intensity atorvastatin (80 mg) or atorvastatin 80 mg/die and

ezetimibe 10 mg/die. The treatment with Evolocumab resulted in significant LDL-C reduction in all groups [226]. RUTHERFORD-2 was a multicentre, randomised, double-blind and placebo-controlled trial, undertaken at 39 sites in different countries around the world. 329 patients with heterozygous FH were randomized to receive Evolocumab (140 mg or 420 mg) or placebo at two weekly and monthly regimens, respectively. Evolocumab treatment significantly reduces LDL-C with both regimens, as compared to placebo after 12 weeks [227]. While RUTHERFORD-2 evaluated efficacy and safety of Evolocumab in heterozygous FH, TESLA trial examined 50 patients with homozygous FH on stable lipid lowering therapy. Addition of Evolocumab (420 mg Q4W) leads to a significant reduction in LDL-C by up to 31%, vs placebo [228]. OSLER-1 (Evolocumab 420 mg Q4W) and OSLER-2 (Evolocumab 140 mg Q2W or 420 mg Q4W) confirmed, in 4465 patients, a very strong reduction in LDL-C with Evolocumab compared to standard therapy [229]. Recently, the results from the FOURIER trial have been presented. The study enrolled 27,564 patients with cardiovascular disease and on a moderate to high intensity statin therapy, in 49 countries. Most patients had a history of heart attack, ischemic stroke and symptomatic peripheral artery disease. Patients were assigned to receive subcutaneous injections of Evolocumab (140 mg Q2W or 420 mg Q4W) or matching placebo, showing that Evolocumab is able to reduce LDL-C by 59%, compared to control group. Interestingly, it was observed a statistically significant 27% reduction in heart attack and a 21% reduction in stroke, despite no effect on cardiovascular mortality by itself [175]. Finally, the TAUSSIG trial (NCT01624142) is still ongoing and is evaluating Evolocumab therapy in 300 patients with severe FH, with the results waited for March 2020 [219].

The side effects of Evolocumab are similar to those of Alirocumab.. The most common adverse effects are nasopharyngitis, upper respiratory tract infection, back pain and nausea, while the most common side effects which lead to drug discontinuation are myalgia, nausea and dizziness. In 2,4% individuals have been observed cardiac disorders including palpitations, angina pectoris and ventricular extra systoles. Anyway, the overall incidence of adverse effects with Evolocumab 140 mg Q2W as compared to placebo were 43,6% vs 41%, respectively. Notably, Evolocumab and Alirocumab have been associated with a higher incidence of cognitive adverse events in patients [219].

Bococizumab and LY3015014

Bococizumab (RN316) is a humanized anti-PCSK9 mAb developed by Pfizer for a longer serum half-life and duration of action on LDL-C lowering. Phase I studies demonstrated that single intravenous or subcutaneous administration of Bococizumab significantly reduces LDL-C in patients with hypercholesterolemia, both with and without concomitant atorvastatin therapy [219]. Gumbiner et al. in a phase II, randomized, placebo-controlled study evaluated the efficacy and safety of Bococizumab in hypercholesterolemic patients on statin therapy but not at target LDL-C. After 12 weeks of treatment they observed a 60% reduction in LDL-C, compared to placebo group. Of note Bococizumab is more potent than other LDL-C lowering mAbs, indeed several patients suspended the treatment after 4 weeks, due to LDL-C levels lower than 25 mg/dL [205]. Bococizumab had undergone the large phase III SPIRE, including SPIRE-HF trial (NCT01968980) in heterozygous FH, SPIRE-HR (NCT01968954) and SPIRE-LDL (NCT01968967) trials which are comparing Bococizumab to statin therapy in patients with high atherosclerotic cardiovascular risk, SPIRE-1 (NCT01975376) and SPIRE-2 (NCT01975389) collecting data on safety and efficacy of this drug [219]. The SPIRE program was planned to involve more than 30,000 subjects worldwide, in order to evaluate efficacy, safety, tolerability, magnitude of reduction in atherogenic lipids as well as in the occurrence of major CV events. However, in November 2016, Pfizer announced the discontinuation of the global clinical development program for bococizumab, due to an unanticipated attenuation of LDL-C lowering over time, as well as a higher level of immunogenicity and higher rate of injection-site reactions, compared to the other agents of this class [230].

LY3015014 (LY), a humanized immunoglobulin G4 (IgG4) monoclonal antibody, binds to a PCSK9 epitope that allows cleavage of the full-length active form of PCSK9 to the inactive form (52kDa), through protease cleavage at Arg218 in the catalytic domain. Preclinical and clinical studies demonstrated that LY binding to a site that permits normal proteolytic cleavage of PCSK9, resulting in a reduction of target-mediated drug disposition, increases potency and durability of the effect on LDL-C levels. Recently, Kastelein et al. showed that the administration of LY dosed Q4W (20, 120, or 300 mg) or Q8W (300 mg), in 527 patients with primary hypercholesterolaemia, resulted in robust and durable reduction of

LDL-C. No clinically relevant safety issues emerged with the administration of LY, although the long-term effects on cardiovascular outcomes require further investigation [231].

4.5.6 Vaccines

Despite mAbs based immunotherapies have significantly improved the treatment of several chronic diseases, they present faults that can limit patient access and clinical use. mAbs are relatively expensive, over the fact that they require to be injected frequently (once or twice a month) and at high doses (140 mg Q2W or 420 Q4W), resulting in tolerability issues and poor compliance. An appealing new alternative to mAbs is the active vaccination against self-antigens involved in chronic diseases. The aim is to provide the same therapeutic effects obtained with the passive administration of mAbs, but with considerably reduced administrations and lower doses, and without the possibility of inducing drug-neutralizing immune responses [232]. In 2012, Fattori et al. demonstrated that immunization with human recombinant PCSK9 in mice is able to raise antibodies that cross-react and neutralize circulating mouse PCSK9 protein. Preventing the PCSK9/LDLR interaction, they showed a considerable increased hepatic LDLR expression, paralleled with a reduction in plasma cholesterol levels, in the immunized mice compared to controls. Interestingly, these findings closely resemble those described in PCSK9 KO mice or in mice treated with anti-PCSK9 mAbs [233]. More recently, the AT04A anti-PCSK9 vaccine was evaluated for its therapeutic potential in improving or even preventing coronary heart disease in the atherogenic APOE*3Leiden.CETP mouse model. AT04A vaccine, when injected in mice fed with a western-type diet for 18 weeks in order to induce hypercholesterolemia and the development of atherosclerosis, reduces the total amount of cholesterol by 53%, atherosclerotic lesions in the aorta by 64%, and systemic and vascular inflammation, compared to unvaccinated mice [234]. In 2015, a phase I clinical study started at the Department of Clinical Pharmacology (Medical University of Vienna – Austria), studying AT04A and AT06A in 72 healthy people to evaluate its safety and activity. The study is expected to complete at the end of this year. Considering that the induced antibodies persist for months after a vaccination, if these findings translate successfully in humans, it could be developed a long-lasting therapy that just needs an annual booster, favouring an higher patient compliance [235].

4.5.7 Mimetic peptides

Mimetic peptides are small protein-like chains designed to mimic the structure of a target protein in order to affect its biological activity. Mimetic peptides have high specificity, are relatively easy to produce and are cheaper compared to antibodies, but their routes of administration are limited. Recently, this approach has been used to interfere with the ability of PCSK9 to interact with the LDLR. In particular, have been developed mimetic peptides towards EGF-A (the PCSK9 binding motif on the LDLR), the catalytic domain, the prodomain and the C-terminal domain of PCSK9 [205]. Shan et al. demonstrated that a synthetic EGF-A mimetic peptide is able to inhibit PCSK9-mediated degradation of LDLR in HepG2 cells, as well as mouse VLDLR and, at a lower rate, ApoER2 [236]. Similarly, another synthetic peptide mimicking the H306Y GOF mutation in the EGF-A domain block the binding of secreted PCSK9 to cell surface LDLR, thus successfully increasing LDLR expression in HepG2 cells [237]. Pep2-8, the smallest peptide that mimics the secondary structure of the EGF-A domain, covering the catalytic domain of PCSK9, restores LDLR recycling and LDL particle uptake in PCSK9-treated HepG2 cells [238]. Beyond mimetic peptides to EGF-A, Saavedra and coworkers have engineered a chimeric protein using the Fc-region of human IgG1 fused to the PCSK9 prosegment, which interacts with the prosegment and the catalytic domain of the PCSK9/prosegment complex and allosterically modulates its function. Moreover, considering that annexin-A2 is a natural extrahepatic inhibitor of the PCSK9-induced LDLR degradation, small mimetic peptides to annexin-A2 have been proposed as a potential approach for PCSK9 inhibition. Finally, the PCSK9 inhibitor SX-PCK9 (Serometrix), a small peptide that interferes with the normal PCSK9 folding and LDLR binding, is currently in preclinical development. Despite there are no clinical trials testing the use of small peptides to inhibit PCSK9 at this time, all these molecules directed against variable parts of PCSK9 could be an interesting approach for LDL-C lowering in the future [175].

4.5.8 Adnectins

Adnectins are a new family of therapeutic proteins derived from the 10th extracellular type III domain of human fibronectin, whose variable loops can be efficiently engineered. Because they are smaller compared to mAbs, adnectins can be simply modified to bind to their target protein (eg, PCSK9) with high specificity and affinity via transforming β -sheet loops, which preserve structural stability [239]. The high-affinity PCSK9-binding adnectin BMS-962476 (Bristol-Myers Squibb/Adnexus) was designed to target the LDLR binding site of PCSK9 and to prevent PCSK9-induced degradation of the LDLR. In hypercholesterolemic mice, which overexpress human PCSK9, a single intravenous injection of BMS-962476 is able to down-regulate both circulating PCSK9 and LDL-C levels. In cynomolgus monkeys the treatment with this adnectin reduces plasma PCSK9 levels to almost zero within 10 min, resulting in a reduction of LDL-C by approximately 55% within 48 h, an effect that persists for nearly 3 weeks. Although adnectins pharmacokinetic has been shown to be favourable with a rapid onset of action in preclinical models, further preclinical and especially clinical trials are needed to assess the possible development of this agent [240].

Aim of the project

PCSK9 is a protein, mainly synthesized and secreted by the liver, which binds to specific target proteins and escorts them towards lysosomes for degradation [1]. The best defined activity of PCSK9 is its ability to modulate the hepatic uptake of LDL-C, by enhancing the intracellular degradation of the LDLR [187]. In humans, several mutations in PCSK9 gene were described, both “gain-of-function” mutations associated to FH [113] and “loss of function” mutations linked to low LDL-C levels [183]. These findings suggest PCSK9 inhibitors as a promising class of drugs for the treatment of patients with severe hypercholesterolemia and/or at very high cardiovascular risk.

Although the liver is the main regulator and target of PCSK9 [148], it is synthesized also in other tissues, pointing to a possible role of this protein beyond the control of hepatic LDLR expression [4]. In particular, the LDLR is abundantly expressed by pancreatic β cells in humans, mice and rats, where it plays a key role in the uptake of plasma LDL-C [2]. Cholesterol homeostasis is crucial for β cells function and survival, and excessive cholesterol accumulation causes a significant reduction in islets’ ability to secrete insulin in response to increased glucose levels [108].

On these premises, the aim of this PhD project was to further investigate the extra-hepatic role of PCSK9. The increasing interest in anti-PCSK9 therapies raises the question of whether pharmacological inhibition of PCSK9 to treat hypercholesterolaemia and associated cardiovascular diseases might impact on non-hepatic tissues, including pancreas and β cells function. Indeed, despite the increasing number of observations, the debate on the exact roles of PCSK9 in extrahepatic tissues is still ongoing, and as very effective drugs inhibiting PCSK9 have become available to the clinician, a better understanding of the biological roles of PCSK9 is warranted. Interestingly, in three different mendelian randomization studies the analysis of the effects of genetic scores consisting of independently inherited polymorphisms in the PCSK9 gene resulted into reduced LDL-C levels and cardiovascular events but was also associated with an increased risk of diabetes [164, 165, 241]; furthermore patients with familial hypercholesterolemia (decreased LDLR function) appear to have a lower risk of diabetes [166]. These data set the stage for further investigating the role of PCSK9 on glucose metabolism and diabetes.

Materials and methods

1. Mice

B6;129Sv-Pcsk9tm1Jdh/J male mice from the Jackson Laboratory (Bar Harbor, ME, USA) were backcrossed to C57Bl6J females for 10 generations. Heterozygous mutant mice from the F10 generation were intercrossed to generate littermates WT and PCSK9 KO mice.

B6.129S7-Ldlrtm1Her/J male mice from the Jackson Laboratory (Bar Harbor, ME, USA) were backcrossed to PCSK9 KO females for 10 generations. Heterozygous mutant mice from the F10 generation were intercrossed to generate littermates LDLR KO and LDLR/PCSK9 DKO mice.

B6.Cg-Tg(Alb-cre)21Mgn/J male mice from the Jackson Laboratory (Bar Harbor, ME, USA) were backcrossed to PCSK9^{LoxP/LoxP} females (provided by Merck Research Laboratories) for 10 generations. Heterozygous mutant mice from the F10 generation were intercrossed to generate littermates AlbCRE-/PCSK9^{LoxP/LoxP} and AlbCRE+/PCSK9^{LoxP/LoxP}.

All the mice were kept under controlled light/dark cycle (12 hours of light/12 hours of dark) and temperature-controlled conditions (21°C). They had free access to food and water, except when fasting (overnight for GTT and fast and refeeding experiment, 4h for ITT) was required.

The investigation conforms to the European Commission Directive 2010/63/EU and was granted approval by the “Direzione Generale della Sanità Animale e dei Farmaci Veterinari” of the Italian Ministry of Health (402/2015-PR, 1162/2016-PR).

2. DNA isolation and genotyping

To identify the genotype of the mice pups the Polymerase Chain Reaction (PCR) technology was performed, followed by agarose gel electrophoresis. DNA for PCR analysis was obtained from ear punches (obtained at 21 days of age), a procedure required for the numbering and the identification of the mice. A 2 mm punch of mouse ear was placed in 0.5 mL of Lysis Buffer [0,5% SDS (Bio-Rad), 0.2 M NaCl (Sigma), 50 Mm Tris HCl pH 8 (Applichem), 4 Mm EDTA (Sigma)] with 25 µL of Proteinase K (10 mg/ml – Roche) for 18 at 56°. The addition of Phenol/Cloroform/Isoamyl alcohol 25:24:1 (500 µL) and subsequently of Ethanol 95%(800 µL) allowed the DNA precipitation, resuspended in 50 µL deionized sterilized water. The PCR reaction, performed with GeneAmp – PCR system 9700

machinery, was prepared using the GoTaq® Flexi DNA Polymerase kit (Promega) and the amplification parameters were set depending on the primers.

PCSK9 KO Primer 0	5'-GAT TGG GAA GAC AAT AGC AGG CAT GC
PCSK9 KO Primer 1	5'-ATT GTT GGA GGG AGA AGT ACA GGG GT
PCSK9 KO Primer 2	5'-GGG CGA GCA TCA GCT CTT CAT AAT CT
LDLR KO Fw Primer	5'-AAT CCA TCT TGT TCA ATG GCC GAT C
LDLR KO Rw Primer	5'-CCA TAT GCA TCC CCA GTC TT
LDLR KO Rw Primer 2	5'-GCG ATG GAT ACA CTC ACT GC
PCSK9 ^{LoxP/LoxP} Fw Primer	5'-GGA TAG TTC AGG GTT CAA AGC ATG GG
PCSK9 ^{LoxP/LoxP} Rw Primer	5'-GGT CTC CTC CAT CAG CAC CAC AAT G
AlbCRE Fw Primer	5'-AGG TGT AGA GAA GGC ACT CAG C
AlbCRE Rw Primer	5'-CTA ATC GCC ATC TTC CAG CAG G

All the primers were provided by Metabion International AG. Once the PCR is done, the agarose gel electrophoresis (1,5%) was performed to check the genotype of the pups, using GelStar™ Nucleic Acid Gel Stain (LONZA).

3. Dietary regimen

WT and PCSK9 KO mice, starting from 8 weeks of age, were fed with a Standard Fat Diet (SFD) or a High Fat Diet (HFD), as a model of diet-induced obesity, for 20 weeks. LDLR KO, LDLR/PCSK9 DKO, AlbCRE-/PCSK9^{LoxP/LoxP} and AlbCRE+/PCSK9^{LoxP/LoxP} mice, starting from 8 weeks of age, were fed with a Standard Fat Diet (SFD) for 12 weeks.

SFD (Research Diets, Inc)

Protein	19,2 g%	20 kcal%
Carbohydrate	67,3 g%	70 kcal%
Fat	4,3 g%	10 kcal%
Total	3,85 kcal/g	100 kcal%

Ingredients	Gm	Kcal %
Casein, 30 Mesh	200	800
L-Cystine	3	12
Corn Starch	452	18080.8
Maltodextrin 10	75	300
Sucrose	174	691.2
Cellulose, BW200	50	0
Soybean Oil	25	225
Lard	20	180
Mineral Mix S10026	10	0
DiCalcium Phosphate	13	0
Calcium Carbonate	5.5	0
Potassium Citrate, H ₂ O	16.5	0
Vitamin Mix V10001	10	40
Choline Bitartrate	2	0
FD&C Red Dye #40	0.04	0
Total	858.15	4057

HFD (Research Diets, Inc)

Protein	24 g%	20 kcal%
Carbohydrate	41 g%	35 kcal%
Fat	24 g%	45 kcal%
Total	4,13 kcal/g	100 kcal%

Ingredients	Gm	Kcal %
Casein, 30 Mesh	200	800
L-Cystine	3	12
Corn Starch	73	291
Maltodextrin 10	100	400
Sucrose	173	691
Cellulose, BW200	50	0
Soybean Oil	25	225
Lard	178	1598
Mineral Mix S10026	10	0
DiCalcium Phosphate	13	0
Calcium Carbonate	5.5	0
Potassium Citrate, H ₂ O	16.5	0
Vitamin Mix V10001	10	40
Choline Bitartrate	2	0
FD&C Red Dye #40	0.05	0
Total	858.15	4057

Both HFD and SFD were given for 12 or 20 weeks. The diet was administered 3 times a week and food intake was measured daily for 4 weeks during both the HFD and SFD treatment, to assess food consumption. Body weights were measured weekly.

4. Glucose Tolerance Test (GTT) and Insulin Tolerance Test (ITT)

GTT and ITT were performed after 12 and 20 weeks of SFD or HFD treatment. For the GTT, mice were fasted overnight (12-16h), weighed and blood glucose was measured by snipping the tail and using a glucose meter (ONE-TOUCH Ultra), before and 20, 40, 60, 120 min after intraperitoneal injection of glucose solution (2g/Kg body weight). For the ITT, mice were fasted for 4h, weighed and blood glucose was measured by snipping the tail and using a glucose meter (ONE-TOUCH Ultra). Insulin solution (0.2IU/kg body weight) was injected in the intraperitoneal cavity and mice were bled as described above after 20, 40, 60, 120 min. Insulin solution was prepared from stock of 100 UI insulin solution (Humuline R 100 UI/mL) and was diluted in a physiological solution (NaCl 0.9%) with 3% of bovine serum albumin (BSA Sigma-Aldrich). At the end of both GTT and ITT the tail wounds were cauterized and the mice were provided with food. The area under the curve (AUC) was calculated for glucose clearance following GTT or ITT.

5. Fasting and refeeding test

Fasting and refeeding experiments were performed at 12 or 20 weeks. Mice were fasted overnight (12-16h), weighted, housed one for cage and refeed ad libitum for 4h (food was weighted at the beginning of the test and after the 4h, to assess food consumption for each animal). Blood glucose was measured by snipping the tail and using a glucose meter (ONE-TOUCH Ultra), both in fasting state and after 4h refeeding.

6. Magnetic resonance for imaging (MRI)

MRI is a test that uses a magnetic field and pulses of radio wave energy to make pictures of organs and structures inside the body. The MRI was used to monitor fat accumulation in the visceral (VAT) and subcutaneous (SCAT) depots after 20 weeks of HFD or SFD, in WT and PCSK9 KO mice. Mice were anesthetize with isoflurane during the MRI analysis. The

identification of fat was allowed by the different amount of water of this tissue compared to muscles: fat depot appeared white while muscles black. A total of 16 pictures were taken from the visceral area; then the area of fat depot was measured in 3 pictures per mouse and the average calculated.

7. Plasma cholesterol and triglycerides measurement

Blood was collected at sacrifice in Eppendorf tubes containing EDTA 0.5%. Blood samples were centrifuged for 14 min at 7000 rpm at 4°C and plasma was collected and immediately stored at -20°C for assays.

Plasma cholesterol levels were measured with ABX Pentra Cholesterol CP kit and according to manufacturer instructions. The calibrator curve was prepared using serial dilution of a cholesterol standard (200 mg/dl - ABX Pentra). The same procedure was followed to detect plasma triglycerides, using the appropriate triglycerides standard (200 mg/dl - ABX Pentra) and reagents (ABX Pentra Triglycerides CP).

8. Insulin, C-Peptide and PCSK9 measurement

Blood was collected at sacrifice in Eppendorf tubes containing EDTA 0.5%. Blood samples were centrifuged for 14 min at 7000 rpm at 4°C and plasma was collected and immediately stored at -20°C for assays.

Insulin levels were measured in plasma with Mercodia Ultrasensitive Mouse Insulin ELISA and according to manufacturer instructions. Plasma insulin was measured also 5 min after intraperitoneal injection of glucose solution (2g/Kg body weight) and after a fasting and refeeding experiment, using blood collected from the tails. For insulin detection in pancreas Mercodia Mouse Insulin ELISA was used. Pancreas were processed in 350 µl of Tissue Protein Extraction Reagents (Thermo Fisher Scientific) containing a cocktail of protease and phosphatase inhibitors (Roche Diagnostics). C-peptide levels were measured in plasma with Mercodia Ultrasensitive Mouse C-peptide ELISA and according to manufacturer instructions. PCSK9 was measured on plasma aliquots collected after overnight fasting and stored at -80°C for up to three weeks by a commercial enzyme-linked immunosorbent assay (ELISA) kit (R&D Systems, Minneapolis, MN). Plasma samples were diluted 50 times and then processed as per manufacturer instructions.

9. Western Blot Analysis

Total cytosolic protein extracts from liver and soleus muscle were obtained by lysing tissues in 350 μ l of Tissue Protein Extraction Reagents (Thermo Fisher Scientific) containing a cocktail of protease and phosphatase inhibitors (Roche Diagnostics). Twenty μ g of proteins and a molecular mass marker (Novex[®] Sharp Protein Standard, Invitrogen[™]; Life Technologies Europe BV) were separated on 4-12% sodium dodecylsulfate-polyacrylamide gel (SDS-PAGE; Novex[®] NuPAGE[®] 4-12% Bis-Tris Mini Gels, Invitrogen[™]; Life Technologies) under denaturing and reducing conditions and then transferred to a nitrocellulose membrane by using the iBlot[™] Gel Transfer Device (Invitrogen[™]; Life Technologies). The membranes were washed with Tris-Buffered Saline-Tween 20 (TBS-T) and non-specific binding sites were blocked in TBS-T containing 5% (BSA; Sigma-Aldrich) for 90 min at RT. The blots were incubated overnight at 4°C with anti-pAKT, (1:150; Millipore) or anti-AKT (1:1,000; Cell Signaling) (5% BSA or non-fat dried milk). Membranes were washed with TBS-T and then exposed for 90 min at RT to a diluted solution (5% non-fat dried milk) of the secondary antibodies. Immunoreactive bands were detected by exposing the membranes to Clarity[™] Western ECL chemiluminescent substrates (Bio-Rad Laboratories) for 5 min and images were acquired with a ChemiDoc[™] XRS System (Bio-Rad Laboratories). Densitometric readings were evaluated using the ImageLab[™] software.

10. Immunofluorescence staining and analysis

For morphological studies, pancreases from wild type and transgenic mice were collected after sacrifice and fixed in 4% (w/v) neutral-buffered formalin, processed and embedded in paraffin blocks. After microwave antigen retrieval (2x5 min in 10 mM citrate buffer, pH 6.0), 5- μ m-thick sections were incubated for two hours with primary antibodies against hormones. The following antibodies were used: anti-insulin polyclonal from guinea pig (Dako; diluted 1:300), anti-glucagon polyclonal from rabbit (R&D Systems, Minneapolis, MN, USA; diluted 1:150), and anti-somatostatin monoclonal from rat (Millipore, diluted 1:100), anti-LDLR (Abcam, diluted 1:300), anti PCSK9 (Cayman, diluted 1:50). Staining with primary antibody was followed by incubation for one hour with rhodamine-

conjugated anti-guinea pig IgG, FITC-conjugated anti-mouse, Cy5-conjugated anti-rabbit and Cy5 or FITC-conjugated anti-rat IgG (Jackson ImmunoResearch Laboratories).

11. Image acquisition and analysis

Microscopic analysis was performed using a Zeiss (Oberkochen, Germany) Axiovert 200 inverted fluorescence microscope equipped with a Retiga SRV charge-coupled device camera (QImaging, Surrey, BC, Canada). Briefly, single-stain wildfield immunofluorescence images were acquired using identical parameters (acquisition time and gain), deblurred using the Nearest Neighbor algorithm (Image ProPlus 6.2 3D Analyser; Media Cybernetics, Rockville, MD) and merged. To quantify the islet's area and composition on digital images, the islet profile was manually outlined and a macro was created in order to automatically quantify the green (somatostatin)-, red (insulin)- and blue(glucagon)-stained areas within the islet regions. For islet composition, single hormone staining was expressed as a percentage of total islet area (insulin+glucagon+somatostatin-stained areas). For each subgroup, a minimum of five islets per pancreas were imaged, in six different animals. Experiments were performed in duplicate.

12. Pancreatic islets isolation and FACS analysis

Islets were isolated from wild type and transgenic mice by injection of 4 ml type II collagenase solution (1 mg/mL, Sigma-Aldrich) within the pancreas. After surgical excision of the pancreas, it was incubated at 37 °C for 10 min and then washed 3 times in minimum essential medium (MEM, Sigma) to remove collagenase. Undigested tissue was removed using a 70 µm filter. Pancreatic islets were separated by Percoll PLUS gradient (GE Healthcare Europe, Milan, Italy), collected and processed for flow cytometry analysis. Antibodies for FACS were used at 1:200 dilutions unless otherwise specified, optimal antibody concentrations for staining were calculated based on manufacturer instructions. Cells from pancreatic islets were suspended in 100 µL of PBS/BSA 5% and incubated with 0.5 µL of Fc block (BD Pharmingen, purified Rat anti-Mouse CD16/CD32, Cat#553142) and with primary antibody against LDLR (Cayman LDL Receptor Polyclonal Antibody, Cat#10007665) for 30 minutes at 4°C. Samples were washed twice with PBS/BSA 5% and

re-suspended in 100 μ L of PBS/BSA 5% with goat anti-rabbit IgG secondary antibody Alexa Fluor 633 (ThermoFisher Scientific, Cat#A-21070) and incubated for 30 minutes at 4°C. After two wash with PBS/BSA 5%, samples were diluted in 500 μ L of PBS/BSA 5% and acquired with Novocyte (ACEA biosciences) and analyzed using Novoexpress 3000 (ACEA biosciences).

13. Cholesterol and fatty acid content in pancreatic islets

Pancreatic islets' homogenates, after thawing and addition of stigmasterol, nonadecanoic acid and cholesteryl heptadecanoate as internal standards, were extracted three times with CHCl₃/CH₃OH 2:1 plus KCl 0,05%. The lipid layers were collected, concentrated and loaded onto a TLC (hexane:diethylether:acetic acid 80:20:1). After run and spraying with dichlorofluorescein, the spots corresponding to FC, FFA and CE were removed and processed as follows. Those containing FC were extracted twice with hexane/isopropanol 3:2, concentrated and detected by gas-liquid chromatography (DANI 1000 equipped with a HTA autosampler; column MEGA FFAP EXT) without derivatization at a constant temperature of 260°C for 10 minutes. The spots containing CE and FFA were derivatized by methanolic HCl 3N for 20-120 minutes at 80°C, extracted by hexane/water and their fatty acid content analyzed by GLC (same equipment as before, with temperature raising from 120 to 260 °C, total run 40 minutes).

The mass of FC was calculated by comparing its AUC with that of the internal standard (stigmasterol), while those of FFA and CE was obtained after summing the AUC of their fatty acids and comparison with that of nonadecanoic acid (FFA) or cholesteryl heptadecanoate (CE). In the case of CE and FFA, obviously also a qualitative profile is available. Each lipid mass was then normalized by sample protein content, evaluated by the bicinchoninic acid, and expressed as ug lipid/mg protein.

14. RNA isolation and real time quantitative polymerase chain reaction (RT-PCR)

RNA was isolated from pancreatic islets (20 mg) collected as described above, using NucleoSpin RNA kit (MACHEREY-NAGEL). 0,5 – 1 ng of RNA was reverse transcribed with iScript™ Reverse Transcription Supermix for RT-qPCR (BioRad), according to manufacturer

instructions. 2 μ L of cDNA were amplified by realtime quantitative PCR with 1X Syber green universal PCR mastermix (BioRad, Italy). The specificity of the Syber green fluorescence was tested as described [242]. Each sample was analyzed in duplicate using the CFX-Cycler (BioRad). The PCR amplification was related to a standard curve ranging from 10⁻¹¹ mol/L to 10⁻¹⁴ mol/L and data were normalized for the housekeeping gene ribosomal protein L13a (RLP13a) [243].

ABCA1 Fw Primer	5'-GGTTTGGAGATGGTTATAACAATAGTTGT
ABCA1 Rw Primer	5'-TTCCCGGAAACGCAAGTC
ABCG1 Fw Primer	5'-TTCATCGTCCTGGGCATCTT
ABCG1 Rw Primer	5'-CGGATTTTGTATCTGAGGACGAA
LXR Fw Primer	5'-CGACAGAGCTTCGTCCACAA
LXR Rw Primer	5'-GCTCGTTCCCCAGCATTTT
SREBP2 Fw Primer	5'-TGACTAAGTCCTTCAACTCTATGATTTTG
SREBP2 Rw Primer	5'-GCGGCAAACACACAATATCATTG
HMGCoA Fw Primer	5'-TGTGGTTTGTGAAGCCGACAT
HMGCoA Rw Primer	5'-TACACCATAGCTCCGTAGTTGTC
ACAT1 Fw Primer	5'-TGGCACGAATTGCAGCAT
ACAT1 Rw Primer	5'-GCAGGCGCAAGTGGAAAA
LDLR Fw Primer	5'-GTGTGACCGTGAACATGACTG
LDRL Rw Primer	5'-CACTCCCCACTGTGACACTTGA

15. Statistical analysis

For animal studies, statistical analyses were performed with GraphPad Prism6 or with IBM-SPSS statistic 19. Data were analyzed by the Wilcoxon rank-sum test or by ANOVA with repeated measures for main effects of treatment time and genotype, followed by a Bonferroni post hoc analysis. Data are presented as mean \pm SEM. A P value <0.05 was considered statistically significant.

Results

1. Setting of a mouse model of obesity and metabolic dysfunction

Weight gain, lipid profile and fat distribution

In order to setting an animal model of metabolic dysfunction, C57BL/6 WT mice were fed a SFD or HFD for 20 weeks. We assessed whether a lipid-rich diet causes alterations in metabolic parameters evaluating plasma lipid profile, body weight, fat distribution and glucose homeostasis.

Starting from the 10th week of diet, mice fed a HFD gained more weight compared to littermates fed a SFD, difference that became significant during the last weeks (13.1 ± 1.9 g vs 7.55 ± 0.6 g, 20 weeks, $p < 0.05$) (Fig 1A). At the end of the 20 weeks of diet, also the total body weight of mice fed a HFD resulted strongly increased compared to controls (37.2 ± 2.4 g vs 29.7 ± 2.6 g, $p < 0.05$). Despite this, food intake was measured daily and no difference occurred between the two experimental groups (Fig. 1B).

As expected, mice fed a HFD showed a significant increase in both circulating cholesterol and triglycerides levels, compared to mice fed a SFD (123.4 ± 5.3 mg/dl vs 79.8 ± 11.0 mg/dl and 61.6 ± 3.7 mg/dl vs 38.6 ± 4.2 mg/dl, respectively, $p < 0.05$) (Fig. 1C/1D).

Regarding the fat distribution, we evaluated both the visceral adipose tissue (VAT) and the subcutaneous adipose tissue (SCAT) accumulation. Mice fed a HFD presented a significantly increased VAT accumulation when compared to mice fed a SFD (+55%, $p < 0.05$), as well as an enhanced SCAT content (+65% vs SFD, $p < 0.05$) (Fig. 1E). Interestingly, also the MRI axial views showed a different fat distribution in the abdomen of SFD WT mice and HFD WT mice (Fig. 1F).

Glucose metabolism

To evaluate the effect of a lipid-rich diet on glucose metabolism, we performed GTT after 12 weeks of SFD or HFD. In spite of similar plasma glucose levels at baseline (o/n fasting), following i.p. glucose injection (2g/Kg body weight), C57BL/6 WT mice fed a HFD showed a significant increased glycemia, compared to those fed a SFD (Fig. 2A). The increase of the plasma glucose AUC confirmed the delay in glucose clearance in HFD WT mice,

compared to control group (AUC +50% vs SFD; $p < 0,05$) (Fig. 2B). GTT was performed also after 20 weeks of diet, obtained similar results (Fig. 2C/2D).

Once shown that a lipid-rich diet is associated with an impaired glucose tolerance in our experimental groups, we investigated whether this effect was the consequence of an impaired insulin tolerance. ITT (4h fasting) was performed in C57BL/6 WT mice, after 12 weeks and 20 weeks of SFD or HFD. The decrease in plasma glucose levels, after i.p. insulin injection (0.2IU/kg body weight), was significantly lower in mice fed a HFD, compared to mice fed a SFD, suggesting the presence of insulin resistance under a lipid-rich diet state (Fig. 2E/2F).

The observation that mice fed a HFD developed alterations in weight gain and lipid metabolism, paralleled with impaired glucose tolerance and insulin resistance, confirmed that we successfully set a mouse model of obesity and metabolic dysfunction.

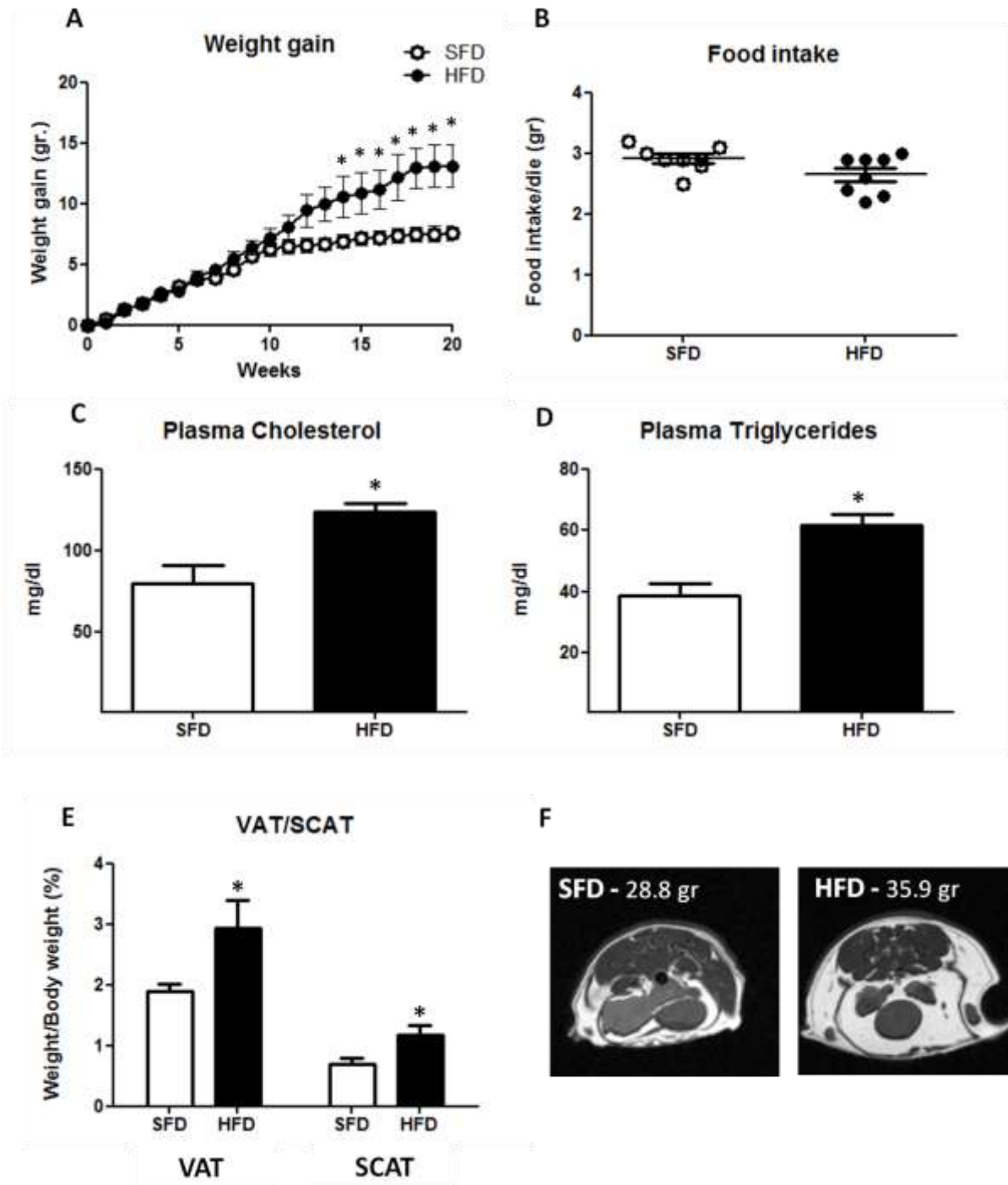


Figure 1. Weight gain and daily food intake of C57BL/6 WT mice fed a standard fat diet (SFD) or high fat diet (HFD) are shown in panel A and B. Panel C and D show the levels of circulating cholesterol and triglycerides of mice fed with SFD or HFD. Weight of visceral adipose tissue (VAT) and subcutaneous adipose tissue (SCAT) is presented in panel E. Weight of each adipose tissue was normalized by total body weight. Data are shown as means \pm SEM; n=8 mice per group; *p<0.05. Panel F reports representative magnetic resonance imaging axial views of C57BL/6 WT fed with SFD or HFD.

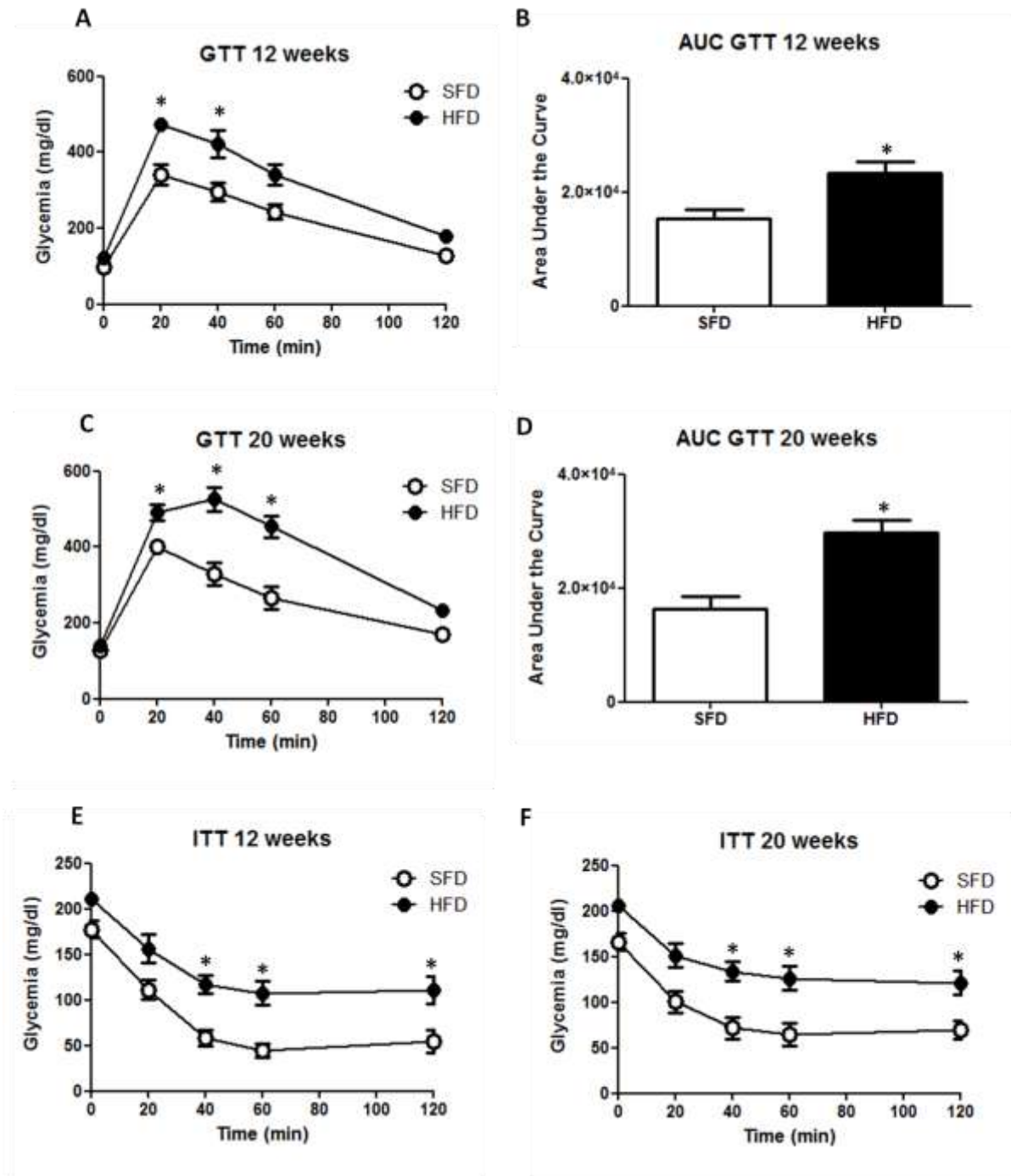


Figure 2. IPGTT was performed and plasma glucose levels were measured at 0, 20, 40, 60, and 120 mins. Data in mice fed a SFD or HFD for 12 weeks or 20 weeks and the AUC for glucose are presented in panels A to D. IPITT was performed and plasma glucose levels were measured at 0, 20, 40, 60, and 120 mins. Data in mice fed a SFD or HFD for 12 weeks or 20 weeks are presented in panels E and F. Data are shown as means \pm SEM; $n = 8$ mice per group. * $p < 0.05$.

2. Impact of PCSK9 deficiency on lipid metabolism and ectopic fat accumulation

Once characterized our mouse model, we focused on the metabolic role of PCSK9, both in a physiological condition (SFD) and in a state of obesity and metabolic syndrome (HFD). Weekly weigh gain and daily food intake of WT and PCSK9 KO mice, fed a SFD or HFD for 20 weeks, were recorded. Interestingly, the absence of PCSK9 did not impact neither the weight gain or the food intake, with both diets (Fig. 3A to 3D).

Plasma cholesterol and triglycerides levels were measured in all experimental groups. Firstly, we confirmed the difference between mice fed a SFD and mice fed a HFD shown in the characterization of the model ($p < 0.05$). Moreover, as expected, PCSK9 KO mice exhibited significantly lower plasma cholesterol levels compared to WT mice (51.8 ± 6.3 vs 81.2 ± 9.1 mg/dl and 86.1 ± 4.7 mg/dl vs 118.6 ± 7.2 mg/dl, SFD and HDF respectively, $p < 0.05$), while no difference in plasma triglycerides concentrations arose both with SFD and HFD (Fig. 3E and 3F).

WT and PCSK9 KO mice presented a different fat distribution in the abdomen, with both diets. Specifically, PCSK9 deficiency was associated with a significantly increased VAT accumulation when compared to WT littermates (+20% with SFD, +50% with HFD), while no differences were observed in SCAT (Fig. 4A/4B). Representative MRI images of the fat distribution in the abdomen of WT and PCSK9 KO mice are reported in Fig 4C.

Here we showed that PCSK9 deficiency, which results in reduced circulating cholesterol levels, is associated with an increased ectopic fat accumulation, both in a physiological condition and in a state of metabolic dysfunction. This observation raises the question of a possible role of PCSK9 in modulating lipids delivery and accumulation in peripheral tissues.

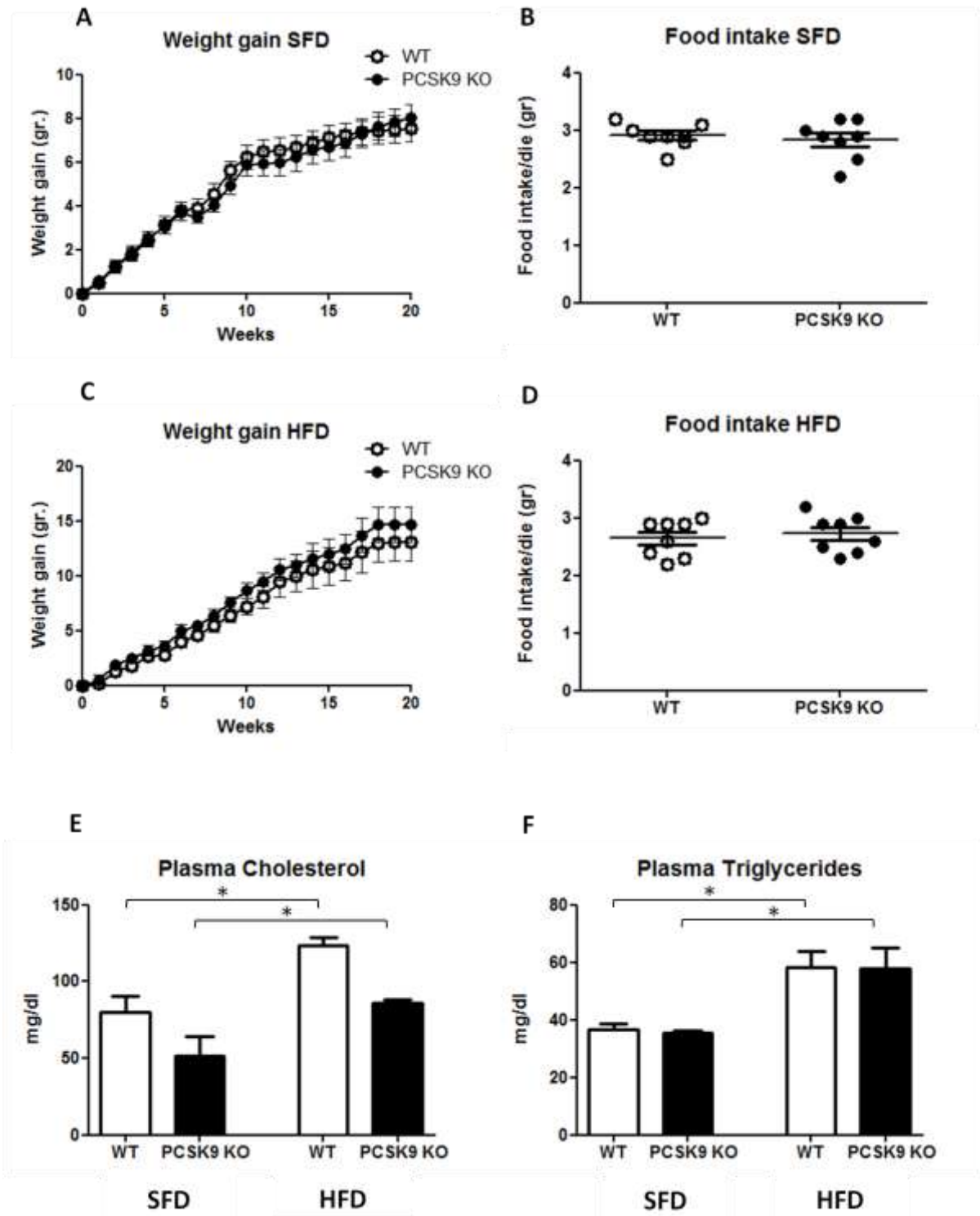


Figure 3. Weight gain and daily food intake of WT and PCSK9 KO mice fed a standard fat diet (SFD) or high fat diet (HFD) are shown in panels A to D. Panel E and F represent the levels of circulating cholesterol and triglycerides of WT and PCSK9 KO mice, fed a SFD or HFD for 20 weeks. Data are shown as means \pm SEM; n=8 mice per group; *p<0.05.

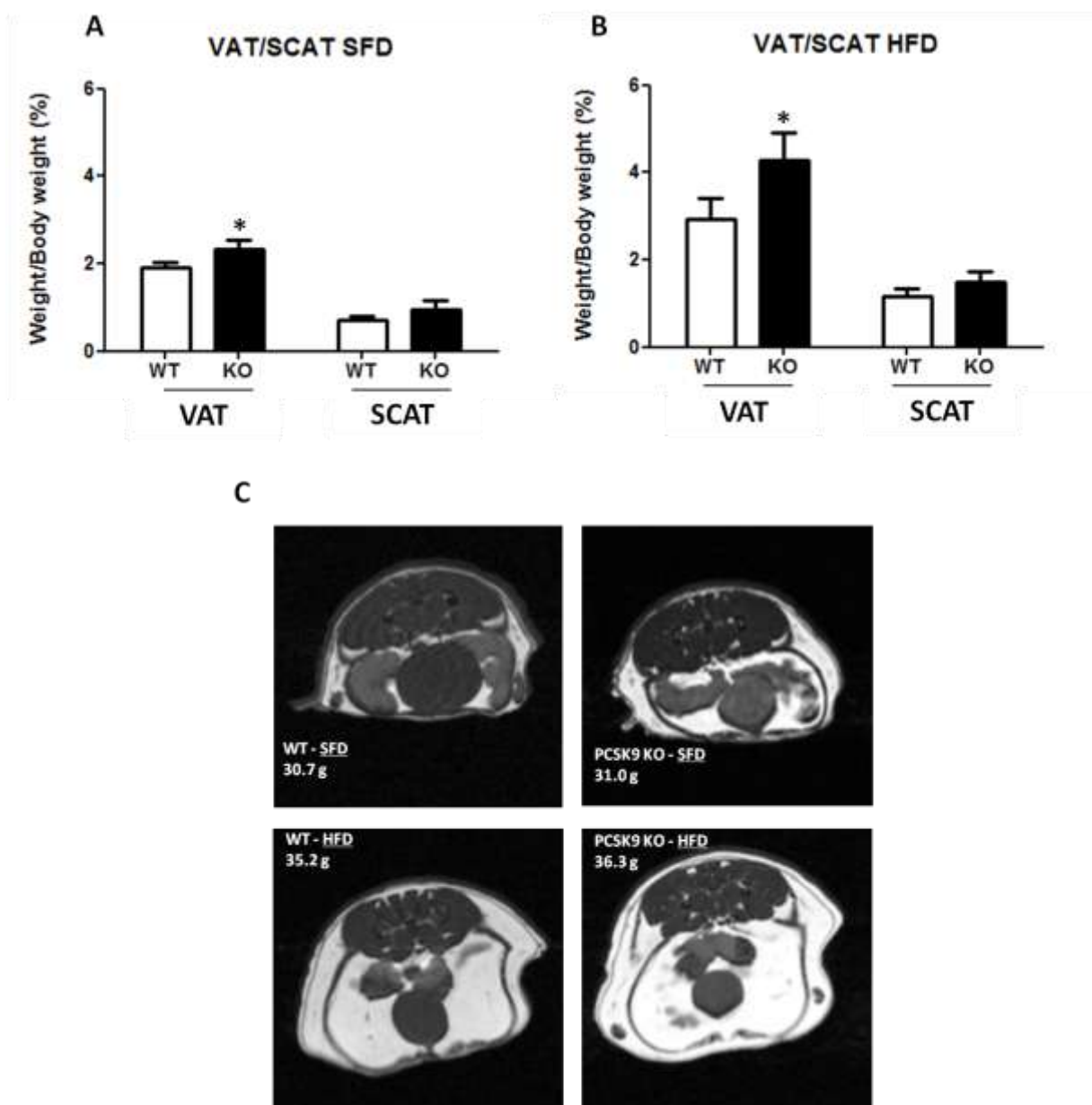


Figure 4. Weights of visceral adipose tissue (VAT) and subcutaneous adipose tissue (SCAT) of WT and PCSK9 KO mice, fed a SFD or HFD for 20 weeks, are shown in panel A and panel B. Weight of each adipose tissue was normalized by total body weight. Data are shown as means \pm SEM; $n=8$ mice per group; $*p<0.05$. Representative magnetic resonance imaging axial views of WT and PCSK9 KO mice are presented in panel C.

3. PCSK9 deficiency results in impaired glucose tolerance but not in insulin resistance

Subsequently, we turned our attention to the role of PCSK9 in glucose metabolism. To evaluate the impact of PCSK9 deficiency on glucose homeostasis, we initially performed GTT in WT and PCSK9 KO mice, fed a SFD or a HFD. In spite of similar plasma glucose levels at baseline, following i.p. glucose injection (2g/Kg body weight), the absence of PCSK9 resulted in a significant delay of glucose clearance, in both the SFD (Fig.5A to 5D) or the HFD (Fig.6A to 6D) groups, after 12 or 20 weeks of diet. Also the plasma glucose AUC was significantly higher in PCSK9 KO mice compared to WT littermates, in all conditions (Fig. 5C/D, 6C/D). The observation that PCSK9 KO mice presented glucose intolerance following GTT, despite comparable baseline glucose levels (following overnight fasting), prompted us to perform a fast and refeeding experiment to better understand possible differences in plasma glucose levels under physiological conditions. After an overnight fasting and ad libitum refeeding (4h), PCSK9 KO mice were characterized by a significant increase in plasma glucose levels compared to WT littermates (266 ± 14 mg/dl vs 216 ± 3 mg/dl with SFD; 322 ± 13 mg/dl vs 252 ± 9 mg/dl with HFD, $p < 0.05$), in spite of similar food consumption ($2,27 \pm 0,43$ g/4h vs $2,18 \pm 0,38$ g/4h with SFD; $2,13 \pm 0,26$ g/4h vs $2,25 \pm 0,28$ g/4h with HFD) (Fig. 5E/F, 6E/F).

These results pointed out the presence of impaired glucose tolerance in PCSK9 KO mice and set the stage for investigating whether this effect was the consequence of impaired insulin tolerance.

To answer this question, ITT was performed in WT and PCSK9 KO mice, after a 4h fast. The decrease in plasma glucose levels, after i.p. insulin injection (0.2IU/kg body weight), was similar in WT and PCSK9 KO mice, fed both a SFD (Fig.7A and 7B) or a HFD (Fig.7C and 7D), after 12 or 20 weeks of diet. These results exclude the presence of insulin resistance under PCSK9 deficient state. Moreover, we measured the ratio between phosphorylated Akt vs total Akt, as an index of downstream activation of the insulin receptor [244], in the liver (Fig. 7E) and in the soleus muscle (Fig 7F) of mice fed a SFD. Interestingly, in these

tissues pAkt/Akt ratio was similar in WT and PCSK9 KO mice, suggesting that downstream activation of insulin receptor might not be affected by PCSK9 deficiency.

GTT, ITT and fasting and refeeding experiments revealed a possible key role of PCSK9 in the regulation of glucose metabolism. PCSK9 KO mice presented impaired glucose tolerance, independent of the type of diet used (high fat or standard fat), but no insulin resistance. IPGTT allowed us to bypass the contribution of GLP-1 on glucose homeostasis, which could interfere during the fasting and refeeding experiment. Several open questions led us to further investigate the mechanisms at the basis of these observations.

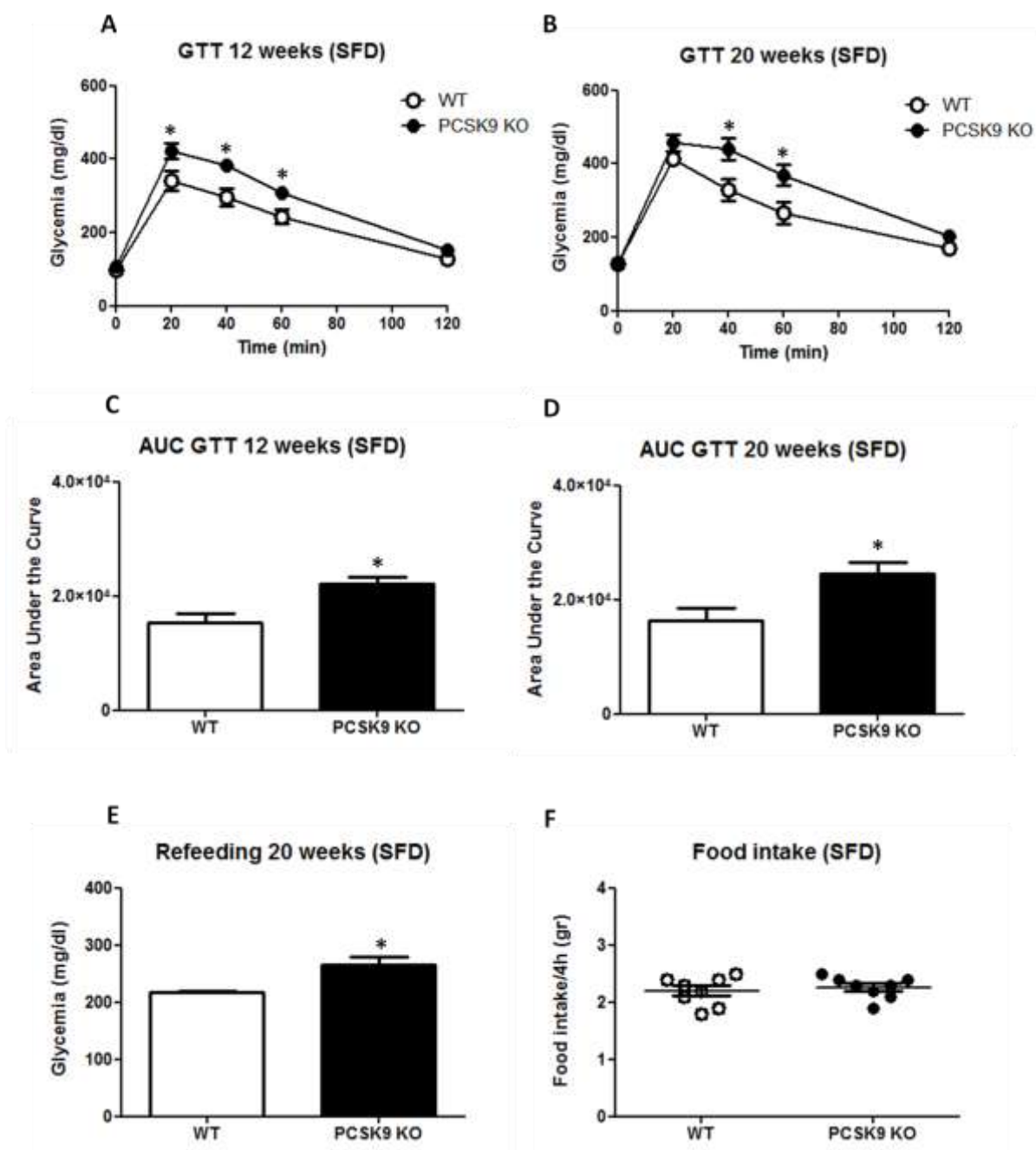


Figure 5. IPGTT was performed and plasma glucose levels were measured at 0, 20, 40, 60, and 120 mins. Data in WT and PCSK9 KO mice, fed a SFD for 12 weeks or 20 weeks and the corresponding AUC for glucose, are presented in panels A to D. Panel E and F show plasma glucose levels and food intake of WT and PCSK9 KO mice after a fasting (overnight) and refeeding (4h) experiment. Data are shown as means \pm SEM; n = 8 mice per group. *p<0.05.

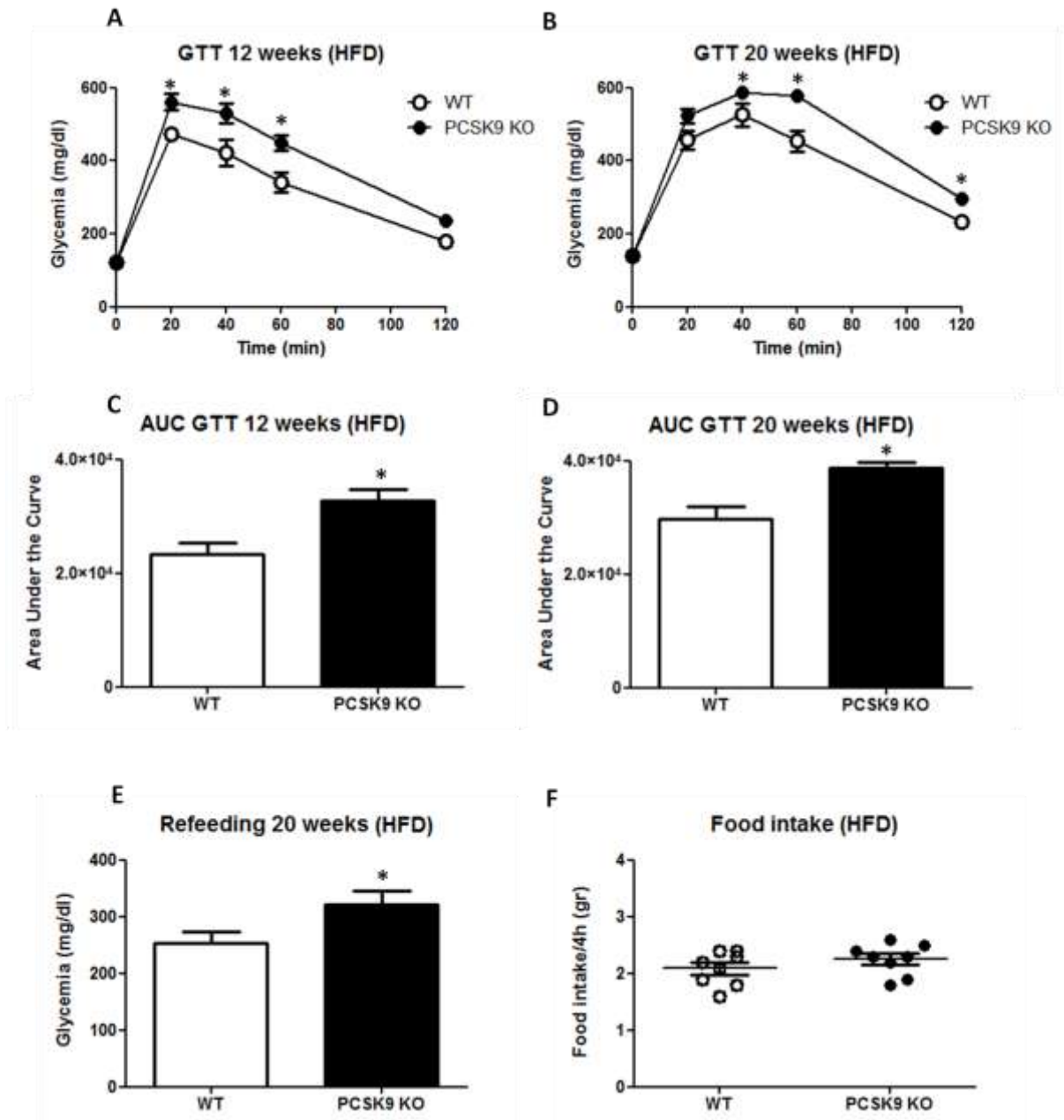


Figure 6. IPGTT was performed and plasma glucose levels were measured at 0, 20, 40, 60, and 120 mins. Data in WT and PCSK9 KO mice, fed a HFD for 12 weeks or 20 weeks and the corresponding AUC for glucose, are presented in panels A to D. Panel E and F show plasma glucose levels and food intake of WT and PCSK9 KO mice after a fasting (overnight) and refeeding (4h) experiment. Data are shown as means \pm SEM; $n = 8$ mice per group. * $p < 0.05$.

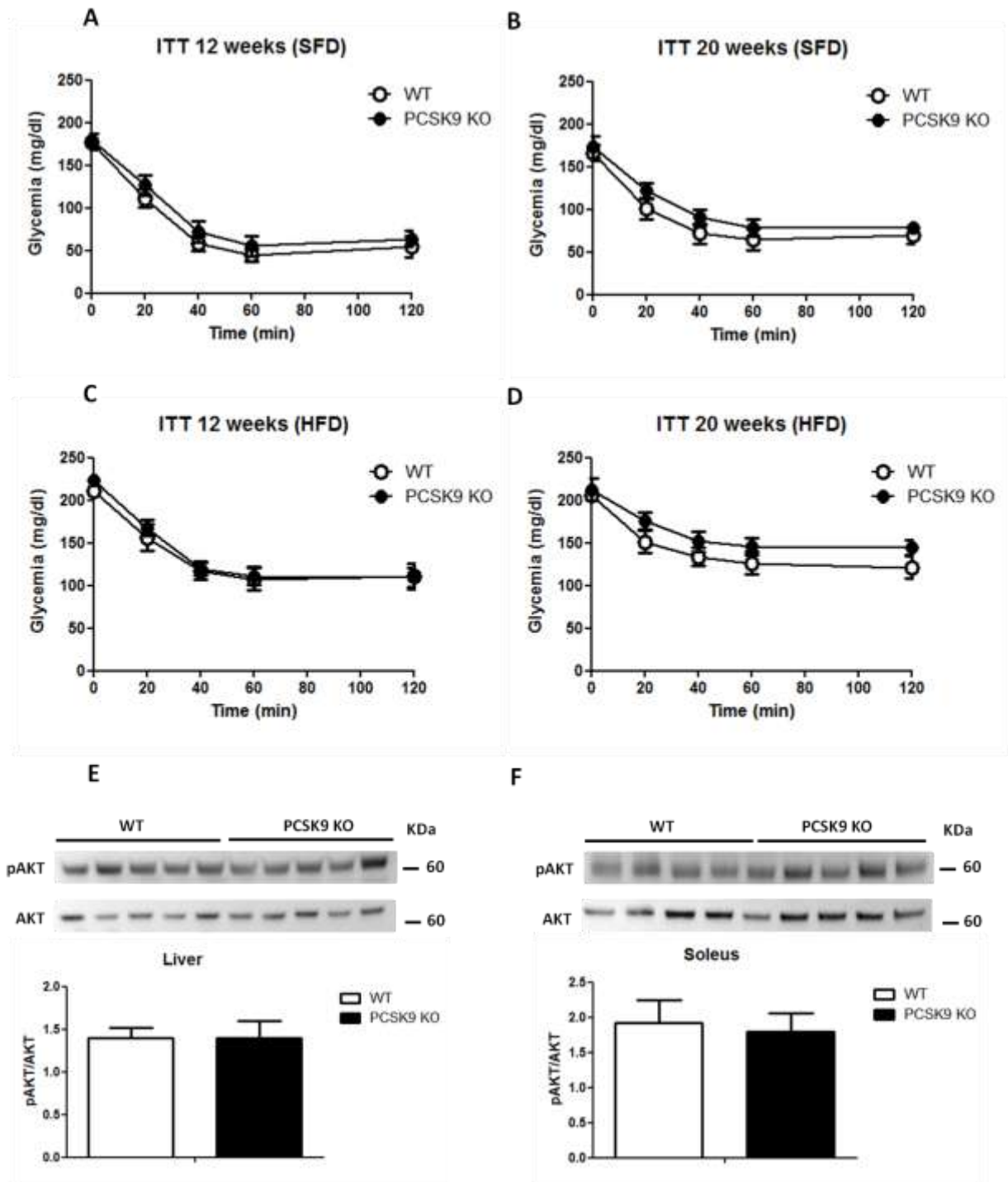


Figure 7. IPITT was performed and plasma glucose levels were measured at 0, 20, 40, 60, and 120 mins. Data in mice fed a SFD for 12 weeks or 20 weeks are reported in panels A and B. Data in mice fed a HFD for 12 weeks or 20 weeks are presented in panels C and D. Data are shown as means \pm SEM; $n = 8$ mice per group. The pAkt/Akt ratio, is presented for the liver (E) and the soleus muscle (F) for PCSK9 KO and WT mice, fed a SFD. Data are shown as means \pm SEM; $n = 5$ mice per group.

4. PCSK9 deficiency results in the impairment of insulin secretion and histological abnormalities in pancreatic islets

To clarify the mechanisms causing impaired glucose tolerance in our mouse model, we subsequently investigated the role of PCSK9 on insulin production and pancreatic β -cells function. Interestingly, plasma insulin and C-peptide levels were significantly decreased in PCSK9 KO mice compared to WT littermates (Fig. 8A/8B), suggesting that PCSK9 deficiency might impair insulin secretion. As a further confirmation, following i.p. glucose injection, plasma insulin levels increased to lower extent in PCSK9 KO mice compared to WT animals (Fig. 8C). Similarly, following fast and refeeding experiment, a reduced increase in plasma insulin levels was observed in the absence of PCSK9 (Fig. 8D).

On the contrary, pancreatic insulin content was significantly increased in PCSK9 KO mice compared to WT controls (Fig 9A). The evaluation of pancreatic islets morphology revealed that PCSK9 KO mice islets present an irregular shape (Fig 9B), a larger size ($10022 \pm 2802 \text{ um}^2$ vs $5061 \pm 1843 \text{ um}^2$, $p < 0.05$) (Fig.9C), and a significant increase in insulin positive areas ($8843 \pm 1432 \text{ um}^2$ vs $3215 \pm 508 \text{ um}^2$, $p < 0.05$) (Fig. 9D) compared to WT littermates.

We confirmed these data also in PCSK9 KO and WT mice, fed a HFD, evaluating plasma insulin levels, pancreatic insulin content and pancreatic islets morphology (Fig. 10). Representative images of pancreatic islets of WT and PCSK9 KO, fed a SFD or a HFD, for 20 weeks, are presented in Fig. 10 C/D.

Here we observed that PCSK9 deficiency is associated with decreased plasma insulin and C-peptide levels, a finding paralleled by altered pancreatic morphology and insulin content. These data suggested an impaired beta cells function in PCSK9 KO mice, independent of the type of diet used, and prompted us to further investigate the mechanisms responsible.

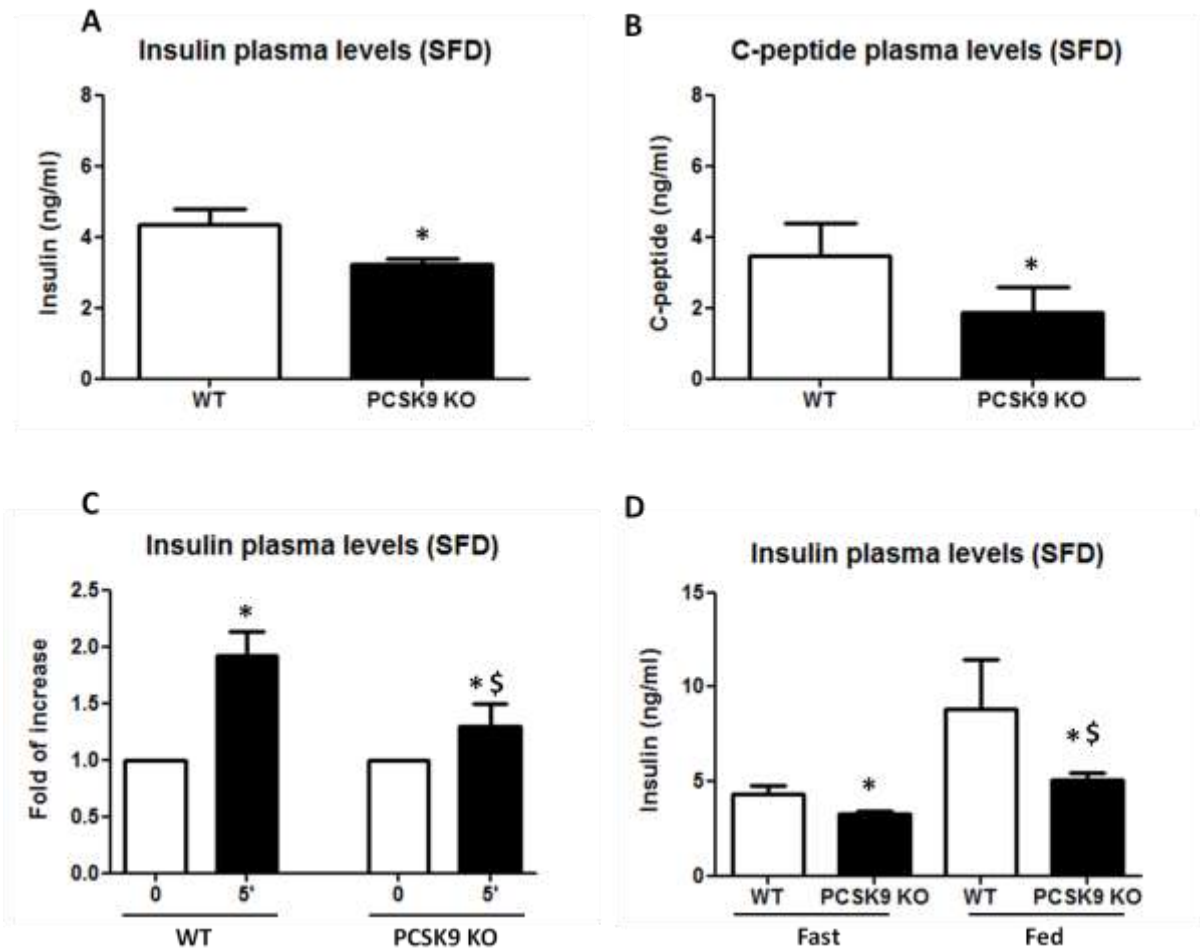


Figure 8. Plasma insulin and C-peptide levels of WT and PCSK9 KO mice, fed a SFD, are shown in panels A and B. Plasma insulin levels before and after 5' of IPGTT are presented in panel C (* $p < 0.05$ vs 0; $^{\S}p < 0.05$ vs 5' WT) while following fasting (overnight) and refeeding (4h) experiment are presented in panel D (* $p < 0.05$ vs WT; $^{\S}p < 0.05$ vs Fasted KO). Data are shown as means \pm SEM; $n = 8$ mice per group.

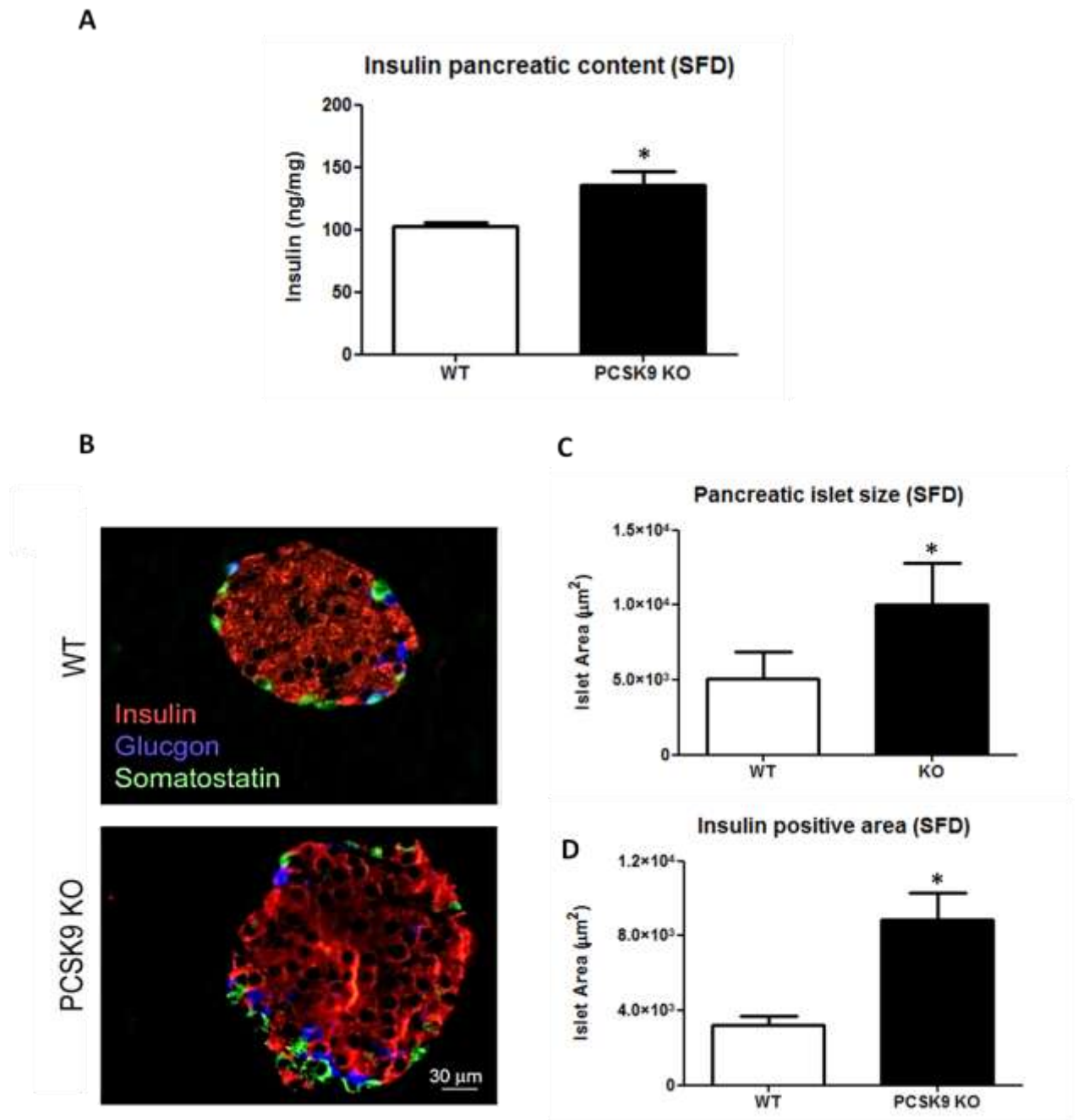


Figure 9. Pancreatic insulin content in PCSK9 KO and WT mice, fed a SFD, is shown in panels A. Data are shown as means \pm SEM; $n = 8$ mice per group. Pancreatic islets morphology shows larger islets in PCSK9 KO mice compared to WT with significantly increased insulin positive areas (panels B to D). A representative image is presented in panel B; data in panels C and D are shown as mean \pm SEM of 6 to 8 representative sections for each pancreas (8 animals for each group); * $p < 0.05$. Scale bar in panel C: 30 μm .

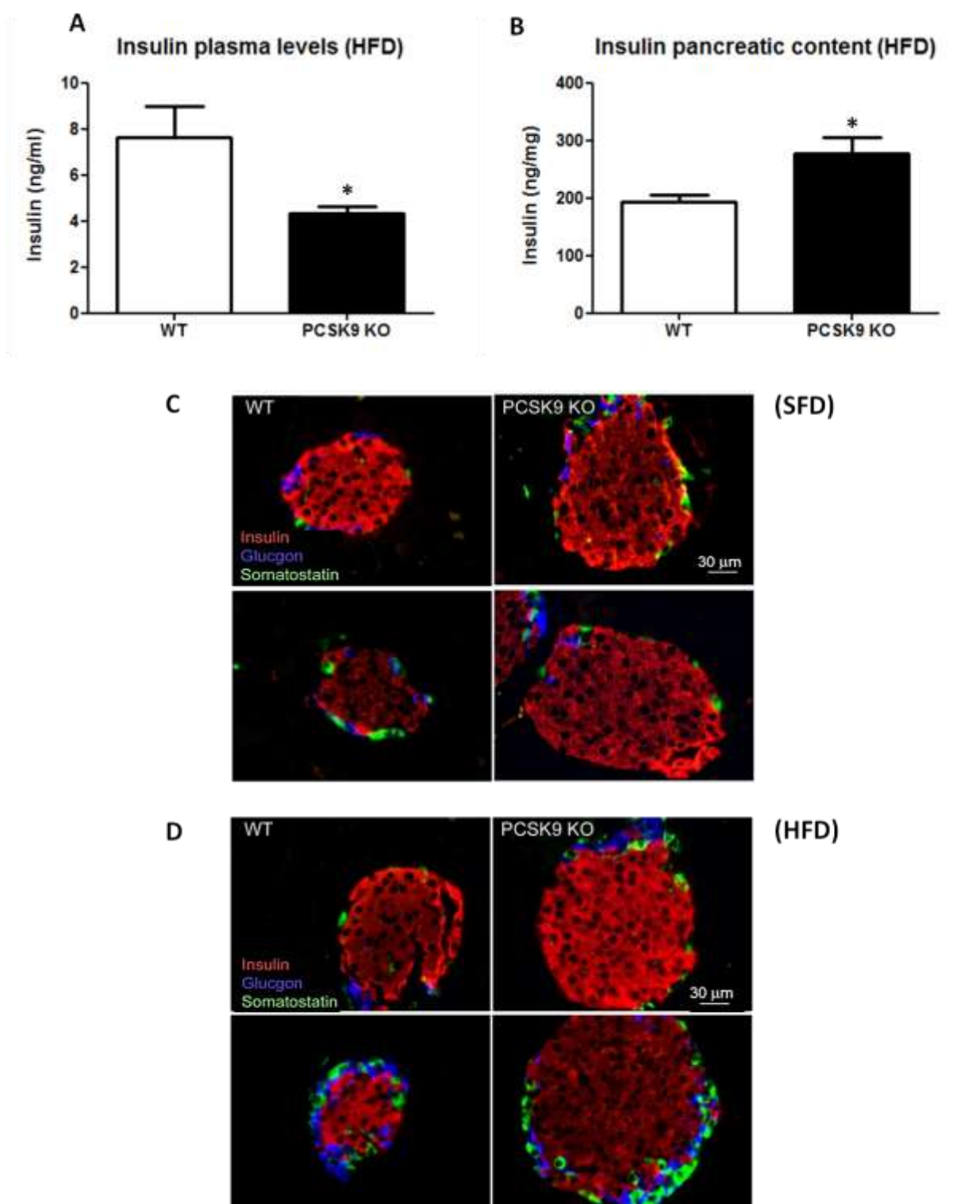


Figure 10. Plasma insulin levels and pancreatic insulin content were measured in PCSK9 KO and WT mice fed a HFD (panel A and panel B). Data are shown as means \pm SEM; $n = 8$ mice per group. * $p < 0.05$. Representative images of pancreatic islets of WT and PCSK9 KO, fed a SFD (panel C) or a HFD (panel D) for 20 weeks, show differences in islets morphology between the two groups. $n = 8$ mice per group.

5. PCSK9 effect on glucose metabolism is dependent on the presence of the LDLR

In order to further investigate the molecular mechanisms responsible for the phenotype observed in PCSK9 KO mice, we focused our attention on the LDLR. The LDLR is abundantly expressed on the surface of pancreatic β cells, where it plays a key role in the uptake of LDL [2]. Moreover, increased β cells cholesterol content was frequently associated with decreased insulin secretion [245, 246].

Firstly, to evaluate the impact of PCSK9 on the pancreatic expression of the LDLR, we performed immunofluorescence analysis of pancreatic sections from WT and PCSK9 KO mice. In agreement with previous observation [156], we showed that LDLR (blue signal) colocalizes with insulin positive areas (red signal), confirming its considerable expression on the surface of pancreatic β cells (Fig. 11). Interestingly, flow cytometry analysis showed that the LDLR expression was significantly increased in the pancreatic islets isolated from PCSK9 KO animals compared to WT littermates (Fig. 12). In addition to increased LDLR expression, pancreatic islets from PCSK9 KO mice presented higher cholesterol esters content compared to WT islets, together with significant changes in fatty acid lipidome (Fig. 13A). This impaired lipid profile was paralleled by the downregulation of genes involved in cholesterol biosynthesis and uptake, including HMGCoA-R and LDLR and the increase of the expression of ACAT1, which promotes cholesterol esterification. A modest but not significant increase was also observed in genes involved in cholesterol efflux, such as ABCA1, ABCG1 and LXR (Fig. 13B).

To further test the hypothesis that the observed phenotype in PCSK9 KO mice could be dependent on the impact on LDLR levels, we created a double KO animal model, PCSK9/LDLR DKO. GTT and ITT were performed in PCSK9/LDLR DKO mice and LDLR KO littermates, fed a SFD. The delayed glucose response observed in PCSK9 deficient conditions was not observed in PCSK9/LDLR DKO mice and, indeed, GTT and ITT curves were superimposable between the two animal groups (Fig. 14A and 14E) and similar to those observed in WT animals. Also the plasma glucose AUC during GTT was similar in the two experimental groups (Fig. 14B). Fast and refeeding experiments confirmed these data, showing no difference in plasma glucose levels between PCSK9/LDLR DKO and LDLR

KO mice (190 ± 6 mg/dl for PCSK9/LDLR DKO compared to 191 ± 7 mg/dl for LDLR KO mice), paralleled with similar food consumption during the 4h of fasting (Fig. 14C and 14D).

Finally, we demonstrated that PCSK9/LDLR DKO mice and LDLR KO littermates were characterized by similar levels of both plasma and pancreatic insulin (5.17 ± 1.08 ng/ml vs 4.67 ± 1.25 ng/ml, $p=ns$) (72.0 ± 21.7 ng/mg of tissue vs 77.7 ± 23.1 ng/mg of tissue $p=ns$) (Fig. 15A and 15B). The evaluation of pancreatic islets morphology revealed no difference in islets shape, size and insulin positive areas between PCSK9/LDLR DKO and LDLR KO mice, whose features are similar to those observed in WT animals (Fig. 15 C to E).

Here we demonstrated that PCSK9 is able to modulate the expression of the LDLR also at the pancreatic level. Moreover, the observations that glucose tolerance, insulin tolerance, plasma insulin levels and pancreatic islets morphology in DKO were similar to those of control mice, suggest the key role of the LDLR in driving PCSK9 dependent pancreatic dysfunction.

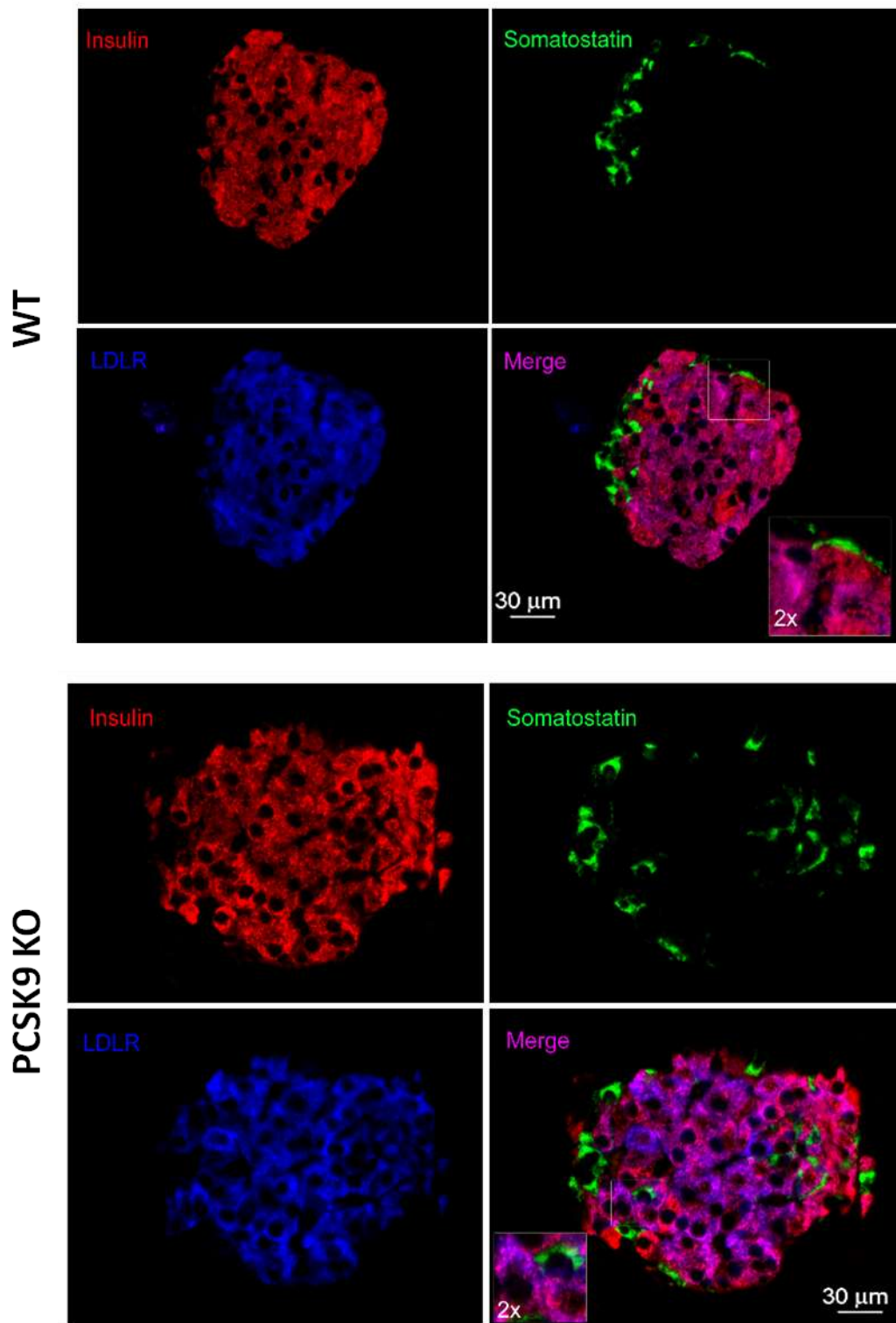


Figure 11. Representative pictures of pancreatic islets from WT and PCSK9 KO mice. The islets were stained for insulin, somatostatin and LDLR, and the results indicated that LDLR colocalizes with insulin positive areas (beta cells). Scale bar: 30 μm.

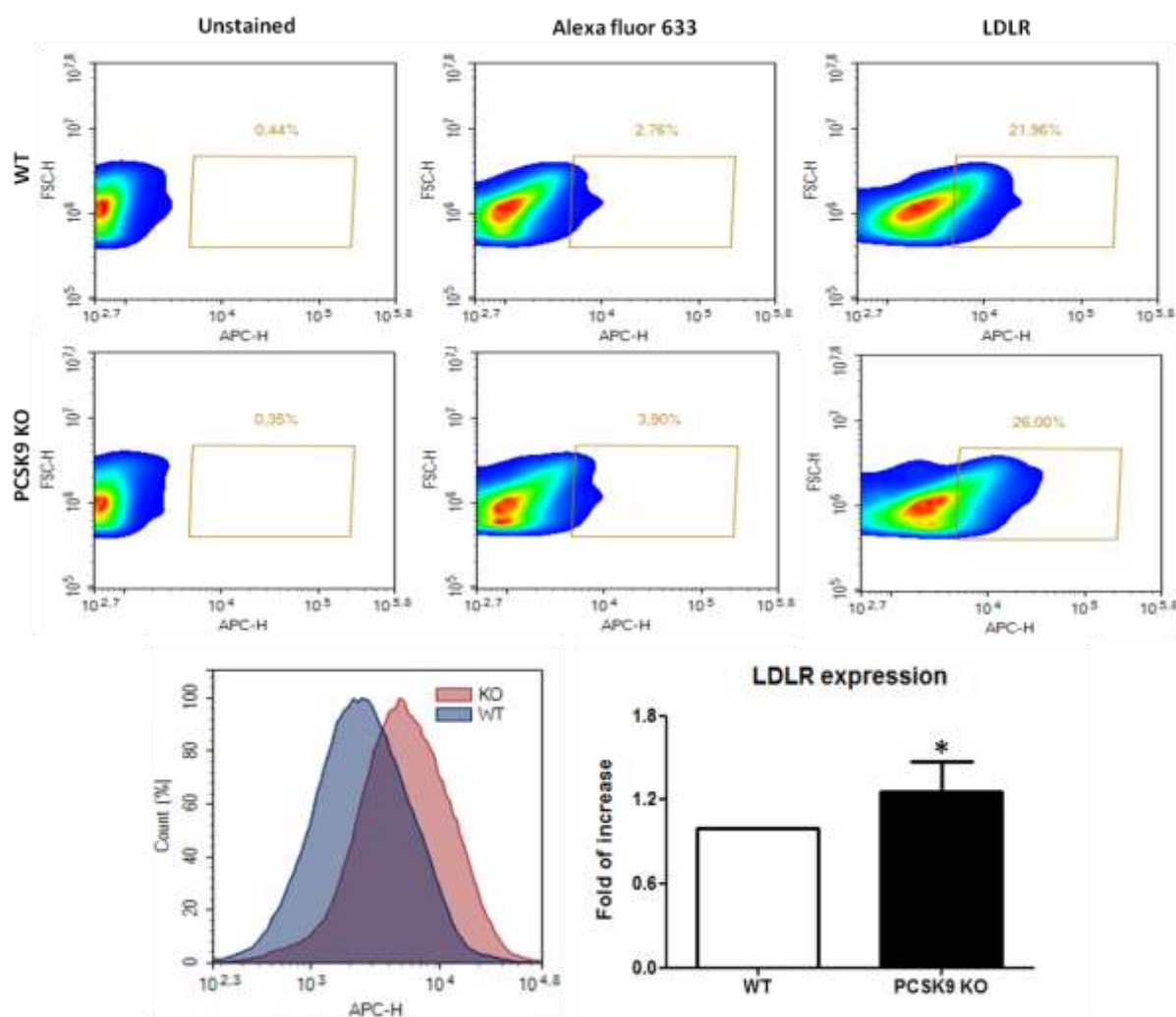


Figure 12. Representative panel for LDLR expression in pancreatic islets isolated from WT mice (upper lane) and PCSK9 KO mice (lower lane). Unstained cells, cells stained only with Alexa Fluor 655 and cells stained with anti-LDLR are shown. The panel presents the overlay of LDLR fluorescence intensity in PCSK9 KO and WT mice and the difference (data are shown as mean \pm SEM, $n=5$, $p<0.05$).

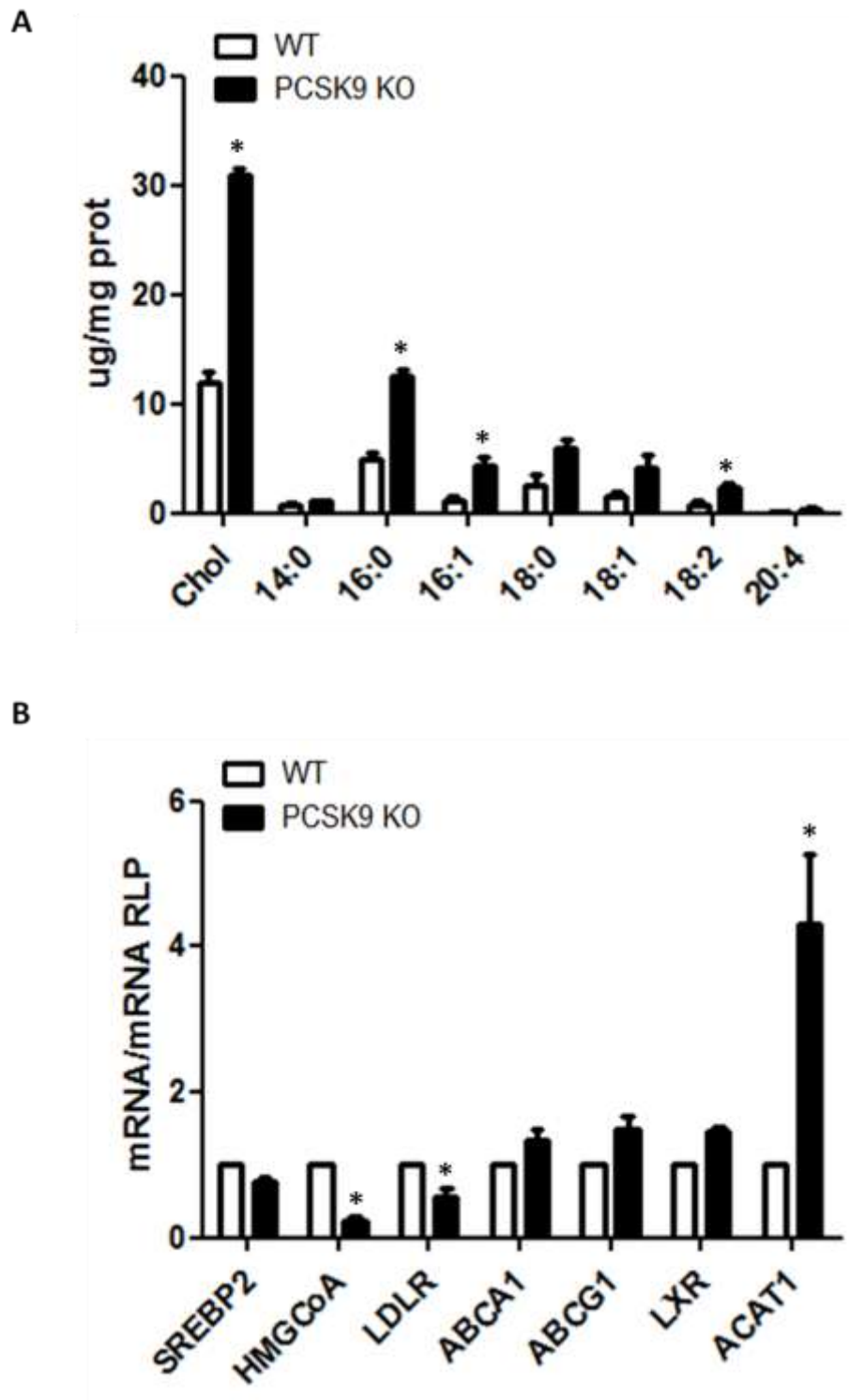


Figure 13. Cholesterol esters and fatty acids content were measured in pancreatic islets from PCSK9 KO and WT mice (panel A). The expression of genes related to cholesterol biosynthesis, uptake and efflux, and the expression of ACAT1 was evaluated in pancreatic islets isolated from PCSK9 KO and WT mice (panel B). Data presented in panel A (* $p < 0.05$; Unpaired T Test; $n = 3$ mice per group) and B (* $p < 0.05$; T Test; $n = 6$ mice per group) are shown as means \pm SEM.

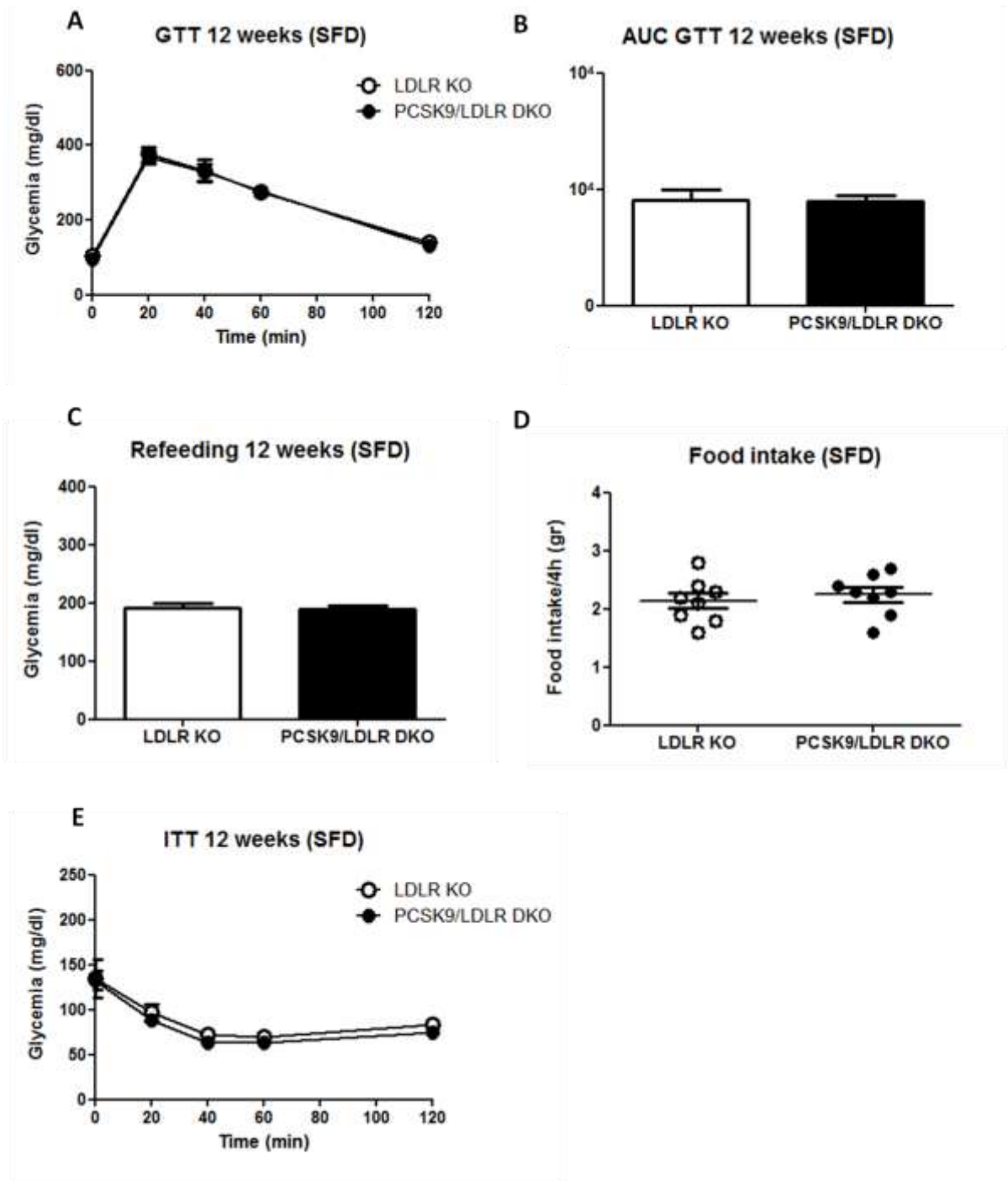


Figure 14. IPGTT was performed and plasma glucose levels were measured at 0, 20, 40, 60, and 120 mins. Data in LDLR KO and PCSK9/LDLR DKO mice, fed a SFD for 12 weeks, and the corresponding AUC for glucose, are presented in panels A and B. Panel C and D show plasma glucose levels and food intake of LDLR KO and PCSK9/LDLR DKO mice after a fasting (overnight) and refeeding (4h) experiment. IPITT was performed in mice fed a SFD for 12 weeks and plasma glucose levels measured at 0, 20, 40, 60, and 120 mins are reported in panels E. Data are shown as means \pm SEM; n = 8 mice per group.

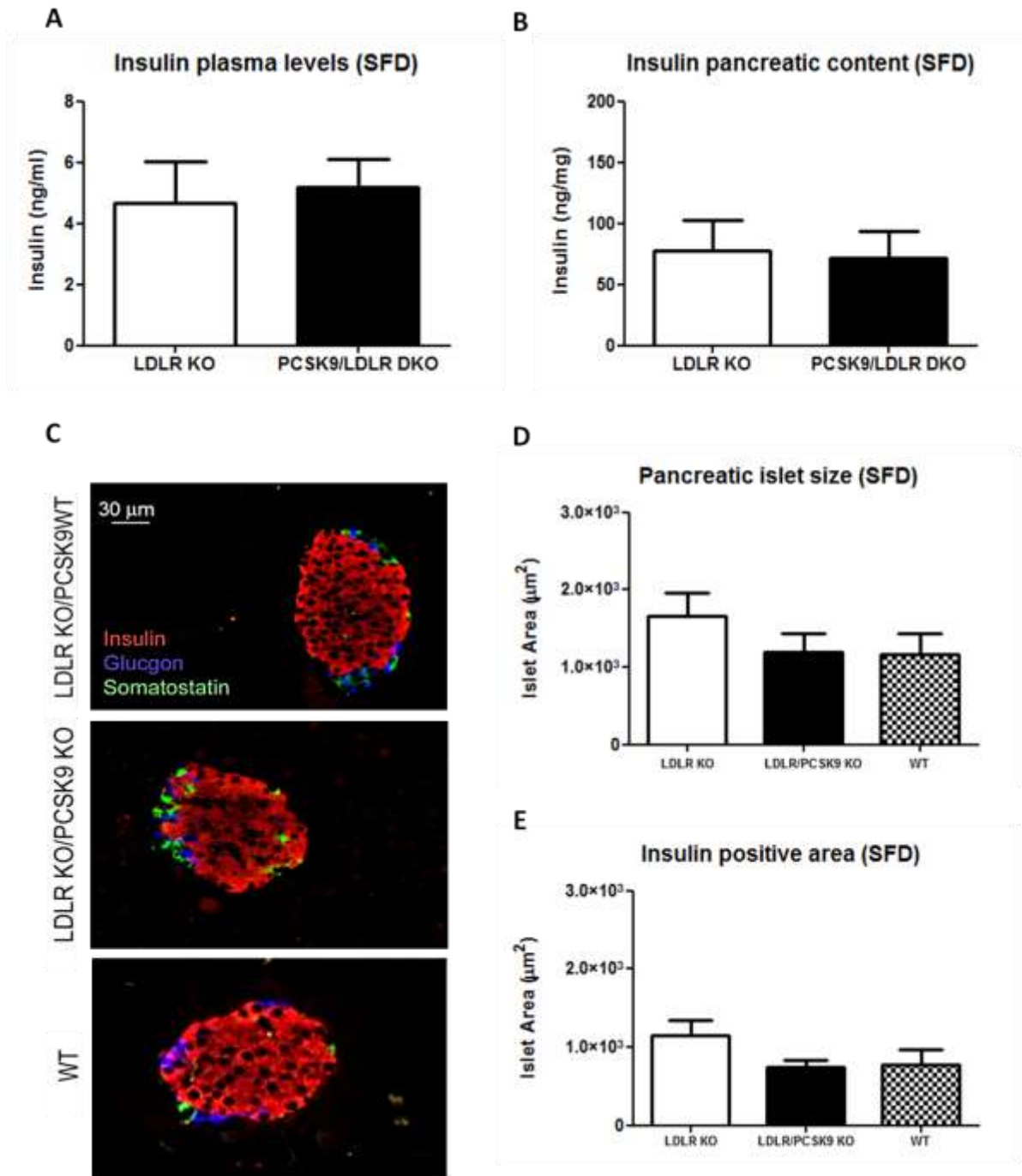


Figure 15. Plasma insulin levels and pancreatic insulin content of LDLR KO and PCSK9/LDLR DKO mice are presented in panel A and panel B. Panel C shows a representative image of pancreatic islet morphology of PCSK9/LDLR DKO, LDLR KO and WT mice, while panels D and E present data on pancreatic islets size and insulin positive areas size. Data in panels A and B are shown as mean \pm SEM; $n = 8$ mice per group. Data in panels D and F are shown as mean \pm SEM of 6 to 8 representative sections for each pancreas (8 animals for each group).

6. Circulating PCSK9 does not impact glucose metabolism and beta cells function

Despite PCSK9 is mainly produced and released by the liver, it is also synthesized to a relevant amount in other tissues, such as the brain, the intestine and the pancreas [1]. Here we investigated if the phenotype observed in PCSK9 KO (full body) mice depends on circulating liver-derived PCSK9 or on PCSK9 produced at the pancreatic level.

Firstly, we demonstrated that in pancreatic islets of WT mice PCSK9 colocalizes with somatostatin positive cells (delta cells) but not with alpha or beta cells (Fig. 16A). As expected, the analysis of islets derived from PCSK9 KO mice confirmed the absence of the protein in delta cells of these animals (Fig. 16B).

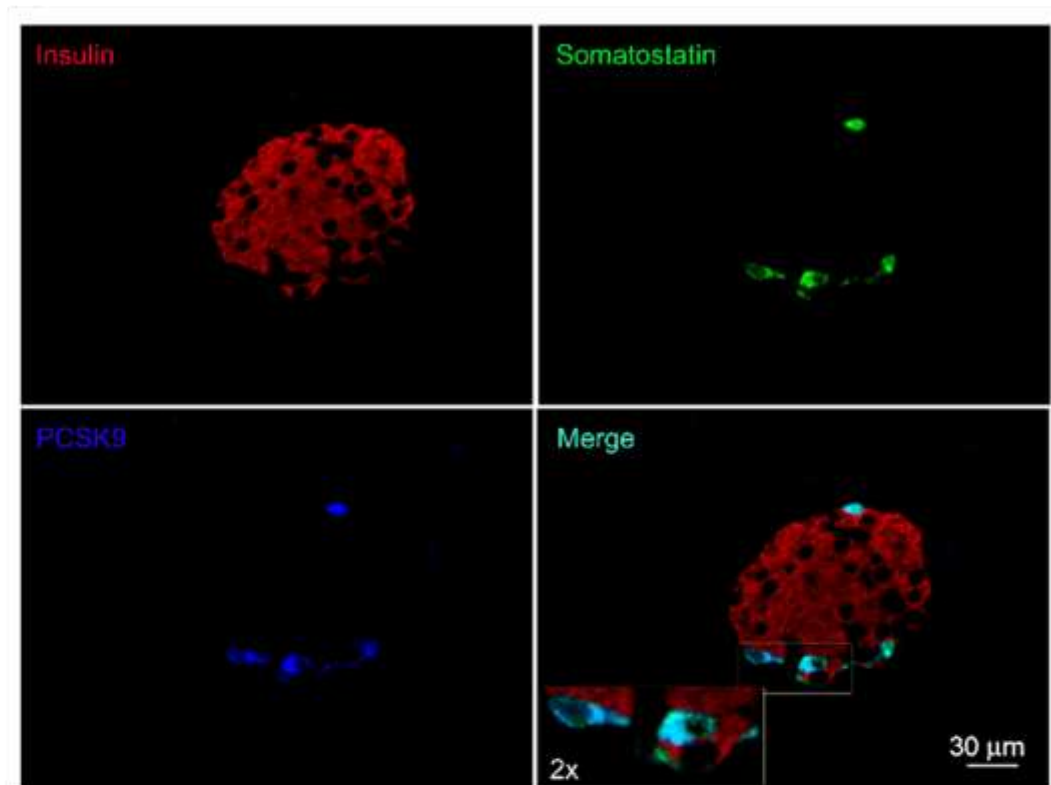
To dissect out the role of circulating liver-derived PCSK9 from those produced in the pancreas, we tested glucose metabolism in SFD fed liver-specific PCSK9 KO mice. PCSK9 mRNA expression was almost abolished in the liver of AlbCre+/PCSK9^{LoxP/LoxP} mice (Fig. 17A). As a consequence, PCSK9 protein was almost undetectable in plasma from AlbCre+/PCSK9^{LoxP/LoxP}, while in AlbCre-/PCSK9^{LoxP/LoxP} mice plasma PCSK9 levels were around 10 fold higher (Fig. 17B). As expected, plasma cholesterol levels in AlbCre+/PCSK9^{LoxP/LoxP} mice were significantly lower compared to AlbCre-/PCSK9^{LoxP/LoxP} (41.8±7.2 mg/dl vs 68.5± 10.2 mg/dl p<0.05) and similar to those observed in PCSK9 KO mice (51.1±14.0 mg/dl), further confirming the key role of circulating, liver-derived PCSK9 on plasma cholesterol levels (Fig. 17C). On the contrary, PCSK9 mRNA expression in pancreas was similar between AlbCre+/PCSK9^{LoxP/LoxP} and AlbCre-/PCSK9^{LoxP/LoxP} mice (Fig. 17A), also confirmed through immunofluorescence analysis of pancreatic islets (Fig. 17D). Flow cytometry analysis revealed that LDLR expression (Fig. 18A) was similar in pancreatic islets from AlbCre+/Pcsk9^{LoxP/LoxP} and AlbCre-/Pcsk9^{LoxP/LoxP} mice and the same was true for cholesterol esters levels (Fig. 18B).

Once characterized our model, we focused our attention on glucose metabolism. Of note, AlbCre+/PCSK9^{LoxP/LoxP} and AlbCre-/Pcsk9^{LoxP/LoxP} mice presented similar GTT and ITT curves (Fig. 19A/B), and the same was true for plasma glucose levels following fast and refeeding experiments (194±8 mg/dl for AlbCre+/Pcsk9^{LoxP/LoxP} mice compared to 192± 5 mg/dl for AlbCre-/Pcsk9^{LoxP/LoxP} mice; p=ns) (Fig. 19C/D). Pancreatic insulin content was

similar in the two animal models (133.6 ± 21.1 ng/mg of tissue vs 119.1 ± 19.3 ng/mg of tissue for AlbCre+/Pcsk9^{LoxP/LoxP} and AlbCre-/Pcsk9^{LoxP/LoxP} mice; $p=ns$) (Fig. 19E), as well as the insulin positive areas (Fig. 19F).

Thus, here we reported that liver-selective PCSK9 KO mice have PCSK9 plasma levels below the detection limit, while maintaining PCSK9 production in other tissues including the pancreas. These mice presented plasma and pancreatic insulin levels, LDLR expression as well as pancreatic islets cholesterol esters levels similar to those of control mice, suggesting that the impaired glucose metabolism observed in PCSK9 KO (full body) mice depends on PCSK9 produced locally in the pancreas.

A



B

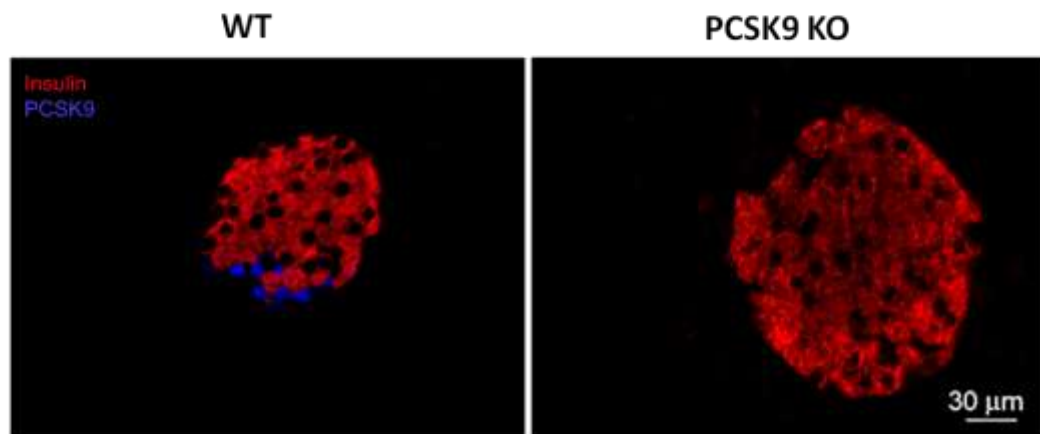


Figure 16. Panel A shows a representative image of the immunofluorescence of pancreatic islets from WT mice indicating that PCSK9 colocalizes with somatostatin positive areas (delta cells). Panel B presents representative images of PCSK9 expression in pancreatic islets from WT and PCSK9 KO mice. Scale bar: 30 μm .

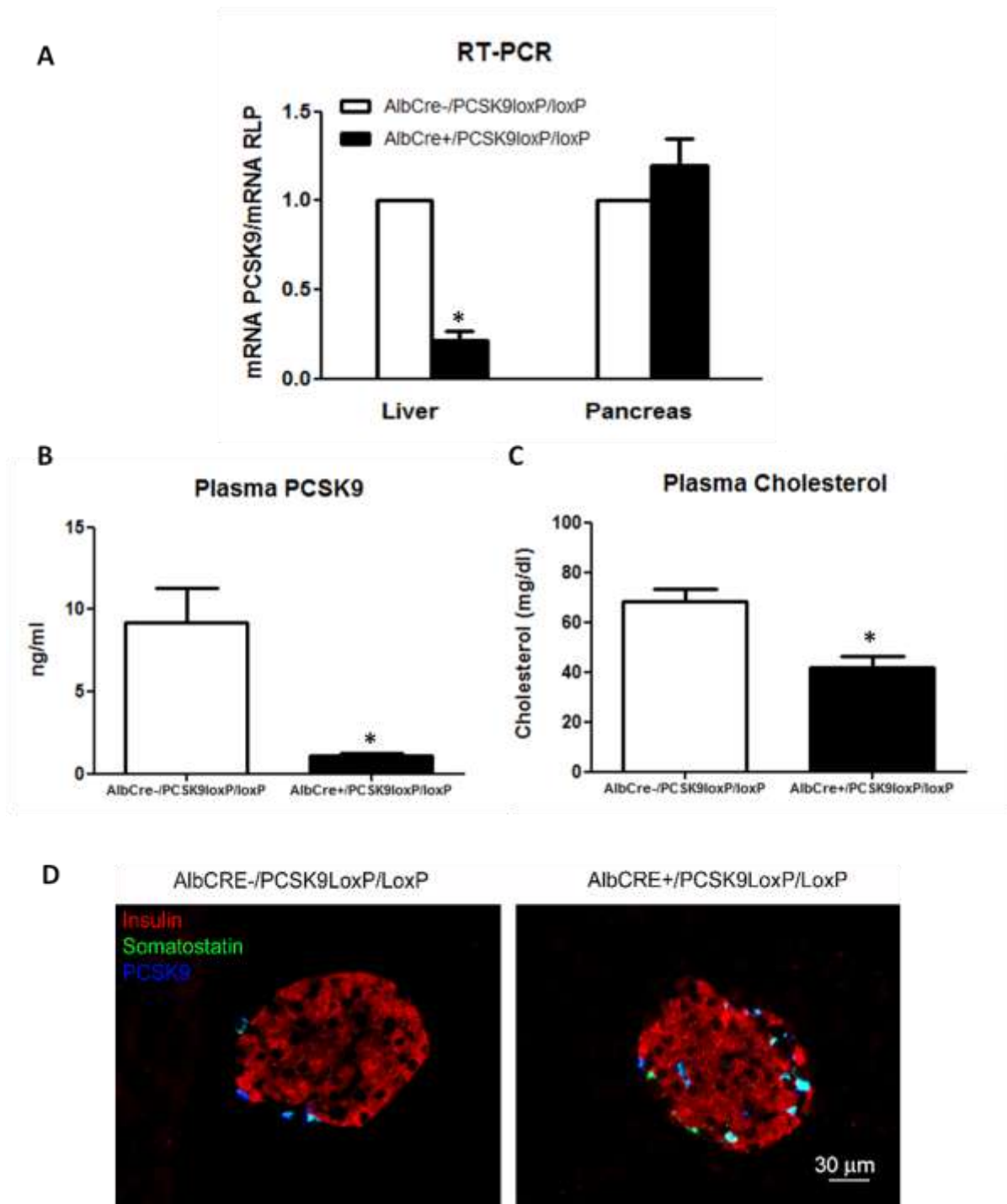


Figure 17. Panel A shows PCSK9 mRNA expression in the liver or in the pancreas of AlbCre+/Pcsk9^{LoxP/LoxP} and AlbCre-/Pcsk9^{LoxP/LoxP} mice. Panel B presents plasma PCSK9 levels of AlbCre+/Pcsk9^{LoxP/LoxP} and AlbCre-/Pcsk9^{LoxP/LoxP} mice, while panel C shows the levels of circulating cholesterol in the same animal groups. Representative images of PCSK9 expression, which colocalizes with somatostatin positive areas (delta cells), of pancreatic islets from AlbCre+/Pcsk9^{LoxP/LoxP} and AlbCre-/Pcsk9^{LoxP/LoxP} mice; Scale bar: 30 μ m (Panel D). Data in panels A, B and C are shown as means \pm SEM; n=8 mice per group; *p<0.05.

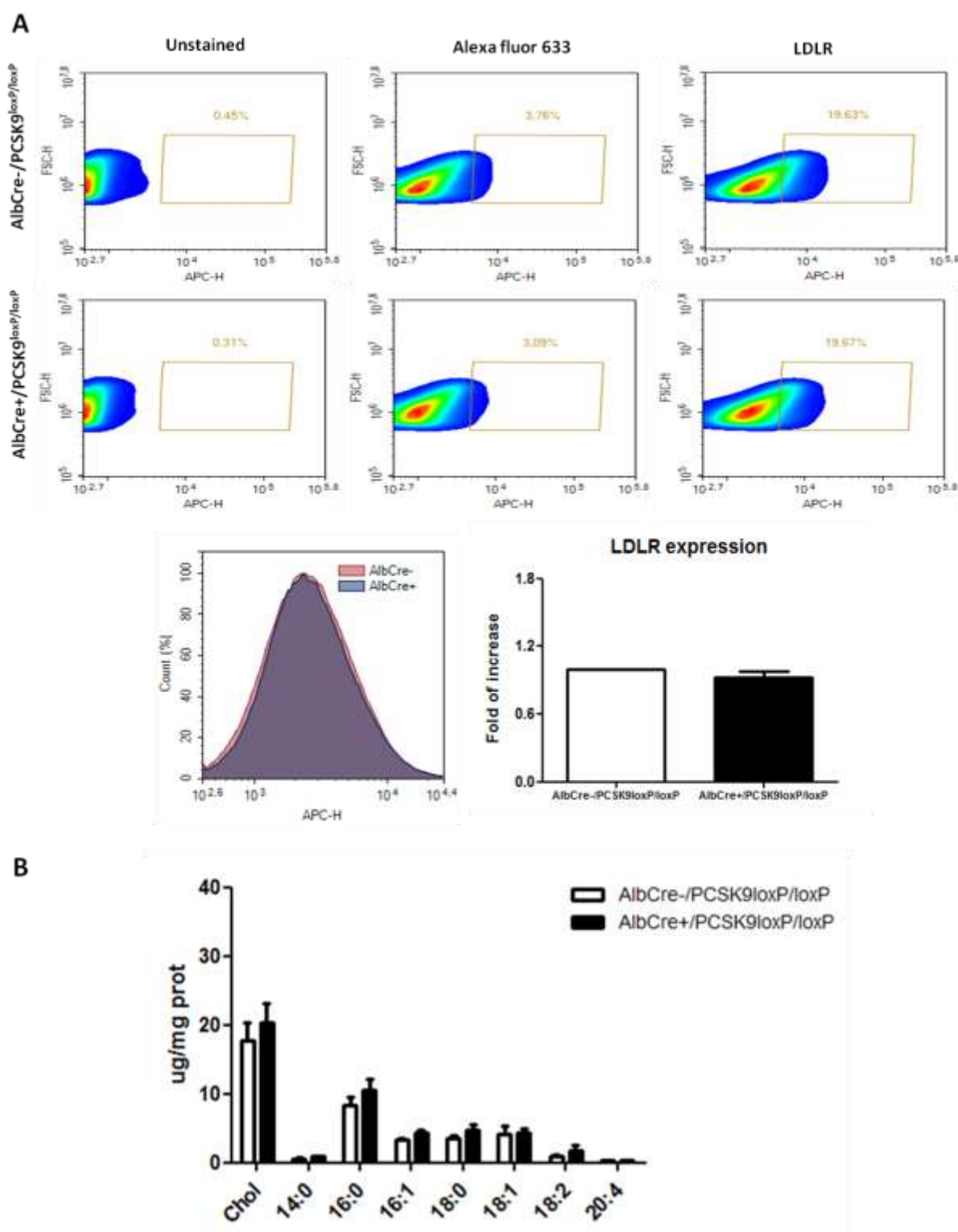


Figure 18. Panel A shows a representative panel for LDLR expression in pancreatic islets isolated from AlbcCre+/Pcsk9^{LoxP/LoxP} and AlbcCre-/Pcsk9^{LoxP/LoxP} mice. The panel presents the overlay of LDLR fluorescence intensity in AlbcCre+/Pcsk9^{LoxP/LoxP} and AlbcCre-/Pcsk9^{LoxP/LoxP} mice and the quantification (data are shown as mean \pm SEM n=5). Panel B shows cholesterol esters and fatty acids content of pancreatic islets from AlbcCre+/Pcsk9^{LoxP/LoxP} and AlbcCre-/Pcsk9^{LoxP/LoxP} mice. Data are shown as means \pm SEM; n = 8 mice per group.

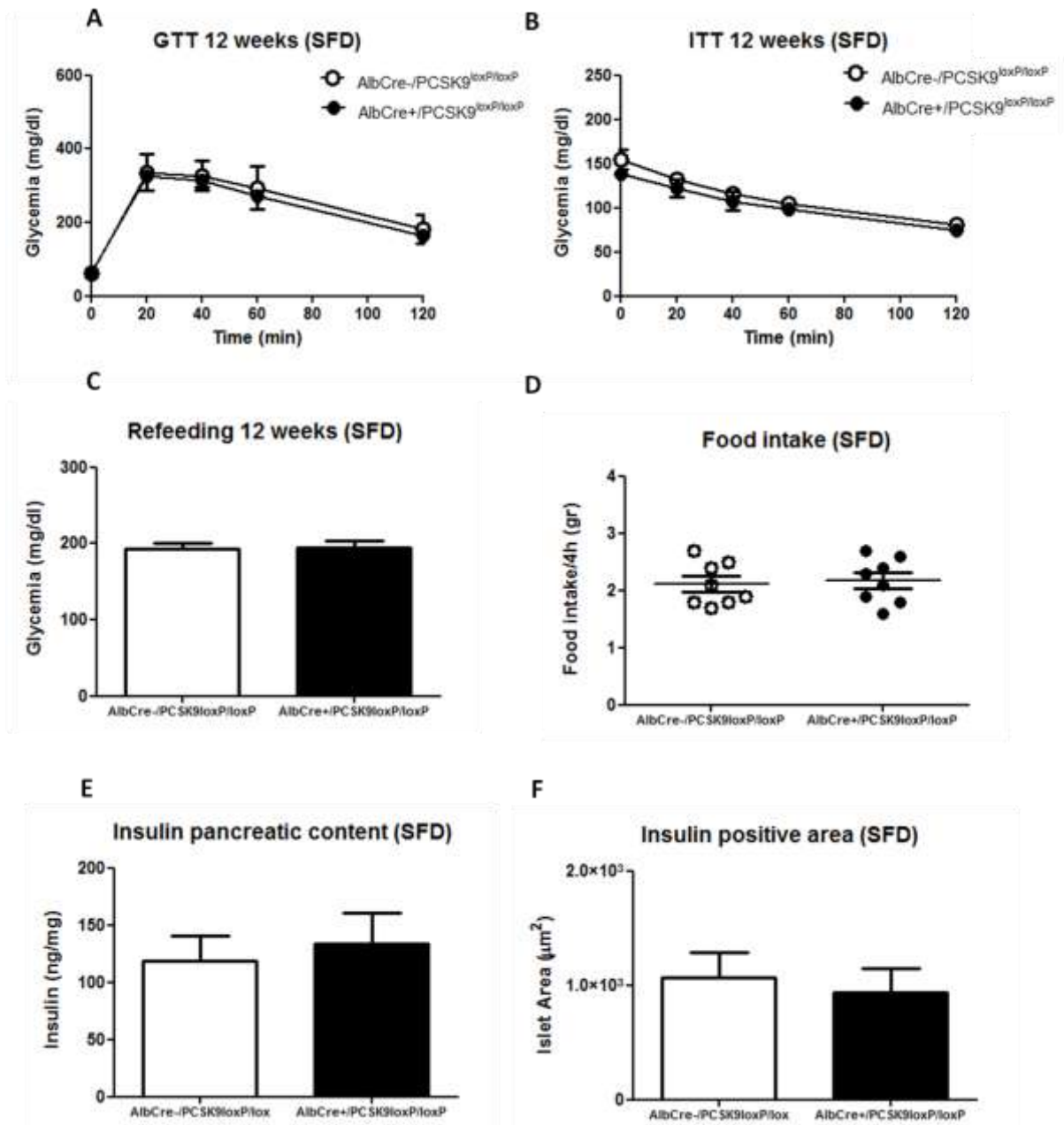


Figure 19. Plasma glucose levels following IPGTT (0, 20, 40, 60, and 120 mins) of AlbCre+/Pcsk9^{LoxP/LoxP} and AlbCre-/Pcsk9^{LoxP/LoxP} mice, fed a SFD for 12 weeks, are presented in panels A. Panel B shows plasma glucose levels in AlbCre+/Pcsk9^{LoxP/LoxP} and AlbCre-/Pcsk9^{LoxP/LoxP} mice following IPITT (0, 20, 40, 60, and 120 mins). Panel C and D show plasma glucose levels and food intake of the same mice after a fasting (overnight) and refeeding (4h) experiment. Pancreatic insulin content and insulin positive areas of AlbCre+/Pcsk9^{LoxP/LoxP} and AlbCre-/Pcsk9^{LoxP/LoxP} mice are presented in panel E and panel F. Data are shown as means \pm SEM; n = 8 mice per group.

Discussion

PCSK9 is a protein, initially discovered to be involved in neuronal development and differentiation, which binds to specific proteins and escorts them towards endosomes/lysosomes compartments for degradation [1, 3]. PCSK9 came to attention of the scientific community in 2003, when it was found mutated in patients affected by FH [113], pointing out its key role in lipid metabolism. The LDLR has been identified as the main target of PCSK9 [247]. Indeed, mice lacking PCSK9 exhibit an increased hepatic LDLR expression, resulting in an increased clearance of circulating LDL-C and hypocholesterolemia [248], while PCSK9 overexpression induces a 2-fold increase in plasma cholesterol levels [124]. In humans, several mutations in PCSK9 gene were described over the years, both “gain-of-function” mutations associated to hypercholesterolemia [113] and “loss of function” mutations linked to low levels of LDL-C [183, 188].

On these premises, anti-PCSK9 therapies have been developed and monoclonal antibodies against PCSK9 are currently available for the treatment of patients with severe hypercholesterolemia and/or at very high cardiovascular risk.

Although the liver is the main contributor to circulating PCSK9 and its most important target [148], other tissues produce PCSK9, pointing to a possible role of this protein beyond the control of the hepatic LDLR expression [4]. Of note, the LDLR is abundantly expressed by pancreatic β -cells in humans, mice and rats, where it plays a key role in the uptake of plasma LDL [2, 157]. The accumulation of cholesterol in pancreatic islets has been associated with reduced glucose induced insulin secretion [108] and cellular toxicity [245, 249], pointing to the critical role of cholesterol metabolism in this tissue. As a consequence of the LDLR-mediated cholesterol influx in β -cells, genetic and acquired conditions increasing LDLR expression, should be associated with altered glucose metabolism. Loss of function variants in the HMGCoA reductase which, by limiting cellular cholesterol biosynthesis, favor cholesterol uptake via LDLR, are associated with increased risk of developing diabetes [164]. On the contrary, FH subjects bearing a loss of function mutation in the LDLR, present a decreased risk of diabetes [166]. Also pharmacological treatments resulting in increased LDLR expression, such as statins, increase the risk of diabetes [250], thus indicating that excessive LDLR activity could be the driver of β -cells dysfunction and diabetes. Interestingly, the same is true for loss of function variants in PCSK9. Indeed, in three different mendelian randomization studies the analysis of the

effects of genetic scores consisting of independently inherited polymorphisms in the PCSK9 gene resulted into reduced LDL-C levels and cardiovascular events but was also associated with an increased risk of diabetes [164, 165, 241]. On these premises and given the great interest in anti-PCSK9 therapies, we investigated in detail how PCSK9 deficiency could impact on non-hepatic tissues, especially pancreas and β -cells function.

The influence of PCSK9 on lipid metabolism and glucose homeostasis was evaluated in two different conditions: a state of obesity and metabolic dysfunction (HFD) and a physiological condition (SFD). The use of a lipid-rich diet, compared to a standard diet, allowed us to investigate the role of PCSK9 in different metabolic settings, thus increasing the knowledge about its biological functions. Firstly we demonstrated that C57BL6 WT male mice, fed a HFD for 20 weeks, developed alterations in weight gain and lipid metabolism, paralleled with impaired glucose tolerance and insulin resistance, confirming that we successfully set a mouse model of metabolic disorders.

Once characterized the model, we investigated the impact of PCSK9 deficiency in both conditions (HFD and SFD). As extensively reported in literature [248], PCSK9 KO mice showed a significant reduction in cholesterol plasma levels compared to WT littermates, ascribable to an increased clearance of circulating LDL-C. However, effects of PCSK9 beyond the LDLR regulation have been proposed [4]. PCSK9 targets not only the LDLR but also the closest family member VLDLR, which is highly expressed in adipose tissue. PCSK9 deficient mice fed a western type diet presented augmented VAT accumulation associated with increased VLDLR expression, a phenotype reverted following the injection of a liver selective PCSK9 transgene [119]. We extended this observation by demonstrating that PCSK9 KO mice presented a significantly increased ectopic fat accumulation compared to WT mice, both in a physiological condition (SFD) and in a state of metabolic dysfunction (HFD). This observation raises the question of a possible role of PCSK9 in modulating lipids delivery and accumulation in peripheral tissues.

However, the main focus of this PhD project regards the role of PCSK9 in glucose metabolism. In spite of similar plasma glucose levels at baseline, depending on an overnight fasting, PCSK9 KO mice showed a significant delay in glucose clearance following intraperitoneal glucose injection (GTT), with both SFD and HFD. The fasting and refeeding experiment, performed to point out possible differences in plasma glucose

levels also under physiological conditions, confirmed the impaired glucose tolerance observed under a PCSK9 deficient state. GLP-1, secreted from L-cells of the gastrointestinal mucosa in response to a meal, is known to be an important blood glucose-lowering agent [251]. However, the intraperitoneal (IPGTT) instead of the oral (OGTT) administration of glucose allowed us to bypass the contribution of GLP-1 on glucose homeostasis, which could interfere during the fasting and refeeding experiment. Interestingly, the altered phenotype described in PCSK9 KO animals, independently of the type of diet used, was not the consequence of an impaired insulin tolerance. Indeed, the glycemic curves resulting from the intraperitoneal injection of insulin (ITT) were superimposable between the two experimental groups, thus excluding the presence of an insulin resistant state under PCSK9 deficiency. To further extend this finding, we measured the ratio between phosphorylated Akt and total Akt, as an index of downstream activation of the insulin receptor [252], both in the liver and in the soleus muscle. In these tissues pAkt/Akt ratio was similar in WT and PCSK9 KO mice, confirming that the absence of PCSK9 do not affect the activation of the insulin pathway.

Once excluded an insulin resistance state, we focused on pancreas and β -cells function to understand the causes on which depends the impaired glucose tolerance observed in PCSK9 KO mice. Plasma insulin and C-peptide levels were significantly decreased in PCSK9 KO mice compared to WT littermates, suggesting that PCSK9 deficiency might impair insulin secretion. As a further confirmation, plasma insulin levels increased to lower extent in the absence of PCSK9 also following both an IPGTT and a fast and refeeding experiment. On the contrary, pancreatic insulin content was significantly increased in PCSK9 KO mice compared to WT controls. These findings, paralleled with the altered pancreatic morphology described in PCSK9 KO animals, led us to hypothesize that PCSK9 could play a central role in β -cells function and to further investigate the molecular mechanisms involved.

The LDLR, which is the main PCSK9 target, is abundantly expressed on the surface of pancreatic β cells, where it plays a key role in the uptake of LDL-C [2, 157]. The PCSK9-mediated LDLR degradation has been extensively characterized in liver, while its role in pancreas is still debate. Firstly we considered the possibility that PCSK9 could modulate the expression of the LDLR also in the pancreas. Interestingly, cytofluorimetric analysis showed a clearly increase of the LDLR expression in islets from PCSK9 KO mice compared

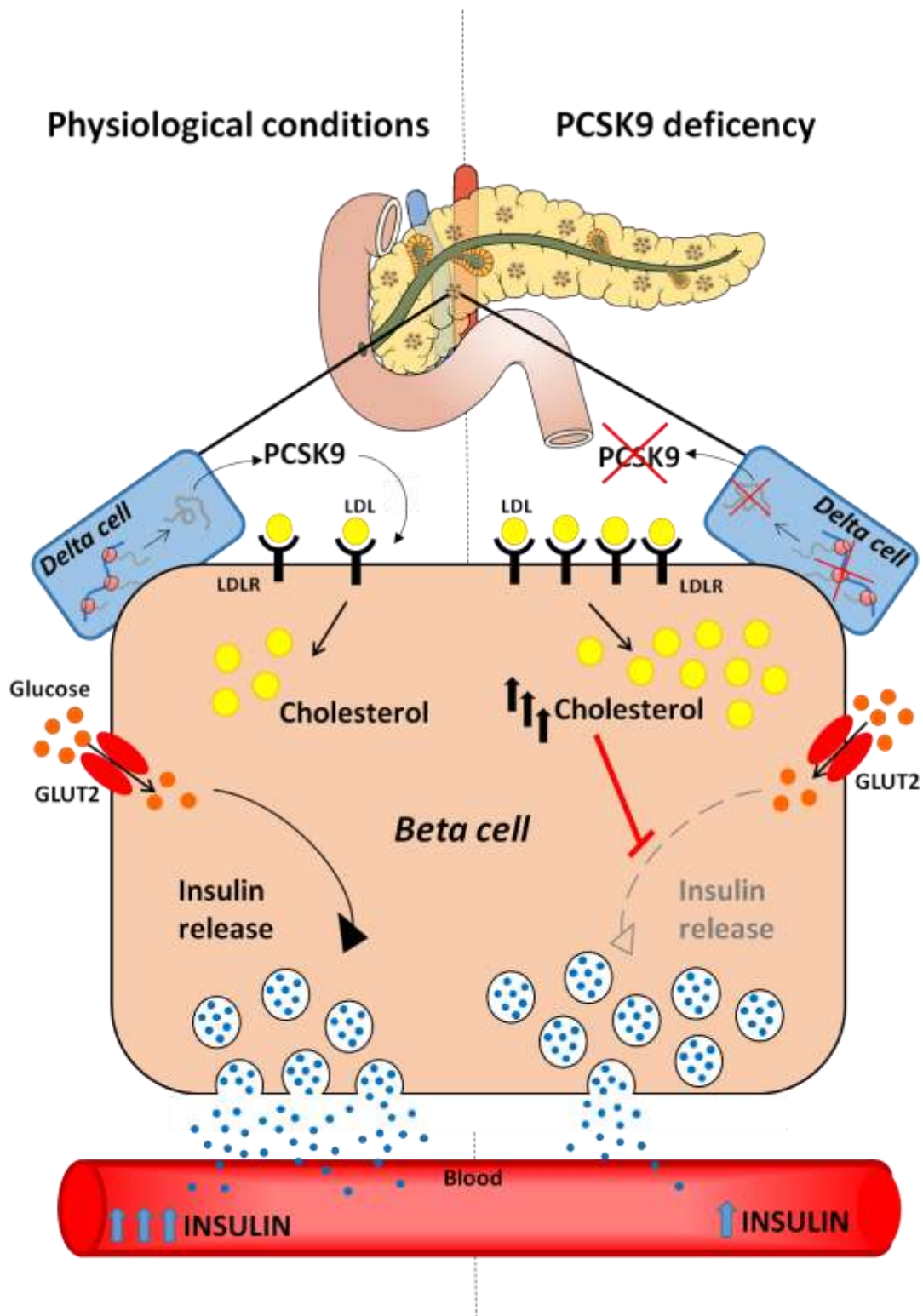
to islets isolated from WT littermates. Recent studies have focused on the potential relationship between cholesterol homeostasis and insulin secretion in β -cells, with a deleterious effect of high intracellular cholesterol content on GSIS [245]. Mice with a selective inactivation of ABCA1 in β -cells, despite normal plasma cholesterol levels, showed an elevated total cholesterol content in islets due to an impaired cholesterol efflux, causing an impaired glucose tolerance [253]. Hence, considering the increased LDLR expression observed in PCSK9 KO mice, we assessed whether PCSK9 deficiency could alter cholesterol content in islets. Lipidomic analysis revealed a higher cholesterol esters content in PCSK9 KO islets compared to WT ones, together with significant changes in fatty acid lipidome. As excess cellular cholesterol is usually stored as cholesteryl esters [254], these findings were paralleled by a strong increase in the expression of ACAT1, a key enzyme in the cholesterol esterification pathway. Moreover, the impaired lipid profile observed in PCSK9 KO islets associated with a downregulation of genes involved in cholesterol biosynthesis and uptake, including HMGCoA-R and LDLR, and with a modest but not significant increase in genes involved in cholesterol efflux. These data showed an altered β -cells lipid metabolism in the absence of PCSK9, which could determine an impairment in β -cells function and in turn explain the impaired glucose tolerance and the reduced insulin secretion observed in PCSK9 KO mice.

To demonstrate that the PCSK9/LDLR axis and not the other known targets of PCSK9, such as VLDLR, ApoER2 or CD36 [118, 119, 255], is responsible for the findings observed, we also investigated glucose metabolism in PCSK9/LDLR DKO mice. Glucose tolerance, insulin tolerance and plasma insulin levels in DKO animals were similar to those of control group, as well as islets morphology and pancreatic insulin content. The lack of differences between LDLR KO and PCSK9/LDLR DKO mice confirmed the key role of the LDLR in driving PCSK9 dependent pancreatic dysfunction.

Taken together these observations are critical, especially given that anti-PCSK9 therapies have been recently approved for the treatment of familial hypercholesterolemia and patients at very high cardiovascular risk. It is possible that, while on the one hand anti-PCSK9 therapies reduce LDL-C levels and related mortality, on the other hand increase the risk of diabetes. Data available from one year of therapy with anti-PCSK9 agents do not appear to increase the risk of diabetes [256], even though the possibility that this effect might appear after longer term treatments could not be ruled out.

However, our data in tissue selective PCSK9 KO mice suggested an alternative explanation. Despite PCSK9 is mainly produced and released by the liver, it is also synthesized to a relevant amount in other tissues, including the pancreas [1]. A liver selective PCSK9 KO model allowed us to investigate if the phenotype observed in PCSK9 KO (full body) mice depends on circulating liver-derived PCSK9 or on PCSK9 produced at the pancreatic level. Liver selective PCSK9 KO mice presented PCSK9 plasma levels below the detection limit, while maintaining PCSK9 production in other tissues, including pancreatic islets. This setting closely mimics the conditions of patients treated with anti-PCSK9 antibodies where PCSK9 is absent in the circulation but still produced in extrahepatic tissues, in contrast to the genetic studies with PCSK9 LOF where all tissues present a PCSK9 deficient condition. Liver selective PCSK9 KO animals showed plasma and pancreatic insulin levels, LDLR expression, islets cholesterol esters content similar to those of control mice, as well as glucose tolerance and insulin tolerance. These data indicate that circulating PCSK9 is not affecting LDLR in pancreas and suggest the possibility that anti-PCSK9 therapies might have a limited impact on inducing LDLR expression in pancreas.

In summary, we demonstrated the crucial role of PCSK9 in glucose metabolism and identified the biological mechanisms involved. PCSK9 critically controls the expression of the LDLR also at the pancreatic level and contributes to maintain a proper cholesterol content in β -cells. PCSK9 deficiency results in increased LDLR expression and cholesterol esters accumulation in pancreatic islets, which is known to be detrimental for cellular functionality. Indeed, cholesterol excess impairs insulin secretion, which could explain the impaired glucose tolerance observed in our model. Moreover, our data indicate that this effect is independent of circulating PCSK9, suggesting the possibility that anti-PCSK9 antibodies or liver specific therapies, such as siRNAs, might have a limited impact on LDLR expression in pancreas and beta cells function. Future studies should aim at addressing, in humans, the safety of targeting circulating PCSK9 on pancreatic β -cell function.



Impact of Pcsk9 deficiency on beta cells function

PCSK9 produced and released from delta cells controls LDLR expression in beta cells. PCSK9 deficiency results in increased expression of the LDLR in beta cells, thus leading to increased accumulation of cholesterol esters which impacts glucose-stimulated insulin secretion, resulting in hyperglycemia and impaired glucose tolerance observed in PCSK9 KO mice.

References

1. Norata, G.D., G. Tibolla, and A.L. Catapano, *Targeting PCSK9 for hypercholesterolemia*. *Annu Rev Pharmacol Toxicol*, 2014. **54**: p. 273-93.
2. Gruppig, A.Y., et al., *Low density lipoprotein binding and uptake by human and rat islet beta cells*. *Endocrinology*, 1997. **138**(10): p. 4064-8.
3. Seidah, N.G., et al., *PCSK9: a key modulator of cardiovascular health*. *Circ Res*, 2014. **114**(6): p. 1022-36.
4. Norata, G.D., et al., *Biology of proprotein convertase subtilisin kexin 9: beyond low-density lipoprotein cholesterol lowering*. *Cardiovasc Res*, 2016. **112**(1): p. 429-42.
5. American Diabetes, A., *Diagnosis and classification of diabetes mellitus*. *Diabetes Care*, 2010. **33 Suppl 1**: p. S62-9.
6. Monje A, C.A., Borgnakke WS., *Association between diabetes mellitus/hyperglycaemia and peri-implant diseases: Systematic review and meta-analysis*. *J Clin Periodontol*, 2017. **44**(6): p. 636-648.
7. Stephen L. Aronoff, K.B., Barb Shreiner, Laura Want, *Glucose Metabolism and Regulation: Beyond Insulin and Glucagon*. *Diabetes Spectrum*, 2004. **17**(3): p. 183-190.
8. Triplitt, C.L., *Examining the mechanisms of glucose regulation*. *Am J Manag Care*, 2012. **18**(1 Suppl): p. S4-10.
9. Wilson JD, F.D., *Glucose homeostasis and hypoglycaemia*. *William's Textbook of Endocrinology*, 1992: p. 1223 –1253.
10. RH, U., *Glucagon physiology and pathophysiology*. *N Engl J Med*, 1971. **285**: p. 443–449.
11. DJ, D., *The biology of incretin hormones*. *Cell Metab*, 2006. **3**: p. 153-165.
12. Sumera Karim, D.H.A., Patricia F Lalor, *Hepatic expression and cellular distribution of the glucose transporter family*. *World J Gastroenterol*, 2012. **18**(46): p. 6771–6781.
13. Agius, L., *Glucokinase and molecular aspects of liver glycogen metabolism*. *Biochem J*, 2008. **414**(1): p. 1-18.
14. Jiang, G. and B.B. Zhang, *Glucagon and regulation of glucose metabolism*. *Am J Physiol Endocrinol Metab*, 2003. **284**(4): p. E671-8.
15. Adeva-Andany, M.M., et al., *Liver glucose metabolism in humans*. *Biosci Rep*, 2016. **36**(6).
16. Berg JM, T.J., Stryer L, *Food Intake and Starvation Induce Metabolic Changes*. *Biochemistry*. 5th edition, 2002. **Section 30.3**.
17. Craig, M.E., et al., *ISPAD Clinical Practice Consensus Guidelines 2014. Definition, epidemiology, and classification of diabetes in children and adolescents*. *Pediatr Diabetes*, 2014. **15 Suppl 20**: p. 4-17.
18. Rewers, M. and J. Ludvigsson, *Environmental risk factors for type 1 diabetes*. *Lancet*, 2016. **387**(10035): p. 2340-8.
19. Vermeulen, I., et al., *Contribution of antibodies against IA-2beta and zinc transporter 8 to classification of diabetes diagnosed under 40 years of age*. *Diabetes Care*, 2011. **34**(8): p. 1760-5.
20. Noble, J.A. and H.A. Erlich, *Genetics of type 1 diabetes*. *Cold Spring Harb Perspect Med*, 2012. **2**(1): p. a007732.
21. Nejentsev, S., et al., *Localization of type 1 diabetes susceptibility to the MHC class I genes HLA-B and HLA-A*. *Nature*, 2007. **450**(7171): p. 887-92.
22. Wang, Z., et al., *Beyond Genetics: What Causes Type 1 Diabetes*. *Clin Rev Allergy Immunol*, 2017. **52**(2): p. 273-286.
23. Longnecker, M.P. and J.L. Daniels, *Environmental contaminants as etiologic factors for diabetes*. *Environ Health Perspect*, 2001. **109 Suppl 6**: p. 871-6.
24. Butalia, S., et al., *Environmental Risk Factors and Type 1 Diabetes: Past, Present, and Future*. *Can J Diabetes*, 2016. **40**(6): p. 586-593.
25. van der Werf, N., et al., *Viral infections as potential triggers of type 1 diabetes*. *Diabetes Metab Res Rev*, 2007. **23**(3): p. 169-83.
26. Akirav, E., J.A. Kushner, and K.C. Herold, *Beta-cell mass and type 1 diabetes: going, going, gone?* *Diabetes*, 2008. **57**(11): p. 2883-8.

27. Buckner, J.H. and G.T. Nepom, *Obstacles and opportunities for targeting the effector T cell response in type 1 diabetes*. J Autoimmun, 2016. **71**: p. 44-50.
28. Kuhn, C., et al., *Regulatory mechanisms of immune tolerance in type 1 diabetes and their failures*. J Autoimmun, 2016. **71**: p. 69-77.
29. American Diabetes, A., *Diagnosis and classification of diabetes mellitus*. Diabetes Care, 2014. **37 Suppl 1**: p. S81-90.
30. Atkinson, M.A., G.S. Eisenbarth, and A.W. Michels, *Type 1 diabetes*. Lancet, 2014. **383**(9911): p. 69-82.
31. Aghazadeh, Y. and M.C. Nostro, *Cell Therapy for Type 1 Diabetes: Current and Future Strategies*. Curr Diab Rep, 2017. **17**(6): p. 37.
32. Staeva, T.P., et al., *Recent lessons learned from prevention and recent-onset type 1 diabetes immunotherapy trials*. Diabetes, 2013. **62**(1): p. 9-17.
33. Han, S., et al., *Novel autoantigens in type 1 diabetes*. Am J Transl Res, 2013. **5**(4): p. 379-92.
34. Biarnes, M., et al., *Beta-cell death and mass in syngeneically transplanted islets exposed to short- and long-term hyperglycemia*. Diabetes, 2002. **51**(1): p. 66-72.
35. Kharroubi, A.T. and H.M. Darwish, *Diabetes mellitus: The epidemic of the century*. World J Diabetes, 2015. **6**(6): p. 850-67.
36. Dabelea, D., et al., *Prevalence of type 1 and type 2 diabetes among children and adolescents from 2001 to 2009*. JAMA, 2014. **311**(17): p. 1778-86.
37. Skyler, J.S., et al., *Differentiation of Diabetes by Pathophysiology, Natural History, and Prognosis*. Diabetes, 2017. **66**(2): p. 241-255.
38. Lyssenko, V., et al., *Clinical risk factors, DNA variants, and the development of type 2 diabetes*. N Engl J Med, 2008. **359**(21): p. 2220-32.
39. Zeggini, E., et al., *Replication of genome-wide association signals in UK samples reveals risk loci for type 2 diabetes*. Science, 2007. **316**(5829): p. 1336-41.
40. Hwang, J.Y., et al., *Genome-wide association meta-analysis identifies novel variants associated with fasting plasma glucose in East Asians*. Diabetes, 2015. **64**(1): p. 291-8.
41. Saxena, M., N. Srivastava, and M. Banerjee, *Association of IL-6, TNF-alpha and IL-10 gene polymorphisms with type 2 diabetes mellitus*. Mol Biol Rep, 2013. **40**(11): p. 6271-9.
42. Chatterjee, S., K. Khunti, and M.J. Davies, *Type 2 diabetes*. Lancet, 2017. **389**(10085): p. 2239-2251.
43. Kolb, H. and S. Martin, *Environmental/lifestyle factors in the pathogenesis and prevention of type 2 diabetes*. BMC Med, 2017. **15**(1): p. 131.
44. Aune, D., et al., *Physical activity and the risk of type 2 diabetes: a systematic review and dose-response meta-analysis*. Eur J Epidemiol, 2015. **30**(7): p. 529-42.
45. Holman, R.R., et al., *10-year follow-up of intensive glucose control in type 2 diabetes*. N Engl J Med, 2008. **359**(15): p. 1577-89.
46. Halban, P.A., et al., *beta-cell failure in type 2 diabetes: postulated mechanisms and prospects for prevention and treatment*. Diabetes Care, 2014. **37**(6): p. 1751-8.
47. Druet, C., et al., *Characterization of insulin secretion and resistance in type 2 diabetes of adolescents*. J Clin Endocrinol Metab, 2006. **91**(2): p. 401-4.
48. Tomita, T., *Apoptosis in pancreatic beta-islet cells in Type 2 diabetes*. Bosn J Basic Med Sci, 2016. **16**(3): p. 162-79.
49. Colagiuri, S., et al., *Glycemic thresholds for diabetes-specific retinopathy: implications for diagnostic criteria for diabetes*. Diabetes Care, 2011. **34**(1): p. 145-50.
50. Thanabalasingham, G., et al., *Systematic assessment of etiology in adults with a clinical diagnosis of young-onset type 2 diabetes is a successful strategy for identifying maturity-onset diabetes of the young*. Diabetes Care, 2012. **35**(6): p. 1206-12.
51. McMacken, M. and S. Shah, *A plant-based diet for the prevention and treatment of type 2 diabetes*. J Geriatr Cardiol, 2017. **14**(5): p. 342-354.

52. American Diabetes, A., 8. *Pharmacologic Approaches to Glycemic Treatment*. Diabetes Care, 2017. **40**(Suppl 1): p. S64-S74.
53. Seino, S., *Cell signalling in insulin secretion: the molecular targets of ATP, cAMP and sulfonylurea*. Diabetologia, 2012. **55**(8): p. 2096-108.
54. Fuchtenbusch, M., E. Standl, and H. Schatz, *Clinical efficacy of new thiazolidinediones and glinides in the treatment of type 2 diabetes mellitus*. Exp Clin Endocrinol Diabetes, 2000. **108**(3): p. 151-63.
55. Nauck, M.A. and J.J. Meier, *The incretin effect in healthy individuals and those with type 2 diabetes: physiology, pathophysiology, and response to therapeutic interventions*. Lancet Diabetes Endocrinol, 2016. **4**(6): p. 525-36.
56. Drucker, D.J. and M.A. Nauck, *The incretin system: glucagon-like peptide-1 receptor agonists and dipeptidyl peptidase-4 inhibitors in type 2 diabetes*. Lancet, 2006. **368**(9548): p. 1696-705.
57. Thrasher, J., *Pharmacologic Management of Type 2 Diabetes Mellitus: Available Therapies*. Am J Med, 2017. **130**(6S): p. S4-S17.
58. Jouvett, N. and J.L. Estall, *The pancreas: Bandmaster of glucose homeostasis*. Exp Cell Res, 2017.
59. Fu, Z., E.R. Gilbert, and D. Liu, *Regulation of insulin synthesis and secretion and pancreatic Beta-cell dysfunction in diabetes*. Curr Diabetes Rev, 2013. **9**(1): p. 25-53.
60. Abel, J.J., *Crystalline Insulin*. Proc Natl Acad Sci U S A, 1926. **12**(2): p. 132-6.
61. Chance, R.E., R.M. Ellis, and W.W. Bromer, *Porcine proinsulin: characterization and amino acid sequence*. Science, 1968. **161**(3837): p. 165-7.
62. Chan, S.J., P. Keim, and D.F. Steiner, *Cell-free synthesis of rat preproinsulins: characterization and partial amino acid sequence determination*. Proc Natl Acad Sci U S A, 1976. **73**(6): p. 1964-8.
63. Egea, P.F., R.M. Stroud, and P. Walter, *Targeting proteins to membranes: structure of the signal recognition particle*. Curr Opin Struct Biol, 2005. **15**(2): p. 213-20.
64. Taylor, K.W., *The biosynthesis and secretion of insulin*. Clin Endocrinol Metab, 1972. **1**(3): p. 601-22.
65. Smith, G.D., W.A. Pangborn, and R.H. Blessing, *The structure of T6 human insulin at 1.0 Å resolution*. Acta Crystallogr D Biol Crystallogr, 2003. **59**(Pt 3): p. 474-82.
66. Weiss, M., D.F. Steiner, and L.H. Philipson, *Insulin Biosynthesis, Secretion, Structure, and Structure-Activity Relationships*, in *Endotext*, L.J. De Groot, et al., Editors. 2000: South Dartmouth (MA).
67. Hay, C.W. and K. Docherty, *Comparative analysis of insulin gene promoters: implications for diabetes research*. Diabetes, 2006. **55**(12): p. 3201-13.
68. German, M., et al., *The insulin gene promoter. A simplified nomenclature*. Diabetes, 1995. **44**(8): p. 1002-4.
69. Shieh, S.Y. and M.J. Tsai, *Cell-specific and ubiquitous factors are responsible for the enhancer activity of the rat insulin II gene*. J Biol Chem, 1991. **266**(25): p. 16708-14.
70. Sander, M., et al., *Genetic analysis reveals that PAX6 is required for normal transcription of pancreatic hormone genes and islet development*. Genes Dev, 1997. **11**(13): p. 1662-73.
71. Naya, F.J., C.M. Stellrecht, and M.J. Tsai, *Tissue-specific regulation of the insulin gene by a novel basic helix-loop-helix transcription factor*. Genes Dev, 1995. **9**(8): p. 1009-19.
72. Naya, F.J., et al., *Diabetes, defective pancreatic morphogenesis, and abnormal enteroendocrine differentiation in BETA2/neuroD-deficient mice*. Genes Dev, 1997. **11**(18): p. 2323-34.
73. Sander, M., et al., *A novel glucose-responsive element in the human insulin gene functions uniquely in primary cultured islets*. Proc Natl Acad Sci U S A, 1998. **95**(20): p. 11572-7.
74. Foulkes, N.S. and P. Sassone-Corsi, *Transcription factors coupled to the cAMP-signalling pathway*. Biochim Biophys Acta, 1996. **1288**(3): p. F101-21.

75. Vander Mierde, D., et al., *Glucose activates a protein phosphatase-1-mediated signaling pathway to enhance overall translation in pancreatic beta-cells*. *Endocrinology*, 2007. **148**(2): p. 609-17.
76. Zhang, W., et al., *PERK EIF2AK3 control of pancreatic beta cell differentiation and proliferation is required for postnatal glucose homeostasis*. *Cell Metab*, 2006. **4**(6): p. 491-7.
77. Mziut, H., et al., *Synergy of glucose and growth hormone signalling in islet cells through ICA512 and STAT5*. *Nat Cell Biol*, 2006. **8**(5): p. 435-45.
78. Itoh, N. and H. Okamoto, *Translational control of proinsulin synthesis by glucose*. *Nature*, 1980. **283**(5742): p. 100-2.
79. Chang, T.W. and A.L. Goldberg, *The metabolic fates of amino acids and the formation of glutamine in skeletal muscle*. *J Biol Chem*, 1978. **253**(10): p. 3685-93.
80. Suckale, J. and M. Solimena, *Pancreas islets in metabolic signaling--focus on the beta-cell*. *Front Biosci*, 2008. **13**: p. 7156-71.
81. Maechler, P. and C.B. Wollheim, *Mitochondrial glutamate acts as a messenger in glucose-induced insulin exocytosis*. *Nature*, 1999. **402**(6762): p. 685-9.
82. Sener, A. and W.J. Malaisse, *L-leucine and a nonmetabolized analogue activate pancreatic islet glutamate dehydrogenase*. *Nature*, 1980. **288**(5787): p. 187-9.
83. MacDonald, P.E., A.M. Salapatek, and M.B. Wheeler, *Glucagon-like peptide-1 receptor activation antagonizes voltage-dependent repolarizing K(+) currents in beta-cells: a possible glucose-dependent insulinotropic mechanism*. *Diabetes*, 2002. **51 Suppl 3**: p. S443-7.
84. Itoh, Y., et al., *Free fatty acids regulate insulin secretion from pancreatic beta cells through GPR40*. *Nature*, 2003. **422**(6928): p. 173-6.
85. Nadal, A., et al., *Rapid insulinotropic effect of 17beta-estradiol via a plasma membrane receptor*. *FASEB J*, 1998. **12**(13): p. 1341-8.
86. Peschke, E., et al., *Receptor (MT(1)) mediated influence of melatonin on cAMP concentration and insulin secretion of rat insulinoma cells INS-1*. *J Pineal Res*, 2002. **33**(2): p. 63-71.
87. Doyle, M.E. and J.M. Egan, *Mechanisms of action of glucagon-like peptide 1 in the pancreas*. *Pharmacol Ther*, 2007. **113**(3): p. 546-93.
88. Ahren, B. and P.J. Havel, *Leptin inhibits insulin secretion induced by cellular cAMP in a pancreatic B cell line (INS-1 cells)*. *Am J Physiol*, 1999. **277**(4 Pt 2): p. R959-66.
89. Petruzzelli, L.M., et al., *Insulin activates a tyrosine-specific protein kinase in extracts of 3T3-L1 adipocytes and human placenta*. *Proc Natl Acad Sci U S A*, 1982. **79**(22): p. 6792-6.
90. Shaw, L.M., *The insulin receptor substrate (IRS) proteins: at the intersection of metabolism and cancer*. *Cell Cycle*, 2011. **10**(11): p. 1750-6.
91. Taniguchi, C.M., B. Emanuelli, and C.R. Kahn, *Critical nodes in signalling pathways: insights into insulin action*. *Nat Rev Mol Cell Biol*, 2006. **7**(2): p. 85-96.
92. Cernea, S. and M. Dobreanu, *Diabetes and beta cell function: from mechanisms to evaluation and clinical implications*. *Biochem Med (Zagreb)*, 2013. **23**(3): p. 266-80.
93. Komatsu, M., et al., *Glucose-stimulated insulin secretion: A newer perspective*. *J Diabetes Investig*, 2013. **4**(6): p. 511-6.
94. Kabra, U.D., et al., *Direct Substrate Delivery Into Mitochondrial Fission-Deficient Pancreatic Islets Rescues Insulin Secretion*. *Diabetes*, 2017. **66**(5): p. 1247-1257.
95. Kyriazis, G.A., M.M. Soundarapandian, and B. Tyrberg, *Sweet taste receptor signaling in beta cells mediates fructose-induced potentiation of glucose-stimulated insulin secretion*. *Proc Natl Acad Sci U S A*, 2012. **109**(8): p. E524-32.
96. Prentki, M., F.M. Matschinsky, and S.R. Madiraju, *Metabolic signaling in fuel-induced insulin secretion*. *Cell Metab*, 2013. **18**(2): p. 162-85.
97. Drucker, D.J., *Incretin action in the pancreas: potential promise, possible perils, and pathological pitfalls*. *Diabetes*, 2013. **62**(10): p. 3316-23.

98. Hotamisligil, G.S. and E. Erbay, *Nutrient sensing and inflammation in metabolic diseases*. Nat Rev Immunol, 2008. **8**(12): p. 923-34.
99. Robertson, R.P., et al., *Beta-cell glucose toxicity, lipotoxicity, and chronic oxidative stress in type 2 diabetes*. Diabetes, 2004. **53** Suppl 1: p. S119-24.
100. Robertson, R.P., et al., *Glucose toxicity in beta-cells: type 2 diabetes, good radicals gone bad, and the glutathione connection*. Diabetes, 2003. **52**(3): p. 581-7.
101. Leibowitz, G., et al., *Glucose regulation of beta-cell stress in type 2 diabetes*. Diabetes Obes Metab, 2010. **12** Suppl 2: p. 66-75.
102. Herchuelz, A., et al., *beta-Cell preservation and regeneration in diabetes by modulation of beta-cell Ca(2)(+) homeostasis*. Diabetes Obes Metab, 2012. **14** Suppl 3: p. 136-42.
103. Sharma, R.B. and L.C. Alonso, *Lipotoxicity in the pancreatic beta cell: not just survival and function, but proliferation as well?* Curr Diab Rep, 2014. **14**(6): p. 492.
104. Poitout, V. and R.P. Robertson, *Glucolipotoxicity: fuel excess and beta-cell dysfunction*. Endocr Rev, 2008. **29**(3): p. 351-66.
105. Giacca, A., et al., *Lipid-induced pancreatic beta-cell dysfunction: focus on in vivo studies*. Am J Physiol Endocrinol Metab, 2011. **300**(2): p. E255-62.
106. Abderrahmani, A., et al., *Human high-density lipoprotein particles prevent activation of the JNK pathway induced by human oxidised low-density lipoprotein particles in pancreatic beta cells*. Diabetologia, 2007. **50**(6): p. 1304-14.
107. Kruit, J.K., et al., *Loss of both ABCA1 and ABCG1 results in increased disturbances in islet sterol homeostasis, inflammation, and impaired beta-cell function*. Diabetes, 2012. **61**(3): p. 659-64.
108. Hao, M., et al., *Direct effect of cholesterol on insulin secretion: a novel mechanism for pancreatic beta-cell dysfunction*. Diabetes, 2007. **56**(9): p. 2328-38.
109. Bogan, J.S., Y. Xu, and M. Hao, *Cholesterol accumulation increases insulin granule size and impairs membrane trafficking*. Traffic, 2012. **13**(11): p. 1466-80.
110. Donath, M.Y., et al., *Cytokines and beta-cell biology: from concept to clinical translation*. Endocr Rev, 2008. **29**(3): p. 334-50.
111. Donath, M.Y., et al., *Islet inflammation impairs the pancreatic beta-cell in type 2 diabetes*. Physiology (Bethesda), 2009. **24**: p. 325-31.
112. Robinson, J.G., et al., *Efficacy and safety of alirocumab in reducing lipids and cardiovascular events*. N Engl J Med, 2015. **372**(16): p. 1489-99.
113. Abifadel, M., et al., *Mutations in PCSK9 cause autosomal dominant hypercholesterolemia*. Nat Genet, 2003. **34**(2): p. 154-6.
114. Seidah, N.G. and A. Prat, *The proprotein convertases are potential targets in the treatment of dyslipidemia*. J Mol Med (Berl), 2007. **85**(7): p. 685-96.
115. Benjannet, S., et al., *NARC-1/PCSK9 and its natural mutants: zymogen cleavage and effects on the low density lipoprotein (LDL) receptor and LDL cholesterol*. J Biol Chem, 2004. **279**(47): p. 48865-75.
116. Mayne J, D.T., Raymond A, Bernier L, Cousins M, Ooi TC, Davignon J, Seidah NG, Mbikay M, Chrétien M., *Novel loss-of-function PCSK9 variant is associated with low plasma LDL cholesterol in a French-Canadian family and with impaired processing and secretion in cell culture*. Clin Chem, 2011. **57**(10): p. 1415-23.
117. Piper, D.E., et al., *The crystal structure of PCSK9: a regulator of plasma LDL-cholesterol*. Structure, 2007. **15**(5): p. 545-52.
118. Poirier, S., et al., *The proprotein convertase PCSK9 induces the degradation of low density lipoprotein receptor (LDLR) and its closest family members VLDLR and ApoER2*. J Biol Chem, 2008. **283**(4): p. 2363-72.
119. Demers, A., et al., *PCSK9 Induces CD36 Degradation and Affects Long-Chain Fatty Acid Uptake and Triglyceride Metabolism in Adipocytes and in Mouse Liver*. Arterioscler Thromb Vasc Biol, 2015. **35**(12): p. 2517-25.

120. Canuel M, S.X., Asselin MC, Paramithiotis E, Prat A, Seidah NG., *Proprotein convertase subtilisin/kexin type 9 (PCSK9) can mediate degradation of the low density lipoprotein receptor-related protein 1 (LRP-1)*. PLoS One, 2013. **8**(5).
121. Huang, S., et al., *Mechanism of LDL binding and release probed by structure-based mutagenesis of the LDL receptor*. J Lipid Res, 2010. **51**(2): p. 297-308.
122. Cunningham, D., et al., *Structural and biophysical studies of PCSK9 and its mutants linked to familial hypercholesterolemia*. Nat Struct Mol Biol, 2007. **14**(5): p. 413-9.
123. Poirier S, M.G., Poupon V, McPherson PS, Desjardins R, Ly K, Asselin MC, Day R, Duclos FJ, Witmer M, Parker R, Prat A, Seidah NG., *Dissection of the endogenous cellular pathways of PCSK9-induced LDLR degradation: Evidence for an intracellular route*. J Biol Chem, 2009. **284**(42): p. 28856-64.
124. Maxwell, K.N., E.A. Fisher, and J.L. Breslow, *Overexpression of PCSK9 accelerates the degradation of the LDLR in a post-endoplasmic reticulum compartment*. Proc Natl Acad Sci U S A, 2005. **102**(6): p. 2069-74.
125. Saavedra YG, D.R., Seidah NG., *The M2 module of the Cys-His-rich domain (CHRD) of PCSK9 is needed for the extracellular low density lipoprotein receptor (LDLR) degradation pathway*. J Biol Chem, 2012. **287**(52): p. 43492-501.
126. Lambert, G., et al., *The PCSK9 decade*. J Lipid Res, 2012. **53**(12): p. 2515-24.
127. Jeong, H.J., et al., *Sterol-dependent regulation of proprotein convertase subtilisin/kexin type 9 expression by sterol-regulatory element binding protein-2*. J Lipid Res, 2008. **49**(2): p. 399-409.
128. Dubuc, G., et al., *Statins upregulate PCSK9, the gene encoding the proprotein convertase neural apoptosis-regulated convertase-1 implicated in familial hypercholesterolemia*. Arterioscler Thromb Vasc Biol, 2004. **24**(8): p. 1454-9.
129. Maxwell, K.N., et al., *Novel putative SREBP and LXR target genes identified by microarray analysis in liver of cholesterol-fed mice*. J Lipid Res, 2003. **44**(11): p. 2109-19.
130. Costet P, C.B., Lambert G, Lalanne F, Lardeux B, Jarnoux AL, Grefhorst A, Staels B, Krempf M., *Hepatic PCSK9 expression is regulated by nutritional status via insulin and sterol regulatory element-binding protein 1c*. J Biol Chem, 2006. **281**(10): p. 6211-8.
131. Li, H., et al., *Hepatocyte nuclear factor 1alpha plays a critical role in PCSK9 gene transcription and regulation by the natural hypocholesterolemic compound berberine*. J Biol Chem, 2009. **284**(42): p. 28885-95.
132. Dong B, W.M., Li H, Kraemer FB, Adeli K, Seidah NG, Park SW, Liu J., *Strong induction of PCSK9 gene expression through HNF1alpha and SREBP2: mechanism for the resistance to LDL-cholesterol lowering effect of statins in dyslipidemic hamsters*. J Lipid Res, 2010. **51**(6): p. 1486-95.
133. Lambert, G., et al., *Fasting induces hyperlipidemia in mice overexpressing proprotein convertase subtilisin kexin type 9: lack of modulation of very-low-density lipoprotein hepatic output by the low-density lipoprotein receptor*. Endocrinology, 2006. **147**(10): p. 4985-95.
134. Lambert, G., et al., *Plasma PCSK9 concentrations correlate with LDL and total cholesterol in diabetic patients and are decreased by fenofibrate treatment*. Clin Chem, 2008. **54**(6): p. 1038-45.
135. Essalmani R, S.-R.D., Chamberland A, Abifadel M, Creemers JW, Boileau C, Seidah NG, Prat A., *In vivo evidence that furin from hepatocytes inactivates PCSK9*. J Biol Chem, 2011. **286**(6): p. 4257-63.
136. Lipari MT, L.W., Moran P, Kong-Beltran M, Sai T, Lai J, Lin SJ, Kolumam G, Zavala-Solorio J, Izrael-Tomasevic A, Arnott D, Wang J, Peterson AS, Kirchhofer D., *Furin-cleaved proprotein convertase subtilisin/kexin type 9 (PCSK9) is active and modulates low density lipoprotein receptor and serum cholesterol levels*. J Biol Chem, 2012. **287**(52): p. 43482-91.
137. Persson L, C.G., Ståhle L, Sjöberg BG, Troutt JS, Konrad RJ, Gälman C, Wallén H, Eriksson M, Hafström I, Lind S, Dahlin M, Amark P, Angelin B, Rudling M., *Circulating proprotein*

- convertase subtilisin kexin type 9 has a diurnal rhythm synchronous with cholesterol synthesis and is reduced by fasting in humans.* *Arterioscler Thromb Vasc Biol*, 2010. **30**(12): p. 2666-72.
138. Careskey, H.E., et al., *Atorvastatin increases human serum levels of proprotein convertase subtilisin/kexin type 9.* *J Lipid Res*, 2008. **49**(2): p. 394-8.
 139. Davignon, J. and G. Dubuc, *Statins and ezetimibe modulate plasma proprotein convertase subtilisin kexin-9 (PCSK9) levels.* *Trans Am Clin Climatol Assoc*, 2009. **120**: p. 163-73.
 140. Nilsson, L.M., et al., *Bile acids and lipoprotein metabolism: effects of cholestyramine and chenodeoxycholic acid on human hepatic mRNA expression.* *Biochem Biophys Res Commun*, 2007. **357**(3): p. 707-11.
 141. Horton, J.D., J.C. Cohen, and H.H. Hobbs, *Molecular biology of PCSK9: its role in LDL metabolism.* *Trends Biochem Sci*, 2007. **32**(2): p. 71-7.
 142. Costet P, H.M., Cariou B, Guyomarc'h Delasalle B, Konrad T, Winkler K., *Plasma PCSK9 is increased by fenofibrate and atorvastatin in a non-additive fashion in diabetic patients.* *Atherosclerosis*, 2010. **212**(1): p. 246-51.
 143. Lakoski, S.G., et al., *Genetic and metabolic determinants of plasma PCSK9 levels.* *J Clin Endocrinol Metab*, 2009. **94**(7): p. 2537-43.
 144. Cui Q, J.X., Yang T, Zhang M, Tang W, Chen Q, Hu Y, Haas JV, Troutt JS, Pickard RT, Darling R, Konrad RJ, Zhou H, Cao G., *Serum PCSK9 is associated with multiple metabolic factors in a large Han Chinese population.* *Atherosclerosis*, 2010. **213**(2): p. 632-6.
 145. Roubtsova, A., et al., *Circulating proprotein convertase subtilisin/kexin 9 (PCSK9) regulates VLDLR protein and triglyceride accumulation in visceral adipose tissue.* *Arterioscler Thromb Vasc Biol*, 2011. **31**(4): p. 785-91.
 146. Jonas MC, C.C., Puglielli L., *PCSK9 is required for the disposal of non-acetylated intermediates of the nascent membrane protein BACE1.* *EMBO Rep*, 2008. **9**(9): p. 916-22.
 147. Sharotri, V., et al., *Regulation of epithelial sodium channel trafficking by proprotein convertase subtilisin/kexin type 9 (PCSK9).* *J Biol Chem*, 2012. **287**(23): p. 19266-74.
 148. Seidah, N.G., et al., *The secretory proprotein convertase neural apoptosis-regulated convertase 1 (NARC-1): liver regeneration and neuronal differentiation.* *Proc Natl Acad Sci U S A*, 2003. **100**(3): p. 928-33.
 149. Rousselet, E., et al., *PCSK9 reduces the protein levels of the LDL receptor in mouse brain during development and after ischemic stroke.* *J Lipid Res*, 2011. **52**(7): p. 1383-91.
 150. Zhao, Z., et al., *Molecular characterization of loss-of-function mutations in PCSK9 and identification of a compound heterozygote.* *Am J Hum Genet*, 2006. **79**(3): p. 514-23.
 151. Koren, M.J., et al., *Anti-PCSK9 monotherapy for hypercholesterolemia: the MENDEL-2 randomized, controlled phase III clinical trial of evolocumab.* *J Am Coll Cardiol*, 2014. **63**(23): p. 2531-40.
 152. C.P., C., *Efficacy and safety of alirocumab in high cardiovascular risk patients with inadequately controlled hypercholesterolemia on maximally tolerated daily statin: results from the ODYSSEY COMBO II.* *Eur Heart J*, 2014.
 153. Hooper AJ, M.A., Tanyanyiwa DM, Burnett JR., *The C679X mutation in PCSK9 is present and lowers blood cholesterol in a Southern African population.* *Atherosclerosis*, 2007. **193**(2): p. 445-8.
 154. Bingham, B., et al., *Proapoptotic effects of NARC 1 (= PCSK9), the gene encoding a novel serine proteinase.* *Cytometry A*, 2006. **69**(11): p. 1123-31.
 155. Piao, M.X., et al., *PCSK9 regulates apoptosis in human neuroglioma u251 cells via mitochondrial signaling pathways.* *Int J Clin Exp Pathol*, 2015. **8**(3): p. 2787-94.
 156. Langhi C, L.M.C., Gmyr V, Vandewalle B, Kerr-Conte J, Krempf M, Pattou F, Costet P, Cariou B., *PCSK9 is expressed in pancreatic delta-cells and does not alter insulin secretion.* *Biochem Biophys Res Commun*, 2009. **390**(4): p. 1288-93.
 157. Roehrich, M.E., et al., *Insulin-secreting beta-cell dysfunction induced by human lipoproteins.* *J Biol Chem*, 2003. **278**(20): p. 18368-75.

158. Mbikay, M., et al., *PCSK9-deficient mice exhibit impaired glucose tolerance and pancreatic islet abnormalities*. FEBS Lett, 2010. **584**(4): p. 701-6.
159. Bonnefond A, Y.L., Le May C, Fumeron F, Marre M, Balkau B, Charpentier G, Franc S, Froguel P, Cariou B; DESIR study group., *The loss-of-function PCSK9 p.R46L genetic variant does not alter glucose homeostasis*. Diabetologia, 2015. **58**(9): p. 2051-5.
160. Saavedra, Y.G., R. Dufour, and A. Baass, *Familial hypercholesterolemia: PCSK9 InsLEU genetic variant and prediabetes/diabetes risk*. J Clin Lipidol, 2015. **9**(6): p. 786-93 e1.
161. Dubuc, G., et al., *A new method for measurement of total plasma PCSK9: clinical applications*. J Lipid Res, 2010. **51**(1): p. 140-9.
162. Baass A, D.G., Tremblay M, Delvin EE, O'Loughlin J, Levy E, Davignon J, Lambert M., *Plasma PCSK9 is associated with age, sex, and multiple metabolic markers in a population-based sample of children and adolescents*. Clin Chem, 2009. **55**(9): p. 1637-45.
163. Yang SH, L.S., Zhang Y, Xu RX, Guo YL, Zhu CG, Wu NQ, Cui CJ, Sun J, Li JJ., *Positive correlation of plasma PCSK9 levels with HbA in patients with type 2 diabetes*. Diabetes Metab Res Rev, 2016. **32**(2): p. 193-9.
164. Ference, B.A., et al., *Variation in PCSK9 and HMGCR and Risk of Cardiovascular Disease and Diabetes*. N Engl J Med, 2016. **375**(22): p. 2144-2153.
165. Lotta LA, S.S., Burgess S, Perry JR, Stewart ID, Willems SM, Luan J, Ardanaz E, Arriola L, Balkau B, Boeing H, Deloukas P, Forouhi NG, Franks PW, Grioni S, Kaaks R, Key TJ, Navarro C, Nilsson PM, Overvad K, Palli D, Panico S, Quirós JR, Riboli E, Rolandsson O, Sacerdote C, Salamanca-Fernandez E, Slimani N, Spijkerman AM, Tjonneland A, Tumino R, van der A DL, van der Schouw YT, McCarthy MI, Barroso I, O'Rahilly S, Savage DB, Sattar N, Langenberg C, Scott RA, Wareham NJ., *Association Between Low-Density Lipoprotein Cholesterol-Lowering Genetic Variants and Risk of Type 2 Diabetes: A Meta-analysis*. JAMA, 2016. **316**(13): p. 1383-1391.
166. Besseling J, K.J., Defesche JC, Hutten BA, Hovingh GK., *Association between familial hypercholesterolemia and prevalence of type 2 diabetes mellitus*. JAMA, 2015. **313**(10): p. 1029-36.
167. Sabatine, M.S., et al., *Efficacy and safety of evolocumab in reducing lipids and cardiovascular events*. N Engl J Med, 2015. **372**(16): p. 1500-9.
168. Ding, Z., et al., *Hemodynamic shear stress via ROS modulates PCSK9 expression in human vascular endothelial and smooth muscle cells and along the mouse aorta*. Antioxid Redox Signal, 2015. **22**(9): p. 760-71.
169. Ferri, N., et al., *Proprotein convertase subtilisin kexin type 9 (PCSK9) secreted by cultured smooth muscle cells reduces macrophages LDLR levels*. Atherosclerosis, 2012. **220**(2): p. 381-6.
170. Wu, C.Y., et al., *PCSK9 siRNA inhibits HUVEC apoptosis induced by ox-LDL via Bcl/Bax-caspase9-caspase3 pathway*. Mol Cell Biochem, 2012. **359**(1-2): p. 347-58.
171. Denis, M., et al., *Gene inactivation of proprotein convertase subtilisin/kexin type 9 reduces atherosclerosis in mice*. Circulation, 2012. **125**(7): p. 894-901.
172. Lee, C.J., et al., *Association of serum proprotein convertase subtilisin/kexin type 9 with carotid intima media thickness in hypertensive subjects*. Metabolism, 2013. **62**(6): p. 845-50.
173. Huijgen, R., et al., *Plasma levels of PCSK9 and phenotypic variability in familial hypercholesterolemia*. J Lipid Res, 2012. **53**(5): p. 979-83.
174. Giunzioni, I., et al., *Local effects of human PCSK9 on the atherosclerotic lesion*. J Pathol, 2016. **238**(1): p. 52-62.
175. Glerup, S., et al., *Physiological and therapeutic regulation of PCSK9 activity in cardiovascular disease*. Basic Res Cardiol, 2017. **112**(3): p. 32.
176. De Smet, E., et al., *Acute intake of plant stanol esters induces changes in lipid and lipoprotein metabolism-related gene expression in the liver and intestines of mice*. Lipids, 2015. **50**(6): p. 529-41.

177. Le May, C., et al., *Proprotein convertase subtilisin kexin type 9 null mice are protected from postprandial triglyceridemia*. *Arterioscler Thromb Vasc Biol*, 2009. **29**(5): p. 684-90.
178. Levy, E., et al., *PCSK9 plays a significant role in cholesterol homeostasis and lipid transport in intestinal epithelial cells*. *Atherosclerosis*, 2013. **227**(2): p. 297-306.
179. Cariou, B., et al., *PCSK9 dominant negative mutant results in increased LDL catabolic rate and familial hypobetalipoproteinemia*. *Arterioscler Thromb Vasc Biol*, 2009. **29**(12): p. 2191-7.
180. Kwakernaak, A.J., G. Lambert, and R.P. Dullaart, *Relationship of proprotein convertase subtilisin-kexin type 9 levels with resistin in lean and obese subjects*. *Clin Biochem*, 2012. **45**(16-17): p. 1522-4.
181. Seidah NG, P.S., Denis M, Parker R, Miao B, Mapelli C, Prat A, Wassef H, Davignon J, Hajjar KA, Mayer G., *Annexin A2 is a natural extrahepatic inhibitor of the PCSK9-induced LDL receptor degradation*. *PLoS One*, 2012. **7**(7): p. e41865.
182. Nguyen, M.A., T. Kosenko, and T.A. Lagace, *Internalized PCSK9 dissociates from recycling LDL receptors in PCSK9-resistant SV-589 fibroblasts*. *J Lipid Res*, 2014. **55**(2): p. 266-75.
183. Cohen, J.C., et al., *Sequence variations in PCSK9, low LDL, and protection against coronary heart disease*. *N Engl J Med*, 2006. **354**(12): p. 1264-72.
184. Farnier, M., et al., *Efficacy and safety of adding alirocumab to rosuvastatin versus adding ezetimibe or doubling the rosuvastatin dose in high cardiovascular-risk patients: The ODYSSEY OPTIONS II randomized trial*. *Atherosclerosis*, 2016. **244**: p. 138-46.
185. Kwakernaak AJ, L.G., Slagman MC, Waanders F, Laverman GD, Petrides F, Dikkeschei BD, Navis G, Dullaart RP., *Proprotein convertase subtilisin-kexin type 9 is elevated in proteinuric subjects: relationship with lipoprotein response to antiproteinuric treatment*. *Atherosclerosis*, 2013. **226**(2): p. 459-65.
186. Jin, K., et al., *Plasma PCSK9 in nephrotic syndrome and in peritoneal dialysis: a cross-sectional study*. *Am J Kidney Dis*, 2014. **63**(4): p. 584-9.
187. Maxwell, K.N. and J.L. Breslow, *Adenoviral-mediated expression of Pcsk9 in mice results in a low-density lipoprotein receptor knockout phenotype*. *Proc Natl Acad Sci U S A*, 2004. **101**(18): p. 7100-5.
188. Cohen, J., et al., *Low LDL cholesterol in individuals of African descent resulting from frequent nonsense mutations in PCSK9*. *Nat Genet*, 2005. **37**(2): p. 161-5.
189. Tibolla, G., et al., *Proprotein convertase subtilisin/kexin type 9 (PCSK9): from structure-function relation to therapeutic inhibition*. *Nutr Metab Cardiovasc Dis*, 2011. **21**(11): p. 835-43.
190. King, P. and S.J. Nicholls, *PCSK9 Inhibitors: Treating the Right Patients in Daily Practice*. *Curr Cardiol Rep*, 2017. **19**(8): p. 66.
191. Bergeron, N., et al., *Proprotein convertase subtilisin/kexin type 9 inhibition: a new therapeutic mechanism for reducing cardiovascular disease risk*. *Circulation*, 2015. **132**(17): p. 1648-66.
192. Sander, J.D. and J.K. Joung, *CRISPR-Cas systems for editing, regulating and targeting genomes*. *Nat Biotechnol*, 2014. **32**(4): p. 347-55.
193. Ding Q, S.A., Patel KM, Ng SL, Gosis BS, Regan SN, Cowan CA, Rader DJ, Musunuru K., *Permanent alteration of PCSK9 with in vivo CRISPR-Cas9 genome editing*. *Circ Res*, 2014. **115**(5): p. 488-92.
194. Wang, X., et al., *CRISPR-Cas9 Targeting of PCSK9 in Human Hepatocytes In Vivo-Brief Report*. *Arterioscler Thromb Vasc Biol*, 2016. **36**(5): p. 783-6.
195. Visser, M.E., et al., *Antisense oligonucleotides for the treatment of dyslipidaemia*. *Eur Heart J*, 2012. **33**(12): p. 1451-8.
196. Graham, M.J., et al., *Antisense inhibition of proprotein convertase subtilisin/kexin type 9 reduces serum LDL in hyperlipidemic mice*. *J Lipid Res*, 2007. **48**(4): p. 763-7.
197. Gupta, N., et al., *A locked nucleic acid antisense oligonucleotide (LNA) silences PCSK9 and enhances LDLR expression in vitro and in vivo*. *PLoS One*, 2010. **5**(5): p. e10682.

198. Lindholm, M.W., et al., *PCSK9 LNA antisense oligonucleotides induce sustained reduction of LDL cholesterol in nonhuman primates*. *Mol Ther*, 2012. **20**(2): p. 376-81.
199. van Poelgeest, E.P., et al., *Antisense-mediated reduction of proprotein convertase subtilisin/kexin type 9 (PCSK9): a first-in-human randomized, placebo-controlled trial*. *Br J Clin Pharmacol*, 2015. **80**(6): p. 1350-61.
200. van Poelgeest, E.P., et al., *Acute kidney injury during therapy with an antisense oligonucleotide directed against PCSK9*. *Am J Kidney Dis*, 2013. **62**(4): p. 796-800.
201. Zatsepin, T.S., Y.V. Kotelevtsev, and V. Koteliansky, *Lipid nanoparticles for targeted siRNA delivery - going from bench to bedside*. *Int J Nanomedicine*, 2016. **11**: p. 3077-86.
202. Frank-Kamenetsky, M., et al., *Therapeutic RNAi targeting PCSK9 acutely lowers plasma cholesterol in rodents and LDL cholesterol in nonhuman primates*. *Proc Natl Acad Sci U S A*, 2008. **105**(33): p. 11915-20.
203. Fitzgerald, K., et al., *Effect of an RNA interference drug on the synthesis of proprotein convertase subtilisin/kexin type 9 (PCSK9) and the concentration of serum LDL cholesterol in healthy volunteers: a randomised, single-blind, placebo-controlled, phase 1 trial*. *Lancet*, 2014. **383**(9911): p. 60-8.
204. Fitzgerald, K., et al., *A Highly Durable RNAi Therapeutic Inhibitor of PCSK9*. *N Engl J Med*, 2017. **376**(1): p. 41-51.
205. He, N.Y., et al., *Lowering serum lipids via PCSK9-targeting drugs: current advances and future perspectives*. *Acta Pharmacol Sin*, 2017. **38**(3): p. 301-311.
206. Pirillo, A. and A.L. Catapano, *Berberine, a plant alkaloid with lipid- and glucose-lowering properties: From in vitro evidence to clinical studies*. *Atherosclerosis*, 2015. **243**(2): p. 449-61.
207. Cameron, J., et al., *Berberine decreases PCSK9 expression in HepG2 cells*. *Atherosclerosis*, 2008. **201**(2): p. 266-73.
208. Dong B, L.H., Singh AB, Cao A, Liu J., *Inhibition of PCSK9 transcription by berberine involves down-regulation of hepatic HNF1 α protein expression through the ubiquitin-proteasome degradation pathway*. *J Biol Chem*, 2015. **290**(7): p. 4047-58.
209. Tsai, S.J. and M.C. Yin, *Antioxidative and anti-inflammatory protection of oleanolic acid and ursolic acid in PC12 cells*. *J Food Sci*, 2008. **73**(7): p. H174-8.
210. Wang, X., et al., *Oleanolic acid improves hepatic insulin resistance via antioxidant, hypolipidemic and anti-inflammatory effects*. *Mol Cell Endocrinol*, 2013. **376**(1-2): p. 70-80.
211. Wong, N.D., P.D. Rosenblit, and R.S. Greenfield, *Advances in dyslipidemia management for prevention of atherosclerosis: PCSK9 monoclonal antibody therapy and beyond*. *Cardiovasc Diagn Ther*, 2017. **7**(Suppl 1): p. S11-S20.
212. Stein, E.A., et al., *Effect of a monoclonal antibody to PCSK9 on LDL cholesterol*. *N Engl J Med*, 2012. **366**(12): p. 1108-18.
213. McKenney, J.M., et al., *Safety and efficacy of a monoclonal antibody to proprotein convertase subtilisin/kexin type 9 serine protease, SAR236553/REGN727, in patients with primary hypercholesterolemia receiving ongoing stable atorvastatin therapy*. *J Am Coll Cardiol*, 2012. **59**(25): p. 2344-53.
214. Roth EM, M.J., Hanotin C, Asset G, Stein EA., *Atorvastatin with or without an antibody to PCSK9 in primary hypercholesterolemia*. *N Engl J Med*, 2012. **367**(20): p. 1891-900.
215. Colhoun, H.M., et al., *Efficacy and safety of alirocumab, a fully human PCSK9 monoclonal antibody, in high cardiovascular risk patients with poorly controlled hypercholesterolemia on maximally tolerated doses of statins: rationale and design of the ODYSSEY COMBO I and II trials*. *BMC Cardiovasc Disord*, 2014. **14**: p. 121.
216. Bays H, G.D., Weiss R, Ruiz JL, Watts GF, Gouni-Berthold I, Robinson J, Zhao J, Hanotin C, Donahue S., *Alirocumab as Add-On to Atorvastatin Versus Other Lipid Treatment Strategies: ODYSSEY OPTIONS I Randomized Trial*. *J Clin Endocrinol Metab*, 2015. **100**(8): p. 3140-8.

217. Moriarty, P.M., et al., *Efficacy and safety of alirocumab, a monoclonal antibody to PCSK9, in statin-intolerant patients: design and rationale of ODYSSEY ALTERNATIVE, a randomized phase 3 trial.* J Clin Lipidol, 2014. **8**(6): p. 554-61.
218. Kastelein, J.J., et al., *ODYSSEY FH I and FH II: 78 week results with alirocumab treatment in 735 patients with heterozygous familial hypercholesterolaemia.* Eur Heart J, 2015. **36**(43): p. 2996-3003.
219. Chaudhary, R., et al., *PCSK9 inhibitors: A new era of lipid lowering therapy.* World J Cardiol, 2017. **9**(2): p. 76-91.
220. Dias, C.S., et al., *Effects of AMG 145 on low-density lipoprotein cholesterol levels: results from 2 randomized, double-blind, placebo-controlled, ascending-dose phase 1 studies in healthy volunteers and hypercholesterolemic subjects on statins.* J Am Coll Cardiol, 2012. **60**(19): p. 1888-98.
221. Giugliano, R.P., et al., *Efficacy, safety, and tolerability of a monoclonal antibody to proprotein convertase subtilisin/kexin type 9 in combination with a statin in patients with hypercholesterolaemia (LAPLACE-TIMI 57): a randomised, placebo-controlled, dose-ranging, phase 2 study.* Lancet, 2012. **380**(9858): p. 2007-17.
222. Koren MJ, S.R., Kim JB, Knusel B, Liu T, Lei L, Bolognese M, Wasserman SM., *Efficacy, safety, and tolerability of a monoclonal antibody to proprotein convertase subtilisin/kexin type 9 as monotherapy in patients with hypercholesterolaemia (MENDEL): a randomised, double-blind, placebo-controlled, phase 2 study.* Lancet, 2012. **380**(9858): p. 1995-2006.
223. Robinson, J.G., et al., *Effect of evolocumab or ezetimibe added to moderate- or high-intensity statin therapy on LDL-C lowering in patients with hypercholesterolemia: the LAPLACE-2 randomized clinical trial.* JAMA, 2014. **311**(18): p. 1870-82.
224. Stroes, E., et al., *Anti-PCSK9 antibody effectively lowers cholesterol in patients with statin intolerance: the GAUSS-2 randomized, placebo-controlled phase 3 clinical trial of evolocumab.* J Am Coll Cardiol, 2014. **63**(23): p. 2541-8.
225. Nissen, S.E., et al., *Efficacy and Tolerability of Evolocumab vs Ezetimibe in Patients With Muscle-Related Statin Intolerance: The GAUSS-3 Randomized Clinical Trial.* JAMA, 2016. **315**(15): p. 1580-90.
226. Blom, D.J., et al., *A 52-week placebo-controlled trial of evolocumab in hyperlipidemia.* N Engl J Med, 2014. **370**(19): p. 1809-19.
227. Raal, F.J., et al., *PCSK9 inhibition with evolocumab (AMG 145) in heterozygous familial hypercholesterolaemia (RUTHERFORD-2): a randomised, double-blind, placebo-controlled trial.* Lancet, 2015. **385**(9965): p. 331-40.
228. Raal, F.J., et al., *Inhibition of PCSK9 with evolocumab in homozygous familial hypercholesterolaemia (TESLA Part B): a randomised, double-blind, placebo-controlled trial.* Lancet, 2015. **385**(9965): p. 341-50.
229. Koren, M.J., et al., *Efficacy and safety of longer-term administration of evolocumab (AMG 145) in patients with hypercholesterolemia: 52-week results from the Open-Label Study of Long-Term Evaluation Against LDL-C (OSLER) randomized trial.* Circulation, 2014. **129**(2): p. 234-43.
230. Ferri, N., et al., *Bococizumab for the treatment of hypercholesterolaemia.* Expert Opin Biol Ther, 2017. **17**(7): p. 909-910.
231. Kastelein, J.J., et al., *Safety and efficacy of LY3015014, a monoclonal antibody to proprotein convertase subtilisin/kexin type 9 (PCSK9): a randomized, placebo-controlled Phase 2 study.* Eur Heart J, 2016. **37**(17): p. 1360-9.
232. Chackerian, B. and A. Remaley, *Vaccine strategies for lowering LDL by immunization against proprotein convertase subtilisin/kexin type 9.* Curr Opin Lipidol, 2016. **27**(4): p. 345-50.
233. Fattori, E., et al., *Immunization against proprotein convertase subtilisin-like/kexin type 9 lowers plasma LDL-cholesterol levels in mice.* J Lipid Res, 2012. **53**(8): p. 1654-61.

234. Landlinger C, P.M., Juno C, van der Hoorn JWA, Pieterman EJ, Jukema JW, Staffler G, Princen HMG, Galabova G., *The AT04A vaccine against proprotein convertase subtilisin/kexin type 9 reduces total cholesterol, vascular inflammation, and atherosclerosis in APOE*3Leiden.CETP mice*. Eur Heart J, 2017: p. 10.1093.
235. Ulrich Laufs, B.A.F., *Vaccination to prevent atherosclerotic cardiovascular diseases*. Eur Heart J 2017: p. 10.1093/eurheartj/ehx302.
236. Shan L, P.L., Zhang R, Murgolo NJ, Lan H, Hedrick JA., *PCSK9 binds to multiple receptors and can be functionally inhibited by an EGF-A peptide*. Biochem Biophys Res Commun, 2008. **375**(1): p. 69-73.
237. McNutt, M.C., et al., *Antagonism of secreted PCSK9 increases low density lipoprotein receptor expression in HepG2 cells*. J Biol Chem, 2009. **284**(16): p. 10561-70.
238. Zhang Y, E.C., Zhou L, Shia S, Li W, Quan C, Tom J, Moran P, Di Lello P, Skelton NJ, Kong-Beltran M, Peterson A, Kirchhofer D., *Identification of a small peptide that inhibits PCSK9 protein binding to the low density lipoprotein receptor*. J Biol Chem, 2014. **289**(2): p. 942-55.
239. Lipovsek, D., *Adnectins: engineered target-binding protein therapeutics*. Protein Eng Des Sel, 2011. **24**(1-2): p. 3-9.
240. Mitchell, T., et al., *Pharmacologic profile of the Adnectin BMS-962476, a small protein biologic alternative to PCSK9 antibodies for low-density lipoprotein lowering*. J Pharmacol Exp Ther, 2014. **350**(2): p. 412-24.
241. Schmidt, A.F., et al., *PCSK9 genetic variants and risk of type 2 diabetes: a mendelian randomisation study*. Lancet Diabetes Endocrinol, 2016. **5**(2): p. 97-105.
242. Norata, G.D., et al., *Oxidised-HDL3 induces the expression of PAI-1 in human endothelial cells. Role of p38MAPK activation and mRNA stabilization*. Br J Haematol, 2004. **127**(1): p. 97-104.
243. Norata, G.D., C. Garlanda, and A.L. Catapano, *The long pentraxin PTX3: a modulator of the immunoinflammatory response in atherosclerosis and cardiovascular diseases*. Trends Cardiovasc Med, 2010. **20**(2): p. 35-40.
244. Dongiovanni, P., et al., *Dietary iron overload induces visceral adipose tissue insulin resistance*. Am J Pathol, 2013. **182**(6): p. 2254-63.
245. Brunham, L.R., et al., *Cholesterol in islet dysfunction and type 2 diabetes*. J Clin Invest, 2008. **118**(2): p. 403-8.
246. Paul, R., et al., *Cholesterol in Pancreatic beta-Cell Death and Dysfunction: Underlying Mechanisms and Pathological Implications*. Pancreas, 2016. **45**(3): p. 317-24.
247. Seidah, N.G., et al., *The activation and physiological functions of the proprotein convertases*. Int J Biochem Cell Biol, 2008. **40**(6-7): p. 1111-25.
248. Rashid, S., et al., *Decreased plasma cholesterol and hypersensitivity to statins in mice lacking Pcsk9*. Proc Natl Acad Sci U S A, 2005. **102**(15): p. 5374-9.
249. Cochran, B.J., et al., *Impact of Perturbed Pancreatic beta-Cell Cholesterol Homeostasis on Adipose Tissue and Skeletal Muscle Metabolism*. Diabetes, 2016. **65**(12): p. 3610-3620.
250. Navarese, E.P., et al., *Meta-analysis of impact of different types and doses of statins on new-onset diabetes mellitus*. Am J Cardiol, 2013. **111**(8): p. 1123-30.
251. Nadkarni, P., O.G. Chepurny, and G.G. Holz, *Regulation of glucose homeostasis by GLP-1*. Prog Mol Biol Transl Sci, 2014. **121**: p. 23-65.
252. Broussard, J.L., et al., *Impaired insulin signaling in human adipocytes after experimental sleep restriction: a randomized, crossover study*. Ann Intern Med, 2012. **157**(8): p. 549-57.
253. Brunham, L.R., et al., *Beta-cell ABCA1 influences insulin secretion, glucose homeostasis and response to thiazolidinedione treatment*. Nat Med, 2007. **13**(3): p. 340-7.
254. Chang, T.Y., et al., *Acyl-coenzyme A:cholesterol acyltransferases*. Am J Physiol Endocrinol Metab, 2009. **297**(1): p. E1-9.
255. Seidah, N.G., *New developments in proprotein convertase subtilisin-kexin 9's biology and clinical implications*. Curr Opin Lipidol, 2016. **27**(3): p. 274-81.

256. Blom, D.J., et al., *Evaluation of the efficacy, safety and glycaemic effects of evolocumab (AMG 145) in hypercholesterolaemic patients stratified by glycaemic status and metabolic syndrome*. *Diabetes Obes Metab*, 2017. **19**(1): p. 98-107.

Ringrazio i Professori Catapano e Norata per avermi seguita con grande professionalità in questo percorso. Li ringrazio per l'esempio che hanno rappresentato.

Ringrazio di cuore tutte le persone conosciute e incontrate in questi anni, che con affetto hanno guidato la mia crescita professionale e umana.